

Asia Pacific Research Initiative for Sustainable Energy Systems 2012 (APRISES12)

Office of Naval Research
Grant Award Number N00014-13-1-0463

Computational Fluid Dynamics (CFD) Applications at the School of Architecture, University of Hawaii: Literature Review of Internal CFD

Task 7

Prepared For
Hawaii Natural Energy Institute

Prepared By
Sustainable Design & Consulting LLC, UH Environmental Research and
Design Laboratory, UH Sea Grant College Program & HNEI

August 2014



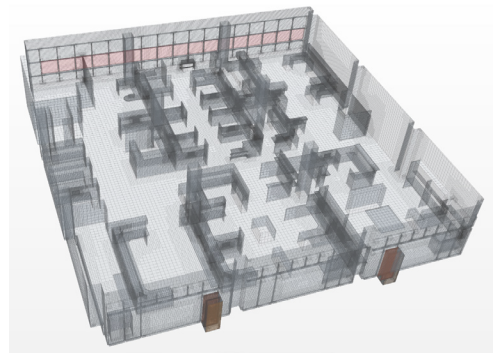
Project Phase 1- 7.B

LITERATURE REVIEW OF INTERNAL CFD

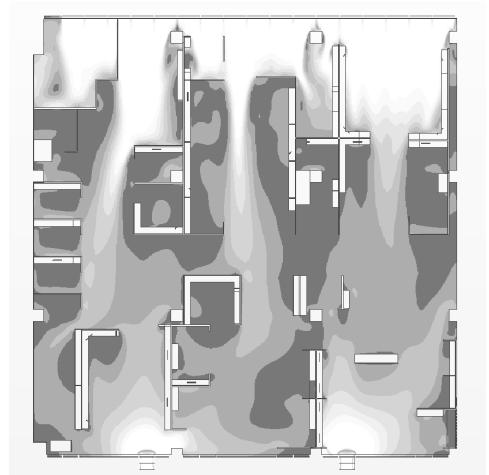
August 10, 2014

6

FINAL REPORT



Prepared by:
Manfred J. Zapka, PhD, PE (Editor)
Tuan Tran, D.Arch
A. James Maskrey, MEP, MBA, Project Manager
Stephen Meder, D.Arch, Director



Contract # N000-14-13-1-0463

Computational Fluid Dynamics (CFD) Applications at the School of Architecture,
University of Hawaii

Project Phase 1 – 7.B

Develop Skill Set for Internal CFD Analysis and Verification at the Building

Project Deliverable No. 6: Literature Review of Internal CFD

Prepared for Hawaii Natural Energy Institute

in support of

Contract #N000-14-13-1-0463

August 10, 2014

Prepared by:

Manfred J. Zapka, PhD, PE (Editor) (*)

Tuan Tran, D.Arch (**)

A. James Maskrey, MEP, MBA, Project Manager (***)

Stephen Meder, D.Arch, Director (**)

(*) Sustainable Design & Consulting LLC

(**) Environmental Research and Design Laboratory (ERDL), School of Architecture, University of Hawaii at Manoa

(***) Hawaii Natural Energy Institute (HNEI), University of Hawaii

Summary and Objectives

This review of scientific and technical literature is conducted to identify previous published research in areas that pertain to predicting airflow inside of buildings with the help of Computational Fluid Dynamics (CFD) investigations. The use of CFD programs to assess ventilation and specifically naturally ventilated buildings has become an important design and analysis tool in fields and their special applications, such as:

- Use of advanced analytical tools to investigate airflow phenomena and thermal performance in buildings.
- Use of CFD to improve the performance of naturally ventilated buildings and contribute to energy reduction by decreasing the need for energy intensive building cooling and ventilation.
- Lowering the barrier for building designers to use powerful numerical simulations for quantitative assessment of building performance.
- Enabling effective CFD use as alternatives to wind tunnel test and lower the costs for pre-construction optimization of building ventilation and conditioning.
- Use of CFD as tools to develop design standards to assess pressure losses in buildings, to enable designers to easily determine effective internal airflow pathways that offer little resistance of naturally induced air flow through the building.

Table of Contents:

1. Basics of Natural Ventilation and Airflow Inside of Buildings	1
1.1 Natural Ventilation of Buildings	1
1.2 Distribution of air in internal spaces	13
1.3 Mechanical Assist Ventilation	17
1.4 Ventilation Opening	28
1.5 Pressure Losses of Building Openings and Airflow Obstructions.....	34
2. CFD as a Design Tool for Natural Ventilation Design	46
3. Internal CFD – Numerical Assessment of Air Movement Inside Buildings.....	62
3.1 Best Practices and Quality Control	62
3.2 Domain Decomposition and Coupled CFD Analysis	76
3.3 Selection of Type of Mesh and Cells	86
3.4 Computational Domain geometry and Grid/mesh Design.....	91
3.5 Surface roughness of grid element	95
3.6 Boundary Conditions	98
3.7 Turbulence Modeling	101
3.8 Steady Flow vs. Unsteady Flow	106
3.9 Grid Convergence.....	109
3.10 Sensitivity Analysis – Guidelines and Evolving Standards	115
3.11 Post Processing.....	124
3.12 Validation of CFD Data through On-site Measurements	127

REFERENCES

1. Basics of Natural Ventilation and Airflow Inside of Buildings

This section provides reviewed literature about basic physical principles of natural ventilation as it relates to the numeric analysis of airflow inside of buildings. A good understanding of physical phenomena is very important in setting up CFD simulations and determining the extent of the domain of the numerical assessment.

1.1 Natural Ventilation of Buildings

In Hawaii, like in most other locations, historic buildings were designed and operated as naturally ventilated. In course of developing to higher standards of living and generally over the past decades, many of these originally naturally ventilated buildings have been modified with the addition of additional internal partitions and adding HVAC systems. Since the mechanical cooling and ventilation requires significant energy and power and with Hawaii featuring the highest energy prices in the nation, efforts have been made to increase the use of natural ventilation again in buildings.

In the course of designing high performance buildings, natural ventilation is being (re)considered as an increasingly attractive method for building designers to reducing energy use and cost, while at the same time ensure providing acceptable indoor environmental quality and maintaining a healthy, comfortable, and productive indoor climate. There are significant challenges to achieve a satisfactory building performance using natural ventilation in the hot and humid climate of Hawaii. However, the benefits of avoiding the ventilation and cooling of buildings solely by mechanical means and using natural ventilation full or in concert with mechanical assist building systems are significant. Based on our own estimates using data from EIA and Hawaii government data, while considering favorable conditions and buildings types, natural ventilation can be used as an alternative to conventional HVAC plants, saving 25% up to 50% of total energy consumption of commercial buildings.

Thermal balance of a room

The basic need for natural ventilation of buildings is twofold, and in this respect natural ventilation does not differ from the premises of mechanical ventilation and cooling.

The first basic need is to provide the internal spaces with sufficient outside air. The required amount, commonly referred to as air exchanges per hour (ACH), is based on applicable local or industry codes. The amount is thereby dependent on the use of the internal spaces or the number of occupants in the space. Where additional considerations are present, such as the presence of certain air borne substances or substance that are liberated as air comes in contact with these substances, a higher amount of ventilation air may be required to provide sufficient dilution and discharge from the space.

The second need for buildings in a hot climate is to expel heat gained in the space to the exterior.

1. Basics of Natural Ventilation and Airflow Inside of Buildings

Heat gain in the building can come from external or from internal heat sources. External heat gain is from radiant, convective and conductive solar heat sources. Internal heat gain is from heat sources such as electric loads or occupants. To achieve a steady state heat environment, the sum of heat inflow, outflow and generation within the system boundaries needs to be zero.

Peterson et al. (Petersen et.al. 1997) provides a comprehensive formulation of a heat balance procedure for determining cooling loads based on a zonal model. The approach presented is to incorporate the heat balance procedure into the load calculation, where accurate calculations of loads are based on basic phenomena that can be examined without the confounding effects of an approximate procedure. The author distinguishes between a surface and air heat balance. (See Figure 1.1)

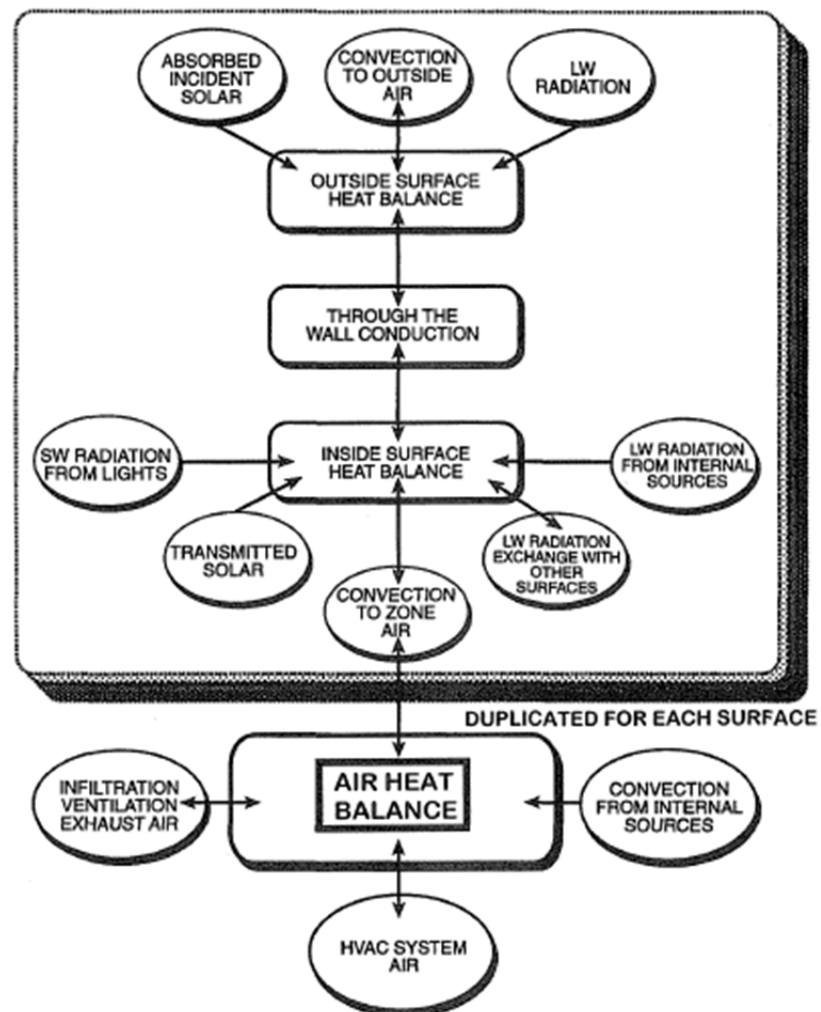


Figure 1.1: Schematic of heat balance processes in a zone (Petersen et.al. 1997)

A central theme of the article is the deviation from conventional norms of defining heat conditions of the internal air mass. Conventional simplification at the time of the article (e.g. in pre-CFD analysis) required a rigorous simplification of zonal air properties. Relying on a well-mixed, or as referred to “well-stirred” air volume and air properties were considered uniform within the zone. The author saw the need for a more rigorous treatment by introducing non-uniformities within the air volume. The author suggested, however, that such treatment would require an enormous increase in computational effort to model a zone. (Remarks: With the current dynamic development of CFD tools, this limitation is becoming less of a factor for comprehensive treatment of heat and especially air heat balance in a space.)

Santamouris (Santamouris, et. a., 1998) defines the thermal zone as a geometric entity limited by an envelope, which can be a single room or a combination of rooms with similar thermal performance. The final thermal equilibrium of the zone in regard to its state variables depends on the interaction of external climatic conditions and internal type and intensity of occupation of the zone. Figure 1.2 illustrates the links between the external and internal state variables as transfer phenomena. Therefore the solution of thermal balance of a zone depends on two physical equations, such as:

- Transfer equations that describe the flow of such properties as heat, mass, chemical agents, etc. where the pertinent transfer equations are:
 - Thermal diffusion (or conduction)
 - Radiation
 - Convection
 - Mass transfer

- Balance equation that define the state, namely pressure, temperature of chemical concentration, where the pertinent balance equations are:
 - Energy
 - Pressure
 - Mass

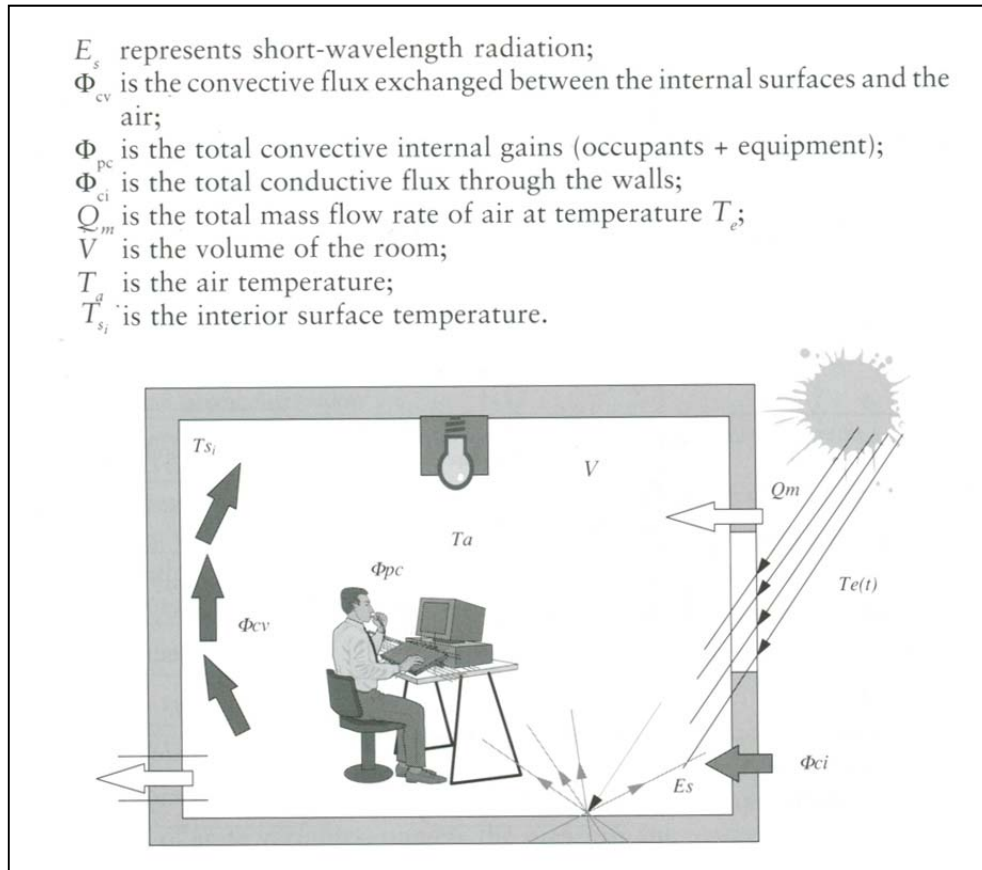


Figure 1.2: Thermal balance of a zone (Santamouris, et. a., 1998)

According to Santamouris the thermal balance of the room can then be expressed:

$$VC_p \frac{dT_a}{dt} = \Phi_{pc} + \sum_{i=1}^{nS} h c_i S_i (T_{s_i} - T_a) + Q_m C_p (T_e - T_a)$$

In regard to the mass airflow rate Q_m there are two main contributors, the airflow from the outdoors, through infiltration or active or passive ventilation, and the interzonal airflow rates due to air mass transfer between various zones.

Driving forces

Naturally ventilated buildings rely on pressure differences to move outside air through buildings. Pressure differences, or driving forces, can result from external wind actions impinging on the building envelope or from internal buoyancy effects caused by air density differences within the buildings. Generally speaking and considering the same site specific wind and climatic conditions, the effectiveness of natural ventilation depends significantly on the size and placement of openings in the building. In systems terms it is helpful to regard the energy and mass balance of building spaces of supply and exhaust. The same pressure driving force does not necessarily result in the same amount of air flowing through the building, since internal pathways create different energy losses. As an example the size and type of openings in the building envelope and between internal spaces and other air resistances along the internal air pathways are determining the amount of internal ventilation.

Wind driving forces: Wind impinging on a building creates a pressure distribution with respect to the background, will mean atmospheric pressure. Walker (Walker, 2010) states that wind actions on a building create a positive pressure on the windward side and a negative pressure on the leeward side of buildings. Due to the pressure difference, air will enter into windward openings and leave the building through leeward openings. Walker suggests a simple relationship between the volume of airflow and wind conditions (expressed by the wind velocity and the characteristics of the openings in the building:

$Q_{wind} = K \times A \times V$, where

Q_{wind}	=	Volume of airflow (m ³ /h)
A	=	Area of smaller opening (m ²)
V	=	Outdoor wind speed (m/h)
K	=	Coefficient of effectiveness (-)

The coefficient of effectiveness depends on the angle of the approaching wind and the relative size of entry and exit openings. The coefficient ranges from about 0.4 for wind hitting an opening at a 45° angle of incidence to 0.8 for wind hitting directly at a 90° angle. There are numerous tables where coefficient of effectiveness is defined for different shapes of buildings.

A difference approach of describing the wind induced driving forces is suggested by Santamouris (Santamouris, et. a., 1998). The resulting pressure representing the driving forces is calculated by correcting the average dynamic pressure of the wind with a pressure coefficient C_p . This results in a relationship of

$$P_s = C_p * P_v$$

With: P_s being the pressure at a specific location of the building envelope

C_p is the wind pressure coefficient

P_v is average dynamic pressure as calculated with $P_v = .5 * \rho * V_H^2$, where ρ is the outdoor air density (e.g. fct. of temperature and atmospheric pressure) and V_H is the mean wind velocity at upwind building height

The coefficient C_p is dependent on a range of variables, such as the approach direction of the wind, the building form and the influence of nearby buildings. Again, tables have been created to provide the building designer with a basic understanding of the results of wind motion around buildings that create pressure distributions. As with all tabulated design figures there are inherent simplifications and generalizations to determine the actual wind induced pressures on the building envelope.

Cóstola, D., et al. (2009) provide a comprehensive summary about C_p values. The authors made a distinction between primary sources of C_p data, such as full-scale measurements, reduced-scale measurements in wind tunnels and computational fluid dynamics (CFD) simulations, and secondary sources, such as databases and analytical models. The comparison suggested that the C_p values are quite different depending on the source adopted. The two influencing parameters for which these differences are most pronounced are the position on the facade and the degree of exposure/sheltering. The comparison of C_p data from different sources for sheltered buildings shows the largest differences, and data from different sources even present different trends. Figure 1.3 shows an example of the distribution of C_p along a path on the building envelope.

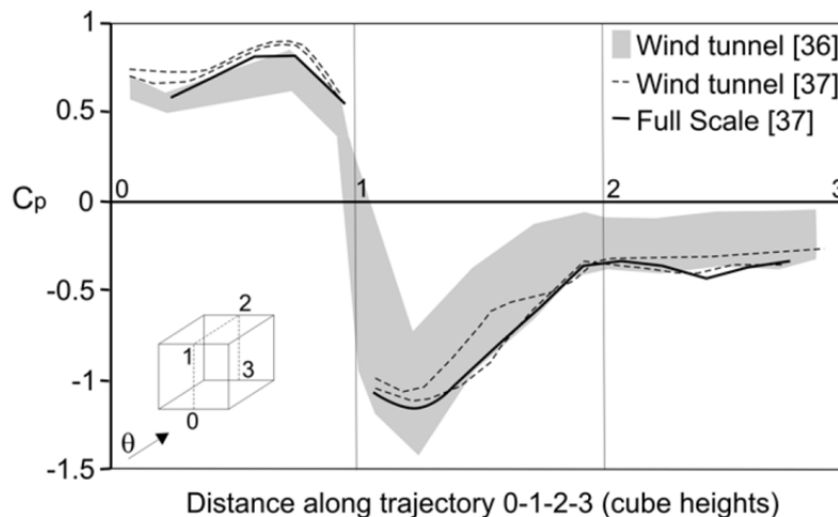


Figure 1.3: Comparison of different wind tunnel experiments (Cóstola, 2009)

Designers often rely standardized on external pressure distribution to determine preferable opening and appurtenances of the building envelope. An example of a 3D distribution of wind induced pressures on the exterior of building is suggested by Lstiburek, J. (2006). Figure 1.4 shows a typical distribution of C_p for standard building geometry. As pointed out before the values of C_p may differ considerably between buildings of the same exterior geometry, due to the influence of neighboring buildings or other obstructing structures or objects that affect the wind field around buildings.

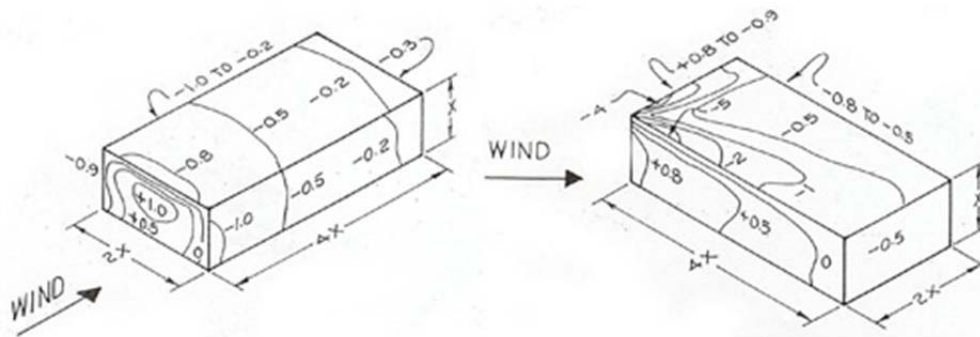


Figure 1.4: Pressure coefficients on walls and roof of rectangular buildings without parapets (Lstiburek, 2006)

The Stack Effect

Stack effect is a physical phenomenon that affects movement of air into and out of buildings, as well as other structures and is driven by buoyancy. The wind movement is created by buoyance due to density differences outside and inside of the building. In the applications that are relevant to natural ventilation air density are mainly dependent on temperature and moisture content of the air. The greater the thermal difference and the height of the structure, the greater the buoyancy force, thus creating the stack effect. The stack effect can be approximated by the following equation.

$$Q_{\text{stack}} = C_d \cdot A \cdot [2gh(T_i - T_o)/T_i]^{1/2}, \text{ where}$$

- Where:
- Q_{stack} = volume of ventilation rate
 - C_d = mean discharge coefficient (has to be determined from tables or experiments)
 - A = Flow area
 - g = the acceleration due to gravity
 - h = vertical distance between inlet and outlet midpoints

T_i = average temperature of indoor air (in absolute temperatures)

T_o = average temperature of outdoor air (in absolute temperatures)

While it is convenient and task oriented for certain design applications to approximate the amount of air drawn into the building through a higher indoor temperature, it is important to keep in mind that it is the difference in pressure that acts as the stack effect driving force. Straube, J. (2007) suggests that although houses might only be 3 to 9 m (9 to 27 feet) tall, stack effect can be a major force driving airflow, particularly in climates with a large temperature difference across the enclosure. The mixing in of air of different temperature in the internal space result in a Neutral Pressure Plane (NPP) located at an elevation in interior space. Figure 5 illustrates this situation.

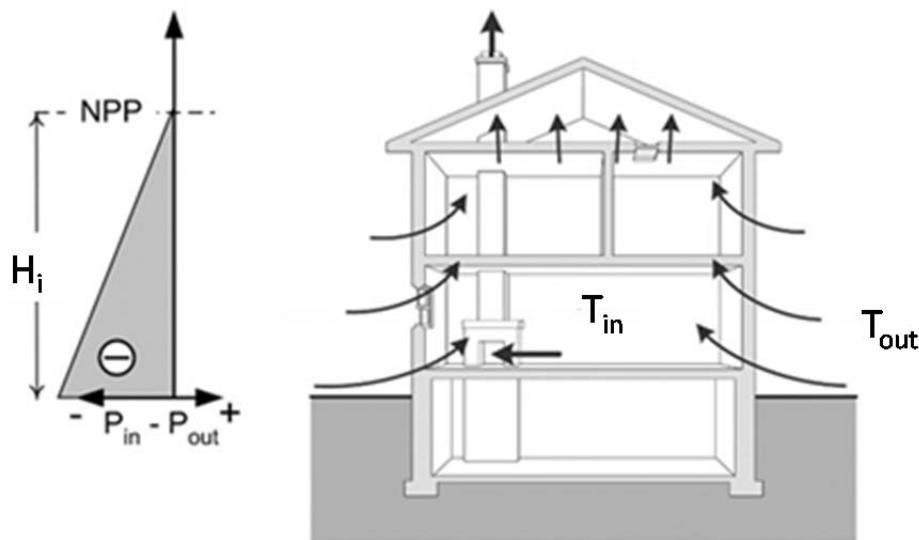


Figure 1.5: *Stack effect in a house* (Straube, 2007); modified by the author

More precisely a stack effect courses not only exist between inside and outside of the building but between zones that share a mass transfer opening. Using two zones m and n the resulting pressure difference created by the stack effect can be evaluated by the following equation:

$$P_{\text{stack}} = \rho_m * g * (z_m - z_i) - \rho_n * g * (z_n - z_i)$$

Where:

ρ_m and ρ_n is the air density in zone m and n, respectively

z_m and z_n are the reference heights in zones m and n, respectively

z_i is the reference height in the zones

Overall Pressure Driving Force and Bernoulli Equation

The sum of wind induced pressures and pressures caused by the stack effect establish the overall pressure driving force which is responsible for air movement inside under the natural ventilation process. The fundamental equation that is necessary to describe air flow in buildings is the so-called Bernoulli equation. This equation is a simpler form of the Navier-Stokes equation and is applicable for steady, incompressible and non-viscous flow. This equation describes the transport effect upon the fluid along a streamline (e.g. air flow path inside the building) in terms of velocity effects, pressure gradient effects and gravity effects.

$$\frac{1}{2} * \rho * v^2 + P + \rho * g * z = \text{constant}$$

The combined velocity, pressure gradient and density effects are set constant as any energy losses are neglected. In a more practical applications energy losses occur along a streamline.

Humidity Effect in Naturally ventilated buildings

Natural ventilation, unlike fan-forced ventilation, uses the natural forces of wind and buoyancy to deliver fresh air into buildings. Fresh air is required in buildings to alleviate odors, to provide oxygen for respiration, and to increase thermal comfort. However, unlike true air-conditioning, natural ventilation is ineffective at reducing the humidity of incoming air. This places a limit on the application of natural ventilation in humid climates.

Design Recommendations for Effective Naturally Ventilated Buildings

Several design recommendation for effective natural ventilation in building design are summarized from various sources. Some of these are presented hereafter:

The specific approach and design of natural ventilation systems will vary based on building type and local climate. However, the amount of ventilation depends critically on the careful design of internal spaces, and the size and placement of openings in the building.

Site selection: Wind-induced ventilation can be maximized by locating the longitudinal axis of the building perpendicular to the prevailing winds. There are various data sets that provide wind

information in regard to wind direction and velocities over extended periods for standard locations such as from the National Oceanographic and Atmospheric Administration (NOAA). The design of naturally ventilated building can however improve by having site specific wind information, such as from local weather stations. The wind regime during the seasons can be quite different so the hottest months should have little obstructions to incident wind. Plants and specifically larger trees or higher hedges can significantly affect the local wind flow.

Cross-ventilation: Wind induced pressure differences on the building can best be used in so called cross ventilation. This means that the building should have effective pathways through the building with large supply and discharge openings. This way the pressure differential across the windward and leeward sides of the building can be effectively used to drive air through the building.

Narrow buildings: Naturally ventilated buildings should have a relatively small width. This recommendation goes hand-in-hand with the need for good connection, which means unobstructed pathways, for wind to transfer the building. Wide building should cause some challenges to distribute outside to all zones in the building using only natural ventilation.

Openings in rooms: In order to use stack effect, each room should have two separate supply and exhaust openings. The exhaust opening should be located at a higher elevation to maximize stack effect.

Provide effective air pathways: Windows should be located across the room and offset from each other to maximize mixing within the room while minimizing the obstructions to airflow within the room. This arrangement avoids dead zones and results in smaller energy losses.

Operable openings: Window and other openings should be operable by the occupants. This allows an effective control of the amount and speed of air movement through the space. Typically, openings should be configured such to allow high flow rates and relatively small pressure differences. However, when stronger winds prevail building occupants should be able to control the flow of air by adjusting the openings. The occupant's involvement in natural ventilation of a building is one of the key elements that increases satisfaction with indoor environmental quality.

Adequate internal airflow: While the primary consideration is the airflow in and out of the building, airflow between the rooms of the building is important. As a measure to ensure privacy, ventilation between spaces can be through high louvers or transoms.

Ventilation through skylights and clerestories: Skylights and clerestories can be used to take advantage of wind induced pressure differences and through stack effect. As wind flows over the roof a lower pressure exists than at the windward side where the stagnation point is located. Warm air, heated by internal loads or through solar gain, rises to the top of the spaces and can effectively vented

through the skylight, or through a clerestory. Figure 1.6 shows an example of the use of clerestory window to maximize natural ventilation.

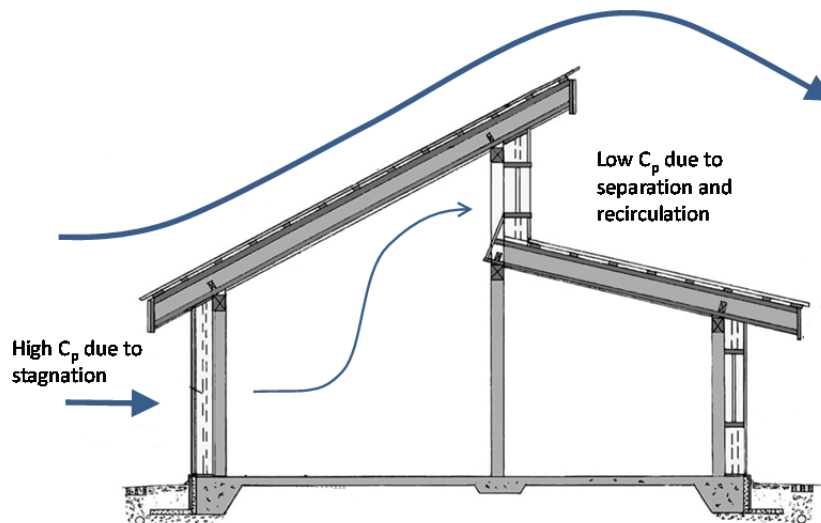
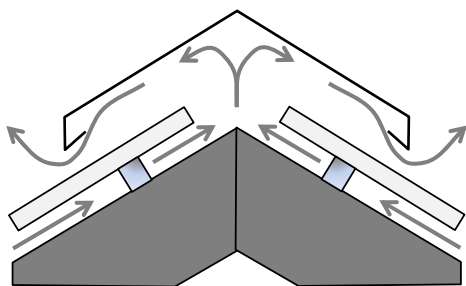


Figure 1.6: clerestory window takes advantage of wind induced pressure and stack effect

Ridge and attic / roof vents: Removing heat from the building through ridge and attic / roof vents can have significant benefits. A ridge vent is located at the highest location of the roof and provides a good outlet for both buoyancy and wind-induced ventilation. (Figure 1.7 (a))The ridge opening needs to be free of obstructions to allow air to freely flow out of the building. An attic or roof vent typically uses a mechanical assist ventilation scheme. The wind turbine in Figure 1.7 (b) is a wind turbine, which is basically a vaned fan which is discharging the roof or attic by using wind power.



(a) Typical ridge vent



(b) Attic and roof vent; wind turbine

Figure 1.7: Typical ridge vent and Attic and roof vent; wind turbine

Fan-assisted ventilation: In mainly cross ventilated buildings natural ventilation can obviously not provide sufficient building ventilation when wind movement provides less than the required pressure differentials to drive air through the building. During these periods of low wind movement whole house fans can contribute to the indoor comfort by removing heat and providing amounts of fresh air. The whole house fans, of course, require electric power to operate but their energy demands are far less than mechanical cooling units.

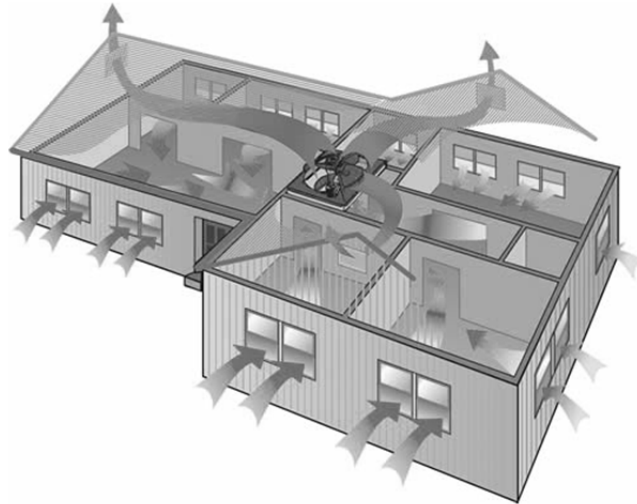


Figure 1.8: A typical whole house fan installation (image obtained from <http://islandcooling.com/wp-content/uploads/whole-house-fan.jpg>)

Open or closed building ventilation approach: A closed ventilation approach is referred to as using night flushing to cool the interior of the building and then close the building during the hot day hours. The best results of the closed ventilation approach is achieved for buildings with massive interior thermal mass and in climates of low night and hot day temperatures. An open-building approach is best applied in warm and humid areas, where the temperature changes are small from day to night. With open-ventilation daytime cross-ventilation is encouraged to maintain indoor temperatures close to outdoor temperatures. In periods of low external wind movement the daytime ventilation can be aided by mechanical assist ventilation.

Using stack effect: Natural ventilated buildings can use open staircases to promote ventilation from stack effect. Other building elements would be atriums or chimneys.

It must be noted that the design recommendations for natural ventilation are only concerned with space ventilation in order to remove heat and provide fresh air. There are also the very important

considerations that naturally ventilated buildings need to ensure building occupant comfort. There are additional measures that increase the comfort in one space over that in another space while the spaces are ventilated in the same way. Such additional measures include ceiling fans which do not increase the amount of air ventilated into or out of the space, but which avoid air stratification and increase the amount of heat transfer from humans to the internal space, of better the human heat rejection. The nature of the increased heat rejection by ceiling fans includes convective, evaporative and radiative effects. The subject of increasing occupant comfort through measures such as ceiling fans or other suitable means will be treated in a later phase of the present research project.

1.2 Distribution of air in internal spaces

The properly distribution of air in the interior of the building is the most important yardstick to gauge the effectiveness of natural ventilation. Different functions of each space in the building, creating effective pathways for interior air movement and openings have to be considered. In the same way the layout and orientation of the building is of importance to create an integrated natural ventilation design strategy.

Therefore optimizing the entire building system, exterior and interior, is more important than only concentrating of individual components. An efficient natural ventilation performance begins with a suitable orientation and siting of the building itself. The topic of external air-movement and the use of CFD in predicting it has been discussed in the project Phase 1 “External CFD” of the present research project. Just as a brief mentioning of the importance of building orientation and siting, Figure 1.9 through 1.12 illustrate examples of building orientation, siting and appurtenances which result in different natural ventilation performances. This means the external building conditions and its surrounding (siting) can significantly affect the effectiveness of internal air movement and therefore effectiveness of the natural ventilation. Figure 1.9 illustrates that an appropriate arrangement of vegetation, here hedges can create a pressure field that is conducive to ventilation. In Figure 1.9 the high pressure is created at the side where the wind stagnates in front of the hedge and low pressure is created in the leeward eddy regions (recirculation zone) of the hedge. When the hedges are arranged symmetrical the same higher pressure field is created which avoid the pressure differential for effective cross ventilation.

1. Basics of Natural Ventilation and Airflow Inside of Buildings

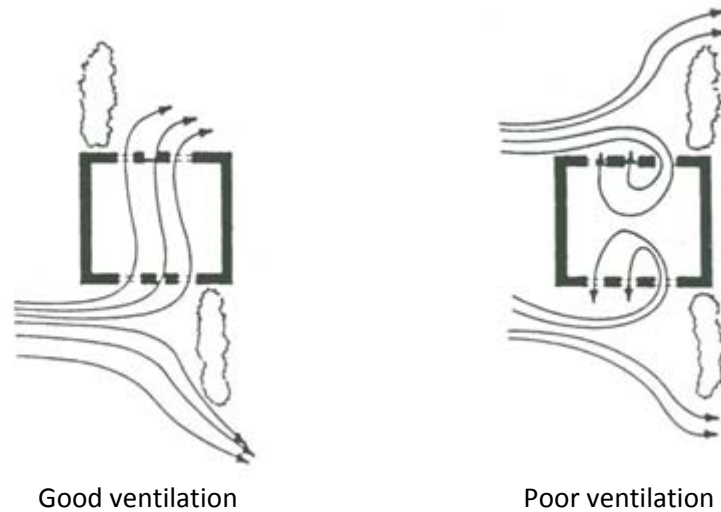


Figure 1.9: The effect of vegetation on pressure field around buildings (Santamouris, 1998)

Figure 1.10 likewise shows the effect of vegetation on the pressure fields and therefore on the wind induced ventilation driving forces. The figure illustrates and describes factors that affect the ventilation effectiveness. Figure 1.11 shows that building orientation and layout have an effect on the ventilation performance. The figure shows areas of low (-) and high (+) pressures which result in pressure differentials that drive air through the building. Figure 1.12 illustrates that windward building configuration can affect the airflow through the building.

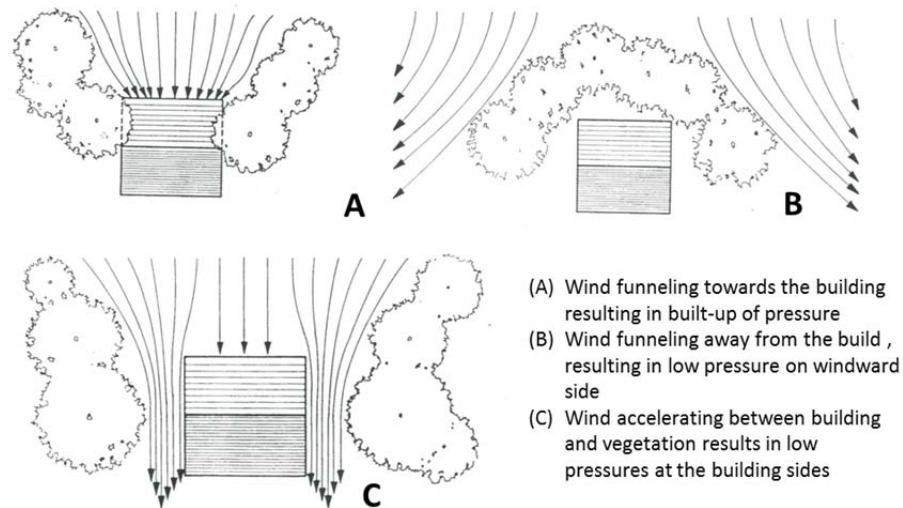


Figure 1.10: The effect of vegetation on pressure field around buildings (Santamouris, 1998)

1. Basics of Natural Ventilation and Airflow Inside of Buildings

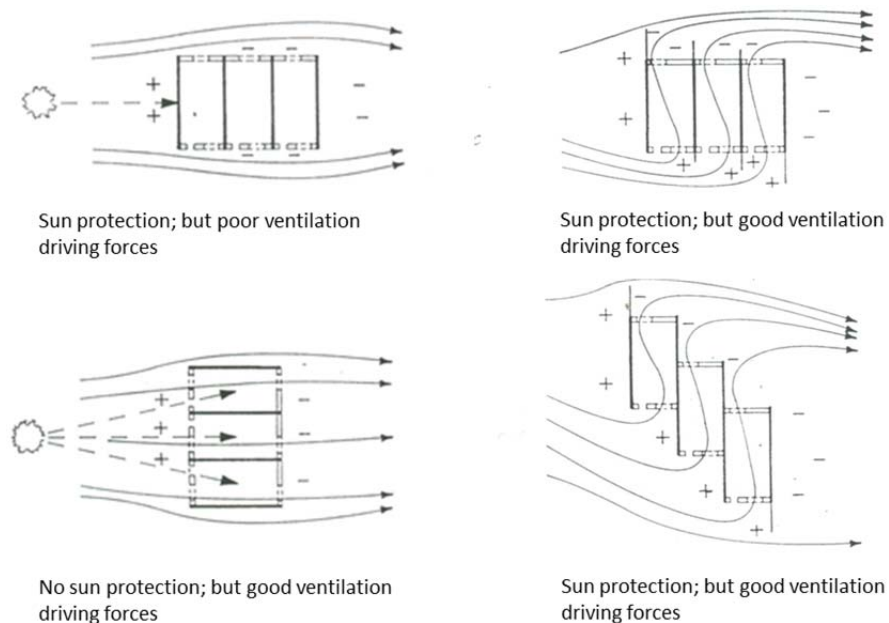


Figure 1.11: The effect of building orientation and appurtenances (Santamouris, 1998)

The external driving forces are important but cannot safeguard good natural ventilation performances on their own. The wind induced external pressure field is a driving force that can only be effective when internal pathways are configured in such a way that decrease pressure, at therefore energy losses.

The horizontal layout should be designed in such a way to maximize effectiveness of cross ventilation. Ventilation through a single opening or at the same side of the building is typically far less effective. Figure 1.12 shows an example of a layout that has good cross ventilation for one particular wind approach direction, while under a different wind approach ventilation is less effective. This example illustrates that building layout needs to allow good ventilation performance for a range of wind directions. In areas where there is a predominant wind direction layout should be optimized for this wind approach while making provisions for secondary wind approach.

In buildings spaces that have potential contaminants or odor, such as bathrooms or kitchen, should be located at the leeward side on the building, preferably with larger windows and providing pathways to the positive pressures on the windward side of the building. In this way, odors are not introduced at the windward side and thus would be carried through the building. Partitions and other flow obstructions, such as large furniture items should be arranged in such a way to still provide good pathways, with a minimum of directional changes to the air streamlines.

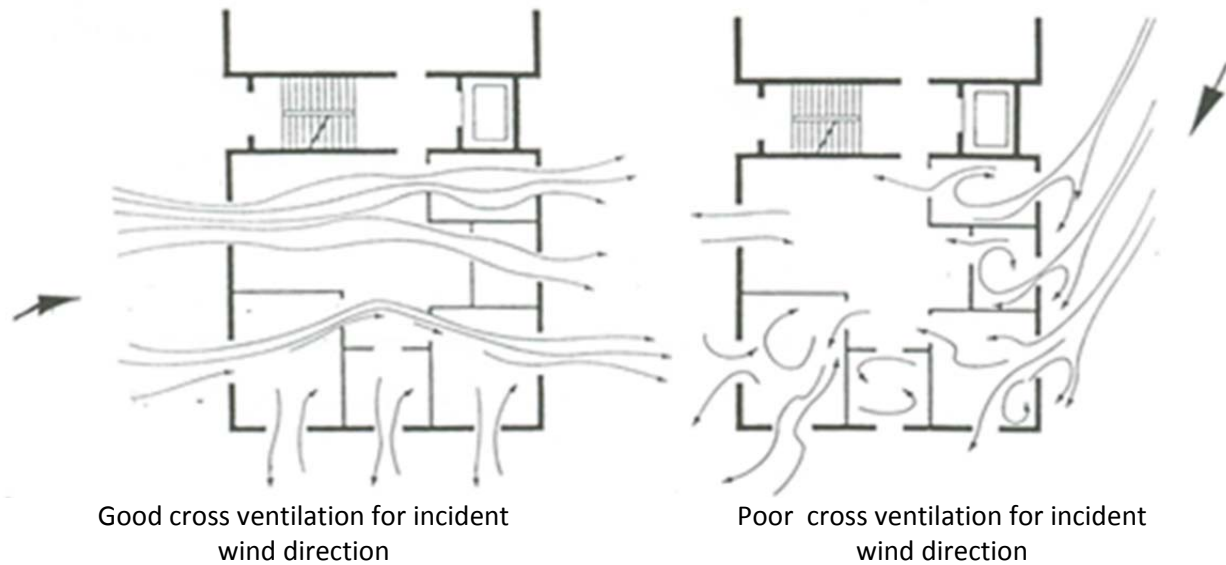


Figure 1.12: Effectiveness of cross ventilation under different wind directions

In office buildings, open spaces should have effective openings on opposite sides, preferable connecting exterior low and high pressure fields. Partitions and cubicle walls should be staggered in order to reduce their resistance to the airflow. Corridors can be used for indirect cross ventilation. In a single-row office layout, the corridor should be placed along the external wall and have large windows. In a two-row office layout, there should be a central corridor which will provide pathways for ventilation air, thereby taking advantage of cross ventilation and pressure differentials. The central corridor can also be used in conjunction with stack effect ventilation.

The vertical layout is primarily affected by stack effect ventilation driving forces. There might be situations where ducting between floors is used to take advantage of cross ventilation pressure differentials but these cases will most likely be few. Since stack effect works best with a large temperature differential space that contain heat sources (such as kitchen or computer rooms) should not be located at higher floors, if possible. In multistory buildings stairways can be used as exhaust-stack ventilation, but provisions have to be made that no warm and stale air enters space at the top floors. In order to enhance the stack effect through wind induced low pressures the opening of the stacks should be positioned to areas of low pressures.

1.3 Mechanical Assist Ventilation

Russell et al (2005) present a comprehensive summary of ventilation technologies. The author's focus is on residential buildings. Then technologies discussed include both mechanical systems and sustainable technologies. The author's treatment of ventilation technologies is very appropriate to consider applications of mechanical ventilation technologies in naturally ventilated buildings. The existing residential housing stock uses infiltration combined with openings in the envelope to provide sufficient ventilation. Residential buildings that use mechanical ventilation and cooling as the only means to condition internal spaces represent a smaller fraction of the existing stock.

Generally speaking, the purpose of ventilation is to provide outdoor air for thermal comfort and to ensure healthy indoor air quality by diluting and discharging contaminants. The author suggested that most of the sometimes resulting in over-ventilation with subsequent energy loss; sometimes resulting in under-ventilation and poor indoor air quality

The authors suggest that a "good ventilation system" should have the following characteristics:

- Provide a controlled amount of unpolluted outdoor air for both comfort and dilution
- Have at least a 15 year life
- Be acceptable to operate by occupants (low noise, low cost)
- Not detract from the safety and durability of the house."

The authors suggest that the type of ventilation discuss in the paper include both mechanical and sustainable technologies. These technologies comprise factors that can be characterized as follows:

- Continuous supply and exhaust systems
- Intermittent supply and exhaust systems
- Combined exhaust and supply (Balanced)
- Infiltration with operable windows
- Passive Stack Ventilation
- Solar Chimney
- Hybrid Systems

Topics treated in the paper (Russell, 2005) which are important for the discussion of naturally ventilated buildings are summarized and their significance to natural ventilation is briefly discussed in the following paragraphs.

Basics of mechanical whole-house ventilation

A variety of mechanical whole-house ventilation approaches are in use used, either individually or in combination. These include exhaust, supply and balanced systems, which operate either continuously or intermittently. These systems may be single-port or multi-port. Differently from natural ventilation, which is prone to intermittent wind action and therefore varying driving force, mechanical ventilation strategies provided more uniform ventilation rates. Thus the great advantage of mechanical ventilation systems over natural ventilation is that the building operator can rely to satisfy mandatory ventilation rates and thereby fulfill code requirements. Mechanical ventilation strategies provided more uniform ventilation rates than natural ventilation. The disadvantage of mechanical ventilation is additional energy required to operate the system and the need to properly maintain. The basic need to always provide a minimum ventilation rate might dictate that mechanical ventilation is added to a natural ventilation system in a building. The great challenge of combining natural and mechanical ventilation systems is that buildings are best designed to operate under either natural or mechanical ventilation modes. Mechanical ventilation systems are typically designed and operated with significantly less pressure differentials than natural ventilation. This results in the design condition that interior ducts and pathways in mechanically ventilated buildings can typically be much smaller than in naturally ventilated buildings.

Exhaust systems

Whole-house exhaust systems provide ventilation by using one or more fans to remove air from the building. As the air is extracted from the building supply air enters the building envelope through gaps (infiltration) or planned opening. When considering infiltration supply air enters the building in an uncontrolled manner and may be pulled in from the outside air or from relatively undesirable areas such as garages or other areas with potential contaminations (i.e. dust). In location with levels of outside environmental contaminants whole -house exhaust systems may not be appropriate. The author points out that in the case of radon gas, researchers have found that exhaust systems may actually increase the indoor levels of contaminants. In moist humid climate zones, exhaust only systems can cause moisture damage to the building structure when moist air enters not well ventilated spaces of when the space is getting in touch with colder surfaces. Since the supply air enters through gaps in the envelope the filtration cannot be reasonably added to an exhaust only ventilation system.

The author suggests that an exhaust system that, if properly installed, can meet current ASHRAE standards for ventilation rates. There are several factors can have a significant effect on whether the installed fan can provide the indicated ventilation rate, such as the tightness of the building envelope, size, quality of ductwork, or placement of ducting). The paper suggests that that from most perspectives exhaust-only mechanical ventilation systems are the most inexpensive of mechanical systems to

operate. The operating costs include mostly energy cost for the fans. Figure 1.13 shows the basic working principle where air is displaced from the building by a mechanical exhaust system and supply air enters the building through infiltration.

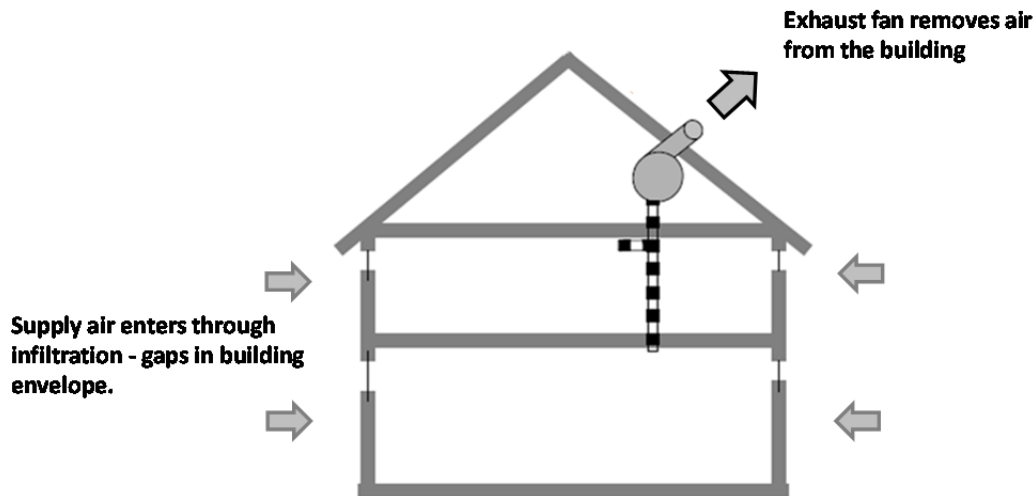


Figure 1.13: Basic mechanical exhaust system where supply air enters through infiltration

Whole-house exhaust system can be built as single-point or multi-point exhaust systems.

A single point exhaust system has the lowest construction and installation costs are the lowest of mechanical systems. The only system components are one fan and possibly some simple ductwork to exhaust the air to the outside. In some cases, the fan can be installed in an exterior wall eliminating the need for extensive ductwork. The disadvantage of single-point ventilation systems is the non-uniform distribution of fresh air especially to closed rooms. The paper points out that in cases where local exhaust depends on kitchen and bathroom fans to provide whole-house ventilation, the results are only marginally better than infiltration alone. The single point systems usually suffers from a poor distribution of supply air where selected rooms received the majority the supply air while other rooms do not receive enough air to meet the applicable ventilation code. The present standards, however, do not require specific distribution.

Multi-point exhaust systems provide better distribution than single-port exhaust systems and therefore they improve room-to-room ventilation uniformity. The disadvantage of multi-point fan systems is the extra cost of installing ductwork between rooms and the central exhaust fan. Reduction of noise levels of the fan can be achieved by installing the fan remotely.

If the building envelope is tight the exhaust system needs to use make-up air inlets. In this case the exhaust fan provides the ventilation driving force but supply air into the building is through dedicated air supply openings. These ventilation openings are also referred to as trickle vents or louvers and they can be located in rooms that need extra ventilation such as the bathroom. Filtration of the supply air is still but the supply air entry point can be controlled to provide cleaner air by installing trickle vents away from polluted areas such as garages, musty basements or dusty attics.

While the exhaust systems discussed so far considers continuous operation, an exhaust system also operates as an intermittent exhaust system.

Often the intermittent exhaust system consists of one central fan to remove stale air from the building, but may also incorporate several fans in areas of high sources (i.e. bathrooms and kitchens). In this case, the fan(s) runs only part of the time at a higher rate and are sized to provide the necessary ventilation. Since the exhaust fans operate not all the time the system has to be designed to handle at a larger capacity than the continuous system. An advantage of intermittent operation is that occupants can reduce or turn off outdoor air supply during periods of the day when the outdoor air quality is poor. Typically energy can be saved and peak loads can be lower to reduce ventilation for certain periods of the day when electricity rates are advantageous.

Providing controls over when the system operates can be simple timers or more sophisticated CO₂ sensors, occupant sensors and humidity sensors. A challenge has been reported by the author if occupants chose to turn off a noisy ventilation fans or override the automatic controls when ventilation would actually be required. The author suggests that that installation and operating costs are similar to the continuous exhaust systems, but may exceed them if sophisticated control systems are installed.

A significant energy saving potential exists when compared to the continuous exhaust system if the intermittent exhaust systems are used in conjunction with natural driving forces to provide adequate ventilation. For example, running the fan at night could reduce cooling costs.

Supply Systems

Supply systems provide pressure to drive outside air into the building. Hereby air is supplied by a central fan ducted to some or all of the rooms. The new air supply forces air in the rooms out of the building through leaks in the envelope. By regulating the ducts supply systems allow the occupant to control the location of the supply air to maximize air quality. Different from exhaust systems filtering the supply air is possible. The author points out that the positive pressure created inside the building by the supply system, which has both advantages and disadvantages. The pressure level that is built up depends on the supply flow and the tightness of the envelope. A positive pressure prevents outside contaminants from entering the building, but it also can force moisture-laden air through the building fabric.

As in the case of the exhaust system the supply system can have either a single point or multiple point supply and can be operated continuously or intermittently. In the single-point supply operation

In Single-point supply strategy, a fan provides outside air through a simple duct to one room of the house, usually the main room. From there air is distributed throughout the building by natural processes. While this system has low costs (only the fan and a small amount of ducting) the system suffers from a poor distribution of supply air, especially to closed rooms in the house. Multi-point systems have the advantage of more uniform distribution and therefore better ventilation performance. However, multiple ducts, and certain cases even multi fans, result in additional installation cost.

The author suggests a combination of exhaust and supply system, which the author refers to as a balanced system, where two fans with separate ducting systems are used. One ducting system supplies outside air and the other remove stale air from the building. A paper published by the Building Science Corporation (BSC, 2010) illustrates the basic operation of a balanced system. Figure 1.14 shows the single-point and multiple-point arrangements of a balance system. As can be seen the balanced system is well suited to install an energy recovery system, where heat energy is recovered. In cooling operation the air that is removed from the building acts as a heat source for the incoming air supply.

This ventilation strategy can be used effectively in any climate. Extensive ducting is used to supply fresh air to living and sleeping rooms, while a separate exhaust system removes stale often moist air from the kitchen and bathrooms. There a several advantages including pre-filtration of the supply air and energy savings from the heat recovery of the exhaust air. Disadvantages are the higher installation and operational cost. Increase noise might also be a problem, but can be mitigated as suggested by references provided in the paper.

Building without forced ventilation systems

Russell et al (2005) points out that most of the applicable codes, such as ASHRAE, do only mention any other way to provided ventilation to new construction. The codes, however, do allow alternative approaches, such as natural ventilation approaches, if they are created by a licensed designer. The basic challenge to natural ventilations approaches is that they might not meet ASHRAE requirements at any given time, due to the intermittent nature of the natural wind driving forces.

1. Basics of Natural Ventilation and Airflow Inside of Buildings

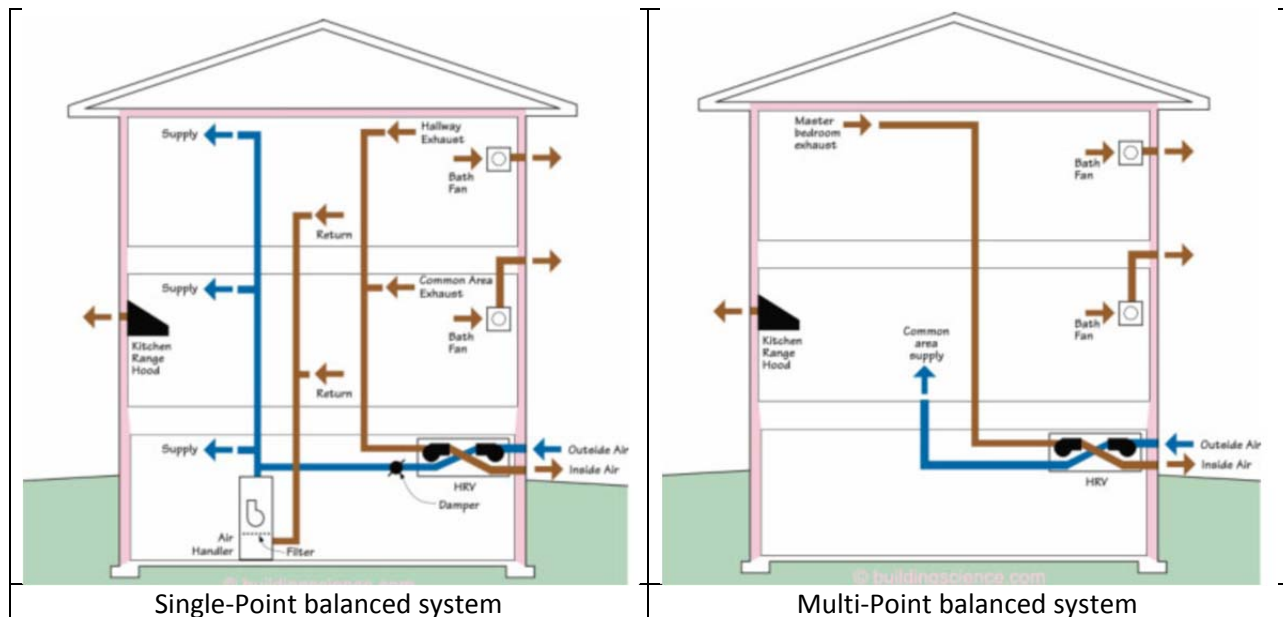


Figure 1.14: Balanced supply and exhaust system with heat recovery (BSC, 2010)

The author suggests that many existing buildings rely on ventilation that is due to infiltration through a porous building envelope for background ventilation and operable windows to provide increased ventilation air when needed. The natural ventilation driving forces are generated by differences in air pressure between the outside and inside of the building that can ventilate a building. Figure 1.15 shows a typical pressure differential between areas of higher (upwind side) and lower (downwind side) pressure. The author points out the intermittent nature of the natural wind driven driving forces. The resulting amount of ventilation is dependent on the placement and number of openings in the building envelope, the internal pathways that the ventilation air takes inside the building and on incident wind direction and speed. This dependency makes the ventilation rate unpredictable and uncontrollable since the driving mechanism is variable over the year and the flow paths are diffused over the building envelope. The author (Russell, 2005) conceded that average ventilation rate over a longer period of time may be predictable. Satisfactory ventilation, however, relies more on the instantaneous ventilation rates or at least on sufficient ventilation rates when required.

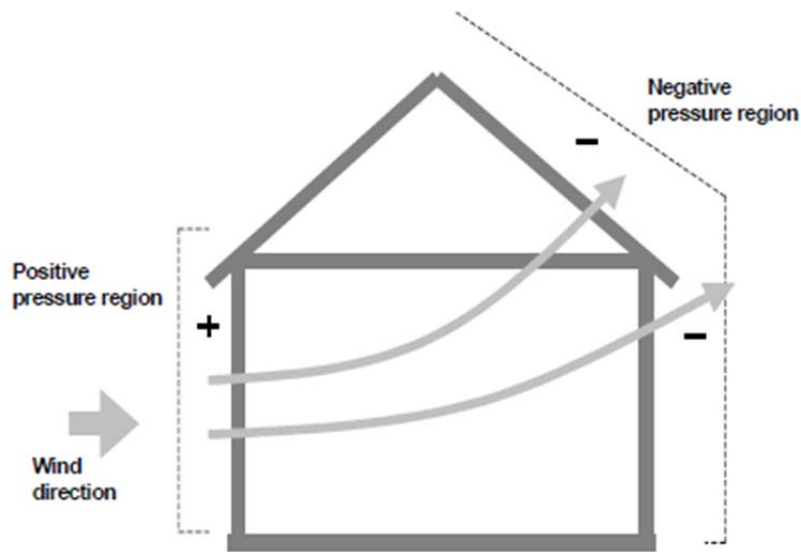


Figure 1.15: Wind induced positive and negative pressure distribution on building envelope (Russell, 2005)

Russell et al (2005) points out that many existing buildings have an annual average air change rate of over one air change an hour due to infiltration; and this high rate can satisfy existing ventilation standards so that many existing buildings do not need any ventilation in addition. Newer buildings might have a tight building envelope and the potential for under-ventilation.

The significant advantage of this basic ventilation system is that there are no extra construction and operating costs. The drawback is the poor control over ventilation rates since a significant indeterminate is the leakiness of the envelope. The basic ventilation mode requires the occupants to open and close windows to provide adequate ventilation when the envelope is tight. During hot summer months the system may under-ventilate since occupants might be tempted to keep the windows closed when there is passive or active cooling. The author suggested that, when climatic conditions are favorable, natural ventilation could be used for cooling and could replace air-conditioning systems.

Since natural ventilation requires an open building there are considerations that have to protect the wellbeing of occupants that are not related to the natural ventilation scheme, such as noise, security, and pollution. Climatic conditions in urban settings, such as the heat island effect, can also impose additional operational limitations. Both the higher temperatures and the decreased wind speeds from adjacent buildings acting as wind obstructions can decrease the potential of natural ventilation systems. Russell et al (2005) points out that through obstructions in densely developed areas wind air flow

through the buildings decreased up to 90 %. Noise abatement can reduce external noise levels (such as traffic noise) somewhat.

The author (Russell, 2005) points out that many researchers have investigated the suitability of various climatic conditions. It was found that of natural ventilation depends not only of the outdoor climate, but also the building site and the design of the building site. While some regions have too harsh climates are for infiltration as a primary source of ventilation there are other climates where the driving forces are too weak for infiltration to be a practical source of primary ventilation. The author suggested that natural ventilation cannot be ruled in or out but has to be appraised on a case by case basis.

Building ventilation through natural driving forces and infiltration depends on many factors so there is no “right” amount of air leakage. Natural ventilation and infiltration will always provide more ventilation than is needed during extreme periods. The design ventilation openings and pathways of the building are always chose in such a way to meet average demands; overdesign is therefore almost unavoidable.

Measures to assist in natural ventilation

Passive stack ventilation can increase and control ventilation rates better than natural ventilation alone. Under this ventilation scheme one or more stacks or towers extract stale air from the building while fresh air enters through provided openings such as trickle vents or louvers. Passive stack air flows use two different naturally occurring driving forces for ventilation. These are wind induced pressures on the building envelope and the stack effect, e.g. differences between the inside and outside temperature that result in a buoyancy effect. The negative pressure at the stack top is often the critical factor. Figure 1.16 illustrates a passive stack ventilation approach.

The author (Russell, 2005) suggests that most of the passive stack ventilation systems are found outside of the US. Stack height and position are important in maintaining a negative pressure at the stack terminus and preventing back flows into the building. A taller stack is less sensitive to wind speed and wind direction. Stacks need to have a larger diameter than mechanical ducting systems would require because usually lower pressure differences prevail and low pressure drop conditions must be maintained.

This form of ventilation can result in significantly varying flow rates from room to room. This is due to the fact that the natural driving forces in the different locations in the building vary. For example, upper and leeward rooms, in particular, may be under ventilated and can easily have no outdoor air. The author stresses that careful design needs to consider measures to control and distribute air flow rates. In regard to operable openings such as trickle vents or louvers can be adjusted to control the flow rate. This of course requires that building envelope is tight to keep uncontrolled infiltration rates are low. The author suggests that it is advantageous that each room has a vent to allow free distribution of the air.

Most of the air distribution measures are relevant for both natural and mechanical ventilation, but these measures are more critical for passive ventilation because of the lower driving forces.

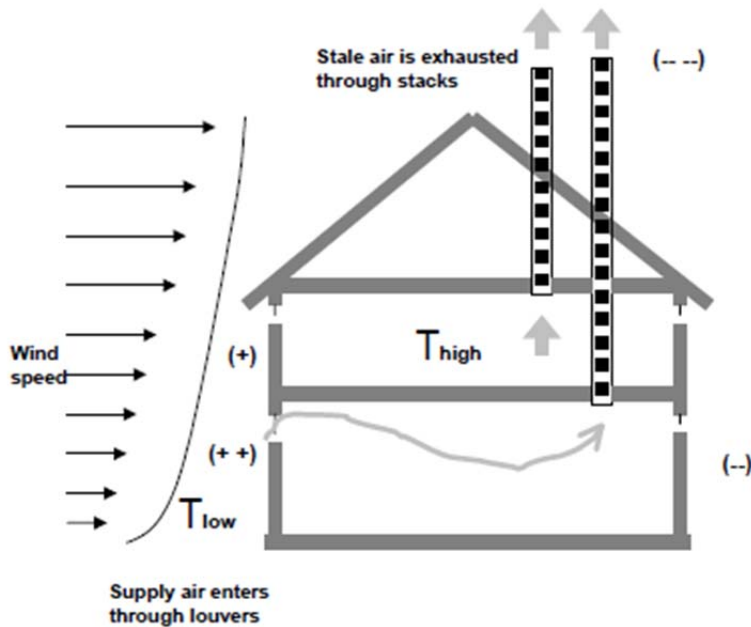


Figure 1.16: Passive stack ventilation uses wind induced pressures and buoyancy forces. (Russell, 2005)

The author (Russell, 2005) cites cases passive ventilation systems have shown the capability of providing adequate long term ventilation, but fall short to provide short term high ventilation when it was required. Most distribution systems are built similar to mechanical systems, but without mechanical components, therefore mechanical equipment costs and operational costs are saved. The author cites some basic design recommendations:

- Provide interior design to allow effective pathways to allow air to flow between the rooms of the building
- Effective location of supply openings
- Larger air distribution ducts are required because of the need to lower flow resistance
- Usually there are some days of the year when weather conditions (low wind speed and/or small indoor/outdoor temperature differences) create insufficient airflow, even with larger air

distribution ducts. At these times proper ventilation may only be attained if the occupant opens a window or otherwise supplements the system.

- Depending in the natural ventilation driving forces under ventilation or over ventilation can be expected at certain times of the year.
- Self-regulating vents are available that can reduce or control over-ventilation. Pressure sensitive ventilators are available that can provide constant ventilation rates over a wide range of pressures
- Passive systems fall short when compared to mechanical systems in the areas of filtration and heat recovery.

Solar chimney is an approach to increase the effectiveness of passive stack system. In solar chimneys, solar heat is added to increase the stack effect and thereby ventilation rates can be increased. Adding of heat can be achieved by effective measures, such as glazed walls on the sun exposed side if the building). The author (Russell, 2005) reports of up the 20% increments in effectiveness of solar chimney over conventional passive stack ventilation. Advantages of this system include increase in reliability of the passive stack system and silent operation. Disadvantages include extra design, installation and cost of the solar glazed panels. Solar chimneys are most appropriate for a sunny, warm climate, such as Hawaii.

Adding fans to stacks can increase ventilation flow through the stacks or vents thereby combining the advantages of a passive system with the reliability of a mechanical system. When fitted with an intelligent control systems these hybrid systems can improve indoor air quality while reducing energy demand through an intelligent controller. A design challenge is given since ducts of passive and active ventilation approaches are performing quite different. The author (Russell, 2005) suggests the following design strategies:

- Provide two independent systems, one passive and one active, linked by a controller to switch from one to the other.
- Fan-assisted natural ventilation where the main ventilation is provided by natural forces, but a low power fan can be switched on to assist ventilation during periods of weak natural forces.
- Include a small fan in a passive stack system to assist in creating optimal pressure differences in the stack.
- Using dampers (energy dissipation) to prevent over ventilation when temperature differences were large
- Use of sophisticated control systems such as CO₂ sensors, room temperature, air flow sensors, motorized windows and even a weather station to activate fans assist ventilation.

Infiltration of air through the building envelope can have a detrimental effect on ventilation effectiveness regardless of the ventilation system, because of the intermittent and weather dependent

nature of the driving forces. For example, balanced ventilation systems may suffer a reduction in performance when air by-passes the heat recovery unit. The amount of infiltration will depend on the air tightness of the building, the difference in indoor and outdoor temperatures, and the wind pressure. A tight building envelope will provide very little ventilation from infiltration and will require a provided ventilation system. Infiltration rates need to be taken into consideration when selecting the ventilation approach.

Operable Windows are required in most buildings, but are required in all buildings that rely on natural ventilation. Occupants are more likely to feel comfortable when they have control over the ventilation system and windows provide a familiar system of ventilation. The author (Russell, 2005) suggests that windows can provide the ventilation rates necessary to meet current codes, if they are use on a daily basis. Window operation is caused by occupant behavior. Conditions under which the windows are typically opened include sunny days, higher occupant density, higher outdoor temperature, low wind speed, and during cleaning or cooking activities. Circumstance may rule out opening windows such as noise, rain or high winds, outdoor pollutants, cold drafts, privacy, security and safety issues, energy loss, or the window may be difficult to operate. Therefore the author concluded that window opening or closing is not always in response to ventilation needs.

Local exhaust fans can mitigate ventilation problems in special rooms, such as kitchens and bathrooms, laundries, utility rooms and lavatories. These local exhausts fans are installed to remove contaminants while they are still concentrated. Therefore they can be regarded as source control measure rather than ventilation in the normal sense. By creating driving forces for building ventilation these exhaust system can add to incidental ventilation, such as powerful kitchen exhaust fans. Due to the intermittent nature of these exhaust fans they cannot be considered towards meeting minimum ventilation requirements. Exceptions exist such as a “double duty” bath fan, where a continuously operating local exhaust fan simultaneously meets the need for local exhaust and also whole-house ventilation.

Energy and Costs

Whenever mechanical ventilation is used energy is required to move the air and to condition the supply air. The energy for only mechanical ventilation, without air conditioning, can account for as much as one third to one half of the total space conditioning (Russell, 2005). In addition, mechanical ventilation requires investment into designing and installing the equipment. Building improvement measures conserve energy while still providing healthy ventilation rates. These measures can include avoiding unnecessary air changes (due to leaky buildings), using good control strategies (not opening windows during periods of heating and cooling), and optimizing fan and equipment efficiencies.

Mechanical ventilation systems can save energy used to condition supply air if the building envelope is tight and infiltration is limited. Energy consumption can be reduced 9 to 21% by installing a mechanical ventilation system with heat recovery (Russell, 2005). A mechanical exhaust system is most likely the least expensive to operate, while multi point recovery ventilation system would be the most expensive to purchase and install. Retrofitting an existing house is more expensive than new construction and multi-point distribution systems are more expensive than a single point system

1.4 Ventilation Opening

Santamouris, Mat, et al (1998) provide recommendations for position and size of openings. Some of these are given below:

- Outlet openings should be equal or larger than the inlet openings in order to avoid excessive air velocities
- For occupant cooling openings should be placed at occupant height, whereas for structural cooling (e.g. night flushing) openings should be placed at height of larger thermal masses, i.e. brick walls. (See Figure 1.17)
- In order to maximize stack effect inlet opening should be located lower than the outlet opening.
- In single-sided ventilation more than one opening is required to increase ventilation performance. The openings should be placed as far apart as possible and measures to change the external pressure regime through envelope appurtenances can create better ventilation performance.

Figure 1.17 (b) illustrates a preferred air flow for structural cooling. In this case an internal thermal mass is cooled down by passing colder air over it during times of colder external temperatures, typically at night. When the thermal mass is in the concrete ceiling, a suspended ceiling cannot be used. Similarly elevated floors can also not be used. Structural cooling of the ceiling work typically better, since hot air rises and heats up the ceiling through convection.



- | | |
|--|--|
| (a) Optimum position of
opening for body
cooling | (b) Optimum position of
opening for structural
cooling |
|--|--|

Figure 1.17: Preferred positions of opening for cooling of occupants and structure (Santamouris, 1998)

Santamouris, Mat, et al (1998) provides four categories of building envelope openings that are of importance to natural ventilation:

Windows: Different types of windows can be categorized according to:

- Plane of placement (e.g. vertical, non-vertical, horizontal, tilted)
- Position of window in the building envelope
- Opening systems (swinging, pivoting)

Screens: Can serve as ventilation as well as shading device.

Doors: Provide interconnections between the exterior and interior and between interior spaces.

Vents and ventilator: Function as means to enhance and direct air movement

The following describes important functions of the four categories of opening in regard to ventilation effectiveness.

Windows: Windows are important air flow control devices. Their effectiveness depends on the size and also on type, or the way they are opening. There are three basic types of windows, single openings window, vertical-vane window and horizontal vane window. Windows are usually installed in walls but some types can also be installed in roofs, such as skylights or horizontal pane windows. The air flow patterns generated by the different windows during their operation significantly affect the effectiveness of natural ventilation. The literature reports on a wide range of air flow patterns. The following general observations of air flow pattern are given:

Simple opening typically do not affect the velocity and direction of the air flow except near the opening.

Vertical vane window exert a wide variety of influence on both pattern and velocity of the airflow. The most common type, the side-hinged casement window, has a great versatility with regard to airflow control.

Horizontal vane windows typically affect the velocity and direction of the air flow mainly in the vertical direction. Projected sash and other horizontal-pivot windows direct the airflow upward. Jalousie windows have the possibility to direct the airflow in either direction according to the position of the sashes.

Figure 1.18, 1.19 and 1.20 show different types of windows.

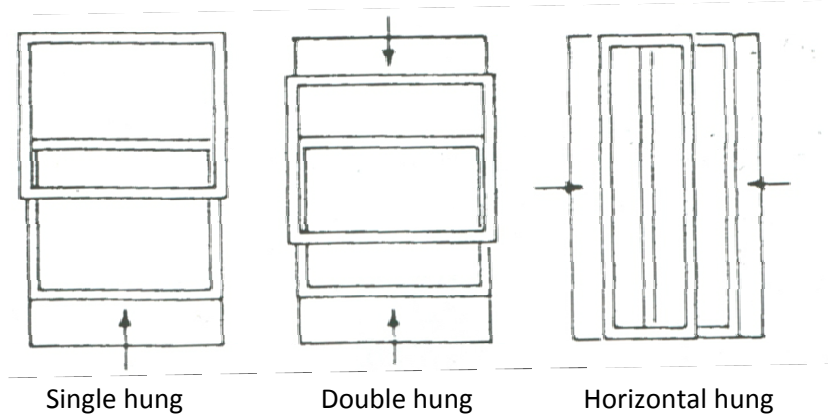


Figure 1.18: Simple opening windows (Santamouris, 1998)

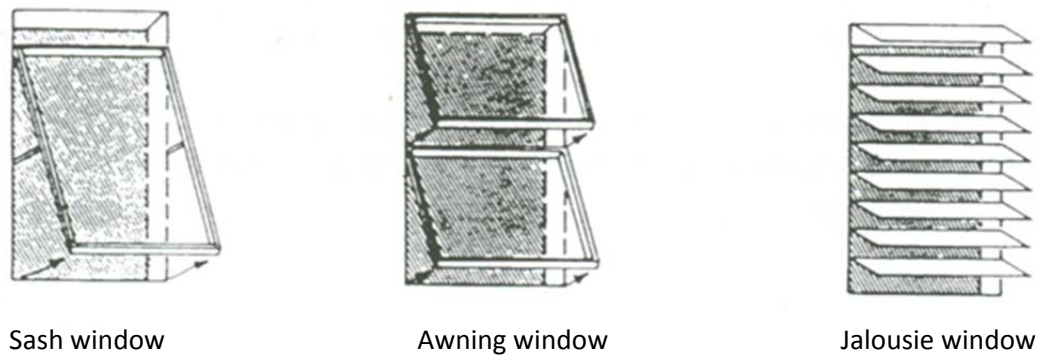
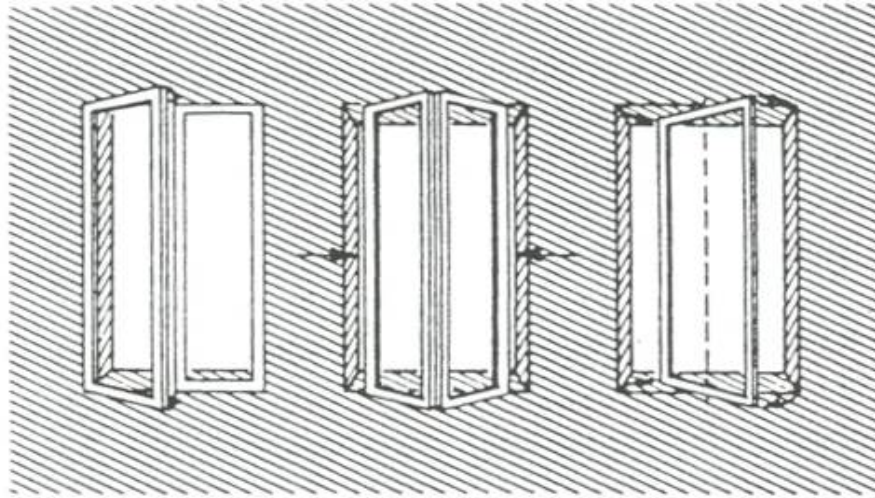


Figure 1.19: Typical horizontal vane windows (Santamouris, 1998)



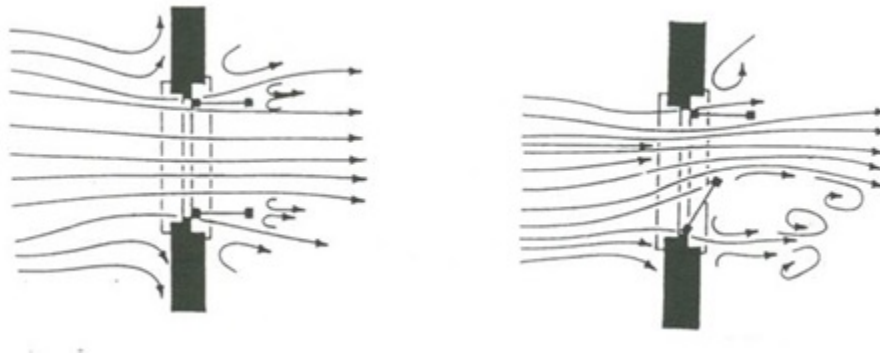
Side-hinged casement

Folding casement

Vertical pivot

Figure 1.20: Typical vertical vane windows (Santamouris, 1998)

The airflow differs significantly between types of windows. As an example of the effects of airflow by windows a fully and partially open vertical vane window is shown in Figure 1.21. While the fully open window allows air to enter relatively uniform over the cross-section of the window, the partially open window generates significant eddies and is deflecting the direction of the airflow.



Fully open in swinging double casement window

Partially open in swinging double casement window

Figure 1.21: Example of effect on airflow from different types of windows; Plan view (Santamouris, 1998)

Screens: Screens can be categorized as either fixed or operable screens. Fixed screens are usually externally fixed screens and function for shading, security or insect deterrent. Operable screens are either exterior or interior screens.

- Fixed exterior screens (i.e. insect screen, safety grilles, etc.) are reducing the approaching airflow in a uniform way over the entire surface, without changing the direction of the airflow.
- Operable exterior screens (i.e. rolling blinds, awning frame, sliding sash shutter, etc.) typically, if slow the airflow as it passes through the screens and they also change the airflow direction. Awning-frame rolling blinds have the best performance as they integrate good shading with good airflow performance.
- Operable interior screens (i.e. vertically and horizontally operating curtains, louvers, etc.) have less airflow deflection and more wind energy absorption, owing to their relative lightness and softness.

As an example of airflow performance Figure 1.22 shows the airflow patterns through a vertical-vane and an awning-frame rolling blind. The figure illustrates that airflow through the awning blind is significantly better

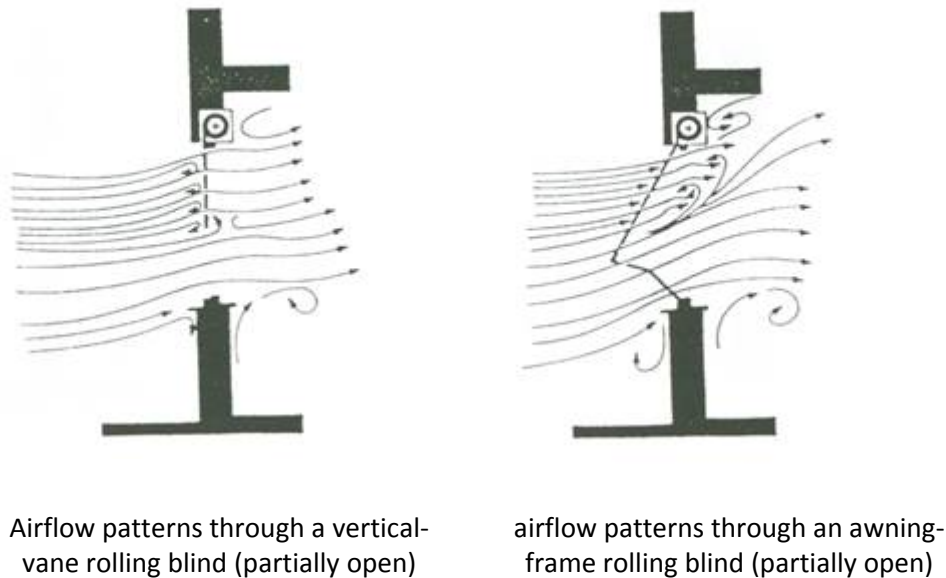


Figure 1.22: Typical airflow pattern through two type of external fixed screen (Santamouris, 1998)

Doors: Doors are normally not used as dedicated airflow control device in the same manner as windows are. The function of doors is significantly different than windows and normally doors remain closed, except maybe doors of businesses which have a considerable number of customers passing through them. Exterior doors can be effectively used as ventilation openings if the door is equipped to let air through but not insects or intruders. Figure 1.23 shows the airflow pattern through an open exterior door that is fitted with a screen. It can be seen that the airflow is effective. The screen slows down the airflow but does not change the flow direction. Many exterior doors cannot be left open without automatic shut controls, because of code requirements such as fire-safety doors. If doors should be used as a ventilation opening an operational schedule has to be considered.

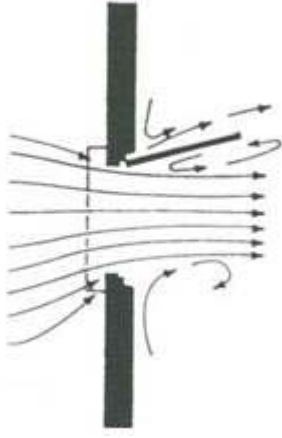


Figure 1.23: Airflow pattern through an open door with exterior screen.

Vents: Vents can be distinguished in non-mechanical and mechanical openings.

1.5 Pressure Losses of Building Openings and Airflow Obstructions

The knowledge of pressure losses of exterior and interior opening and passageways is an important design factor for naturally ventilated buildings. The exterior pressure distribution around the building acts as the driving force for the airflow through the interior spaces. With the same exterior pressure differentials between sections of the envelope the pathway with the least pressure losses, or flow resistance, will have the higher airflows through the space.

Hulk et al (Hulk, 2009) suggests that in passively ventilated spaces, key design considerations are the number and size of the vents as well as the resistance to flow along the flow path. Factors that act to reduce flow through the space such as friction and flow contraction are most significant where the cross-sectional area open to the flow is smallest. It is standard practice in airflow calculations to model the effects of friction and flow contraction through large openings using a so-called discharge coefficient. The discharge coefficient is the ratio of the actual flow to the ideal flow.

$$Q = C_d A \sqrt{\frac{2\Delta P}{\rho}},$$

Where, Q is the flow rate through the opening, A is the area of the opening, DP is the pressure difference across the opening and r is the fluid density.

Hulk et al (Hulk, 2009) determined the discharge coefficient for pivoted windows as a function of window angle and aspect ratio. The cooling and ventilation capacity due to wind and buoyancy driven flows is strongly dependent on the window discharge coefficient, so the accuracy of the coefficient can have a substantial impact on the ability of a model to predict performance. CFD simulations were used and validation was done through wind tunnel tests. The author concluded that CFD results and data from validation measurement agree well.

Figure 1.24 shows the results of the improved discharged coefficient pivoted windows. The graph shows the original (---) and modified (—) EnergyPlus parameterizations, the different markers represent validation tests. As can be seen the modified discharge coefficients are significantly larger than the original. The author concluded that current pivoted window parameterization used in airflow network models such as EnergyPlus may underestimate the cooling capacity for passive ventilation by up to 50%. These results illustrate that accurate discharge coefficients are instrumental for a reliable prediction of airflow through openings. The paper also suggests that CFD simulations are a reliable tool to predict discharge coefficients.

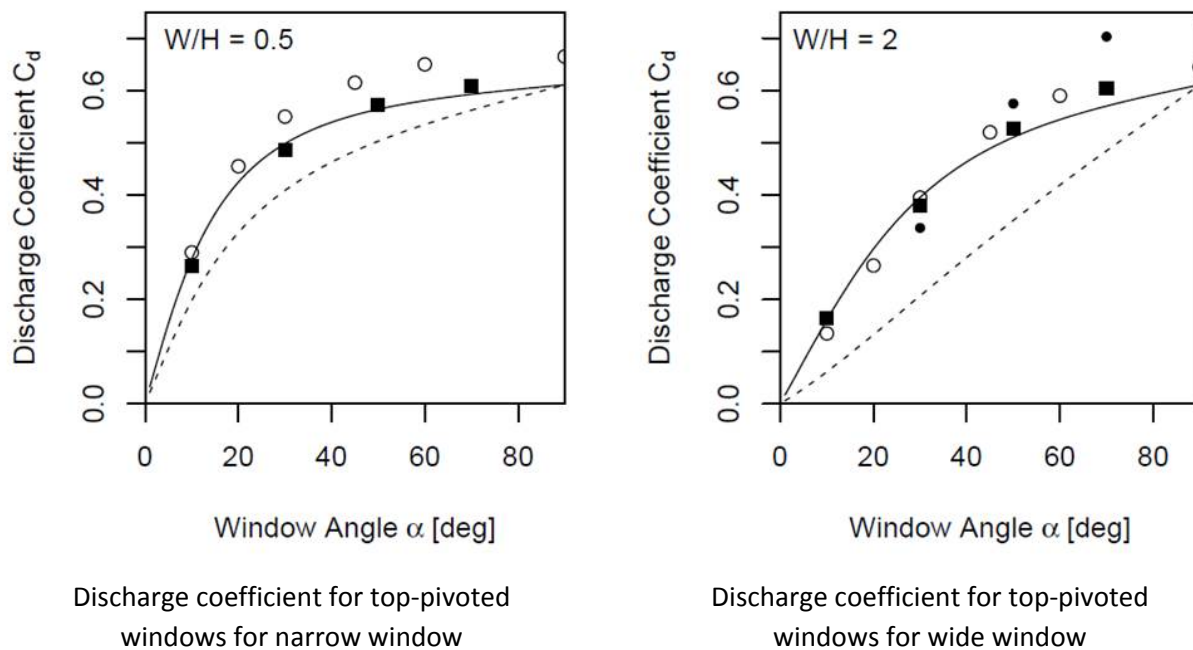


Figure 1.24: Discharge coefficient for top-pivoted windows; depiction of original (---) and modified (—) EnergyPlus parameterizations (Hulk, 2009).

The discharge coefficient is affected by the inlet configuration of the opening. An example of the effect if inlet configuration on orifices of the same diameter is illustrated in Figure 1.25 (SFTG, 2007).

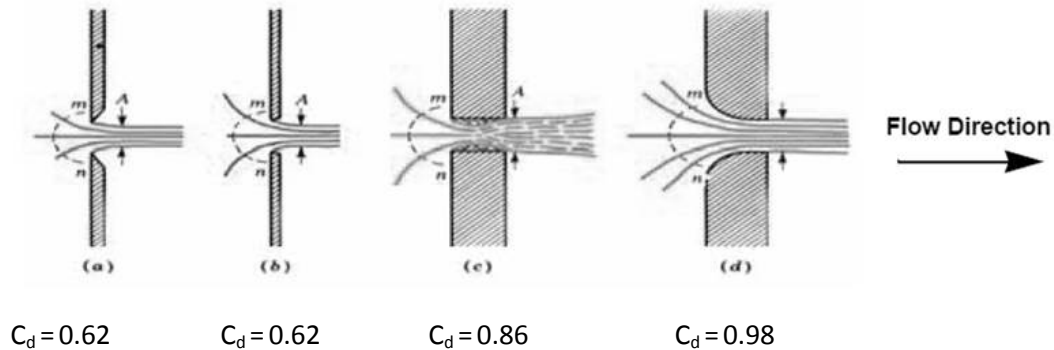


Figure 1.25: Discharge coefficients for orifices (noted as C_d) with the same diameter but with different inlet geometries (SFTG, 2007).

In predicting air flow through a building the Bernoulli Equations can be used (as discussed earlier in this report). The airflow problem can thus be reduced to the hydrodynamic properties along an air pathway, or streamline. The air density related part of the equation, and therefore a change in overall energy of the air particle due to an elevation change along the pathway, is negligible in comparison with the pressure and kinetic energy parts. Therefore the Bernoulli equation for air has two significant parts, the static pressure and the kinetic pressure. The energy along the streamline is therefore described by the static and dynamic pressures and the viscous losses are considered as a multiple of the dynamic pressure.

An example of the relationship between static and dynamic pressures in airflow inside an air duct is illustrated by the pressure curve depicted in Figure 1.26.

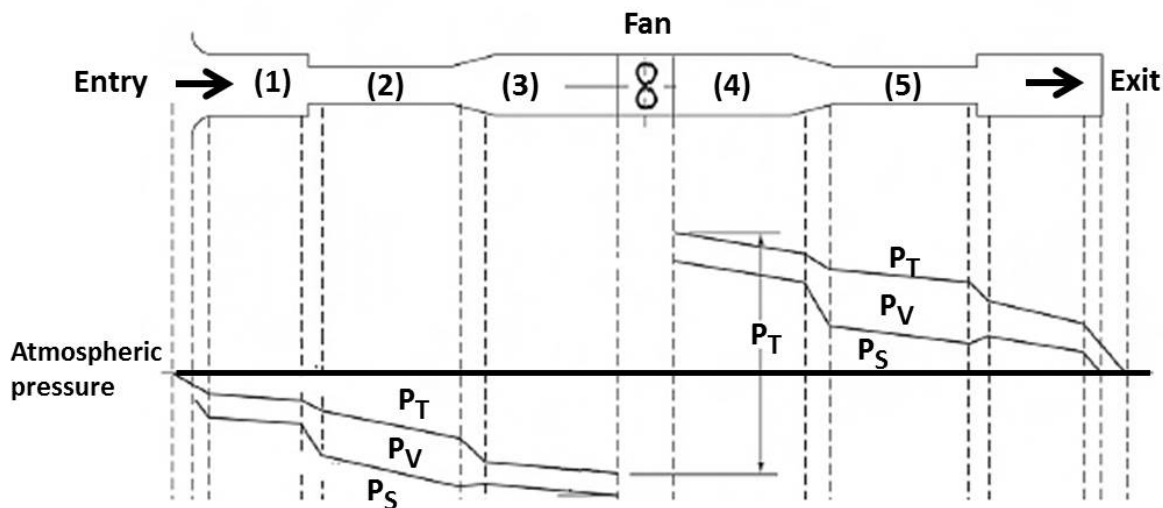


Figure 1.26: Pressure distribution and losses in an air conveyance systems (Lstiburek, 2000; modified)

Figure 1.26 illustrates the pressure distribution along the streamline starting in the example conveyance (duct) systems. The notations are as follows: P_S is the static pressure at that point on the streamline, P_V is the velocity pressure (often also referred to as the dynamic pressure) and P_T is the sum, of the P_S and P_V . The pressure at the entry of the duct is the atmospheric pressure, the air velocity at this point is considered as zero and therefore the velocity pressure is zero. As the air enters the duct the velocity increases which means that P_V increases and the P_S decreases. The pressure loss between entry and Point (1) is a major loss due to air friction at the duct walls and energy losses due to turbulences in the duct. Point (1) on the streamline is a sudden contraction where a pressure, or energy loss, occurs. P_V in segment (2) is larger than in the first segment since the cross-sectional area is smaller and therefore the velocity larger. At point (3), an expansion occurs resulting in another pressure loss. The fan provides a pressure increase by exerting mechanical work in the airflow. Downstream of the fan pressure losses occur. At the exit the pressure is again equal the atmospheric pressure.

This simple example of pressure losses along a streamline illustrate that in order to calculate the air flow the pressure losses along the streamline have to be known. We can apply this simple procedure of airflow through a bounded conveyance system to the pressure situation inside the building an air flows from the higher pressure entry to the lower pressure exit. In the case of the airflow through the building the pressure losses P_T through the building have to be the same as the available pressure differential between upwind and downwind locations of the building envelope.

Generic values for pressure losses of typical building openings is still not as readily available as pressure losses in conventional HVAC systems. However, the physical principles and calculation procedures of these two fields of interest are similar same. Some of the pressure losses of building can be approximated from known pressure losses in HVAC systems.

The following pages present pressure losses estimates for various openings or air conveyance components. Major losses are defines as pressure losses due to resistance along the conveyance system, or streamline. Minor losses are pressure losses at locations of flow disturbances. Both minor and major losses are defines either as absolute pressures, in inch Ws or Pascal, or as coefficients of the velocity pressure P_v , as a dimensionless number.

Figure 1.27 shows the major losses of air flow inside an air duct system. The friction losses are defined as pressure losses per length of duct. Pressure losses are smaller with smaller air velocities. While the functions depicted in Figure 1.27 are obtained from airflow test in ducts it is possible to obtain similar relationships between air velocities and pressure losses in internal pathways.

Figure 1.28 shows a tabulated relationship that determines the minor pressure losses based on air velocity and minor loss coefficients. The minor loss coefficient, listed as the in the abscissa in Figure 5, represents the minor loss coefficient of either one airflow resistance or the overall resistances of the conveyance system (such as illustrated in the example in Figure 1.26. In order to obtain the sum of all minor losses to airflow each airflow resistance, such as bends, contractions, expansions, valves, inlet and outlet structures, are determines and then summarized.

Figure 1.29 shows the procedure of determining the minor losses for a bend in the duct. The round bend, or a segmented bend as an approximation, results in significantly lower pressure losses than a sharp bend. Figure 1.30 shows minor loss coefficients for inlets and outlets. As evident, airflow conduits that result in less directional changes and abrupt acceleration of the airstream create lower pressure losses. Figures

Figures 1.31 and 1.32 present tabulated values for different components of duct systems either minor losses (as dimensionless coefficients) or minor pressure losses (in dimensions of pressure).

1. Basics of Natural Ventilation and Airflow Inside of Buildings

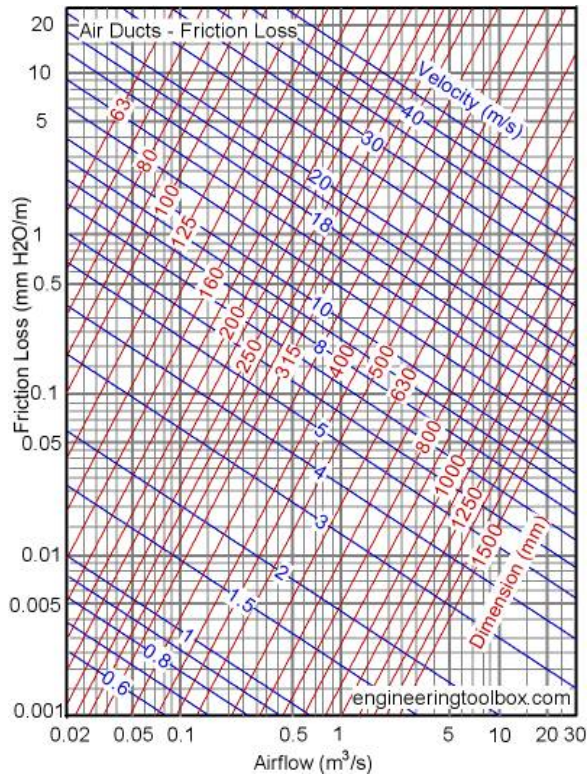


Figure 1.27: Major pressure losses in an air duct (engineeringtoolbox.com)

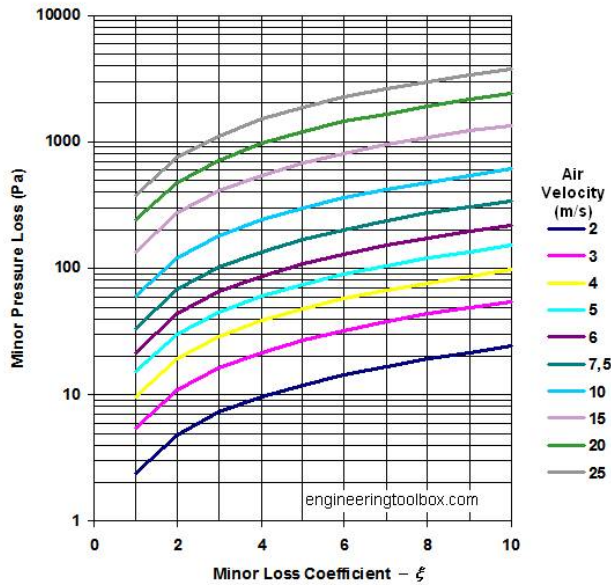


Figure 1.28: Conversion of minor losses to minor pressure loss (engineeringtoolbox.com)

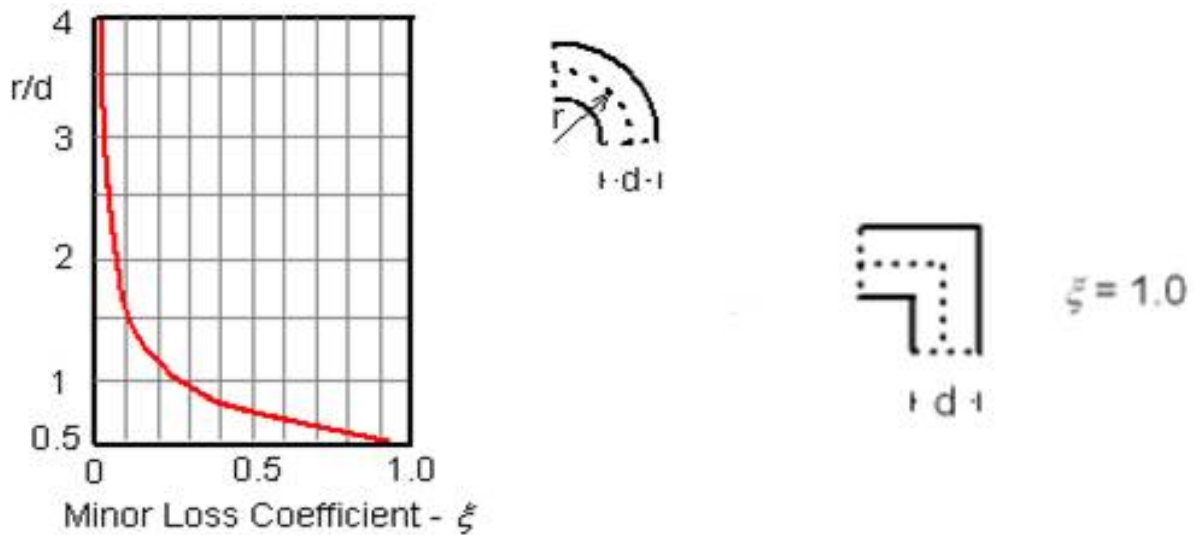


Figure 1.29: Minor loss assessment for rounded and sharp bend in duct (engineeringtoolbox.com)

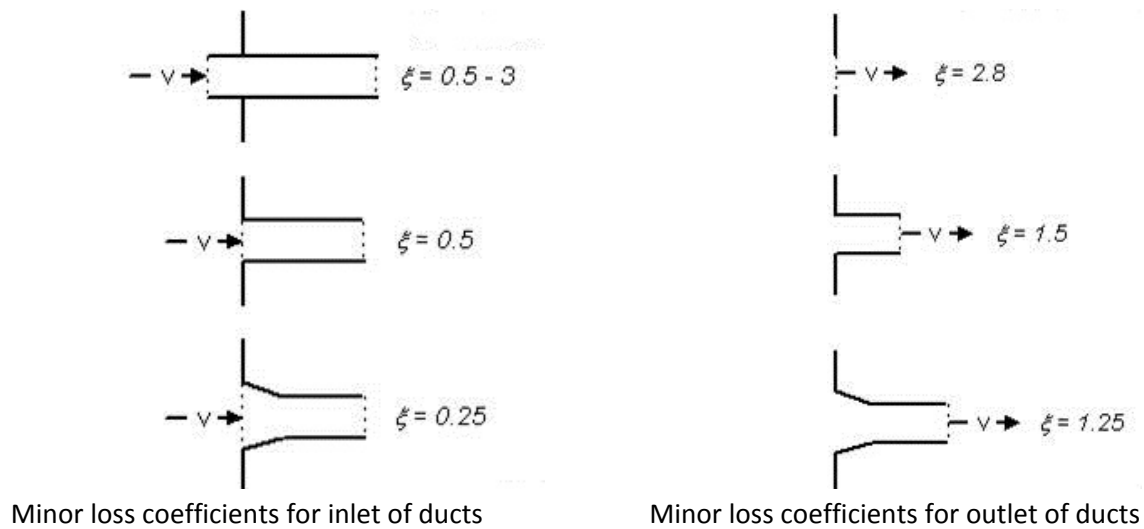


Figure 1.30: Minor loss coefficients for different inlet and outlet configurations (engineeringtoolbox.com)

1. Basics of Natural Ventilation and Airflow Inside of Buildings

Component or Fitting	Minor Loss Coefficient - ξ -
90° bend, sharp	1.3
90° bend, with vanes	0.7
90° bend, rounded radius/diameter duct <1	0.5
90° bend, rounded radius/diameter duct >1	0.25
45° bend, sharp	0.5
45° bend, rounded radius/diameter duct <1	0.2
45° bend, rounded radius/diameter duct >1	0.05
T, flow to branch (applied to velocity in branch)	0.3
Flow from duct to room	1.0
Flow from room to duct	0.35
Reduction, tapered	0
Enlargement, abrupt (due to speed before reduction) (v_1 = velocity before enlargement and v_2 = velocity after enlargement)	$(1 - v_2 / v_1)^2$
Enlargement, tapered angle < 8° (due to speed before reduction) (v_1 = velocity before enlargement and v_2 = velocity after enlargement)	$0.15 (1 - v_2 / v_1)^2$
Enlargement, tapered angle > 8° (due to speed before reduction) (v_1 = velocity before enlargement and v_2 = velocity after enlargement)	$(1 - v_2 / v_1)^2$
Grilles, 0.7 ratio free area to total surface	3
Grilles, 0.6 ratio free area to total surface	4
Grilles, 0.5 ratio free area to total surface	6
Grilles, 0.4 ratio free area to total surface	10
Grilles, 0.3 ratio free area to total surface	20
Grilles, 0.2 ratio free area to total surface	50

Figure 1.31: Minor loss coefficients for different components and fittings of a duct system
(engineeringtoolbox.com)

1. Basics of Natural Ventilation and Airflow Inside of Buildings

Component Type		Pressure Drop (Pa)				
		Air Velocity (m/s)				
		2.0	2.25	2.5	2.75	3.0
Intake damper		5	5	5	5	5
Mixing chamber	straight	35	45	55	70	85
	90°	40	55	70	85	100
Filter	short EU2	70	75	80	90	95
	short EU3	100	110	120	135	145
	long EU3	70	75	80	80	85
	long EU5	115	125	140	150	165
	long EU7	140	150	165	175	185
	long EU9	160	175	190	210	230
Heater	water, size 1	5	5	10	10	10
	water, size 2	10	15	15	20	20
	water, size 3	20	25	30	30	35
	electrical, size 1	10	10	15	15	20
	electrical, size 2	15	20	30	35	40
	electrical, size 3	35	45	55	70	85
Cooler	size 1	20	25	30	35	40
	size 2	25	35	40	45	55
	size 3	35	45	50	60	70
	drop separator				45	50
Humidifier	60%	50	60	75	90	110
	90%	75	100	120	160	180
Noise damper	750 mm	5	10	10	15	15
	1425 mm	10	15	15	20	25
Rotating heat exchanger	big rotor	120	140	160	180	195
	little rotor	150	170	195	220	245
Air-fluid-air exchanger	lamella 2 mm, size 1	50	60	75	90	105
	lamella 2 mm, size 2	75	90	110	130	155
	lamella 2 mm, size 3	95	120	145	175	205
	lamella 4 mm, size 1	30	35	45	55	65
	lamella 4 mm, size 2	45	55	65	80	90
	lamella 4 mm, size 3	55	70	85	100	120
	drop separator				45	50
Plate exchanger		65	80	105	125	150
	with drop separator					200

Figure 1.32: Minor pressure losses for different components of a duct system (engineeringtoolbox.com)

While the reviewed literature provides pressure loss predictions for air ducts, there are few publications that provide pressure loss predictions for pressure losses along streamlines in buildings. Pressure losses

are used in nodal air flow calculations, such as provided by the popular EnergyPlus program. A reliable assessment of pressure losses of typical airflow obstructions, such as windows, screens, vents, directional shifts in corridors, to name a few will make the pressure loss predictions of naturally ventilated building much more reliable and valuable. Several technical articles which discuss pressure losses associated with natural ventilation are presented here.

Baker and Shearin (2010) discuss the effectiveness of screens to keep pests out of greenhouses without the need of significant application of pesticides. The authors suggest that a risk benefit analysis has to be done to weight effectiveness of the screen against the pressure losses, which reduce the effectiveness of ventilation. The authors tested different screen materials and the resulting pressure losses. Their results suggest that screen materials with small holes are often better for pest exclusion but are usually more resistant to airflow. If a greenhouse operator decides to apply a fabric with a very small hole size but under-estimates the area of material needed, the ensuing screen may block airflow resulting in high static pressure drop, inadequate air exchange, higher energy consumption by the fans, excessive wear and tear on the fans, and high greenhouse temperatures. Figure 1.33 shows the result of their pressure loss tests.

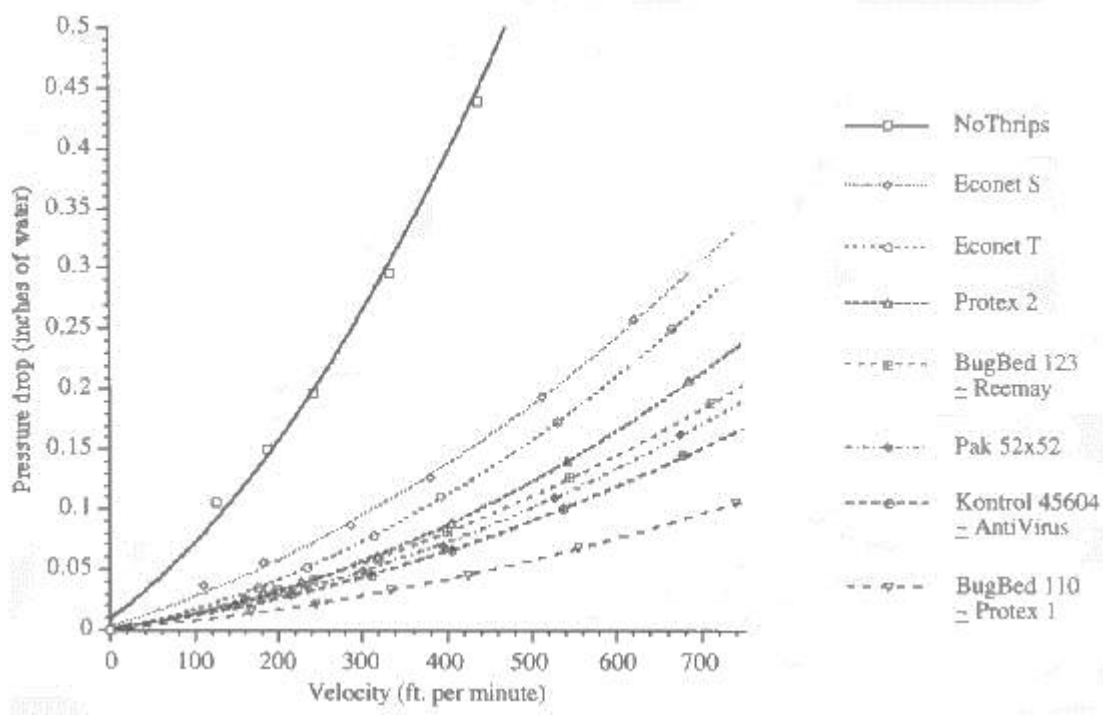


Figure 1.33: Pressure losses of air passing through different types of insect screens (Baker and Shearin, 2010)

1. Basics of Natural Ventilation and Airflow Inside of Buildings

The decision on what screen to select depends on the required exclusion efficiency against intrusion of insects. Figure 1.34 suggests the performance of different types of screen to keep certain insects out of the buildings. In tropical climates, such as in Hawaii, the appropriate choice of screen is an important design consideration for natural ventilation effectiveness.

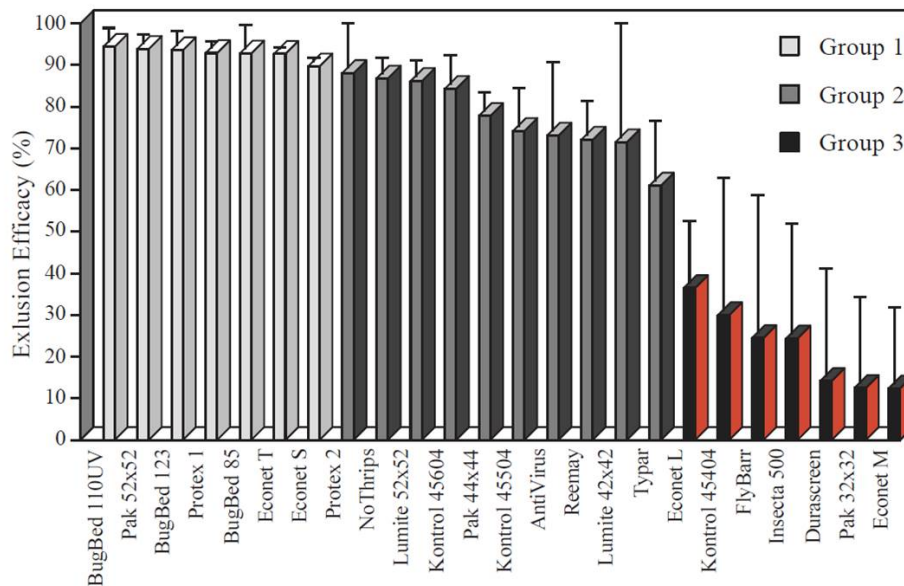


Figure 1.34: performance of different types of screen to keep certain insects out of the buildings (Bell and Baker, 1997)

Harrington and Ray (2014) report on pressure losses in architectural louvers. The authors suggest that louvers should be selected with several performance criteria in mind, such as free area, water penetration, and resistance to airflow (pressure loss). The authors present an optimization procedure to select louvers with high air flow and the least water penetration. Figure 1.25 shows the airflow resistance of a sample louver.

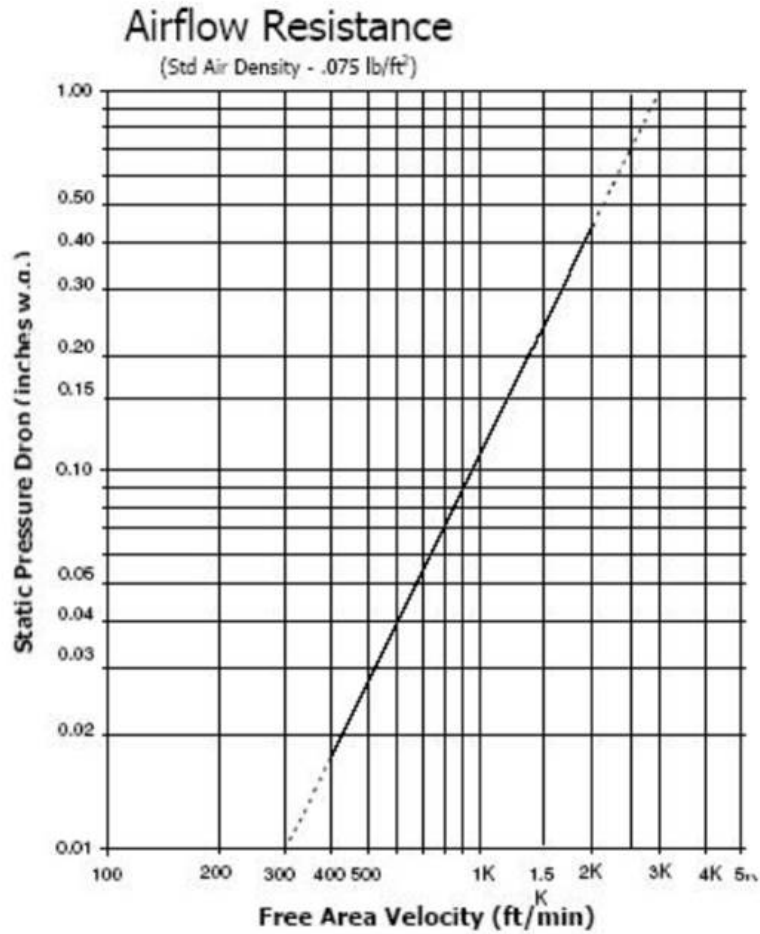


Figure 1.35: Airflow resistance of architectural louvers (Harrington and Ray, 2014)

2. CFD as a Design Tool for Natural Ventilation Design

Over the past three decades the role of CFD as a tool to assess effective solutions has been investigated by numerous building science practitioners. Most of the studies concluded that CFD is a promising design for naturally ventilated buildings, but several authors in the literature review caution that CFD, being simplified, and sometimes oversimplified, virtual model of the actual conditions, should be regarded with some skepticism. The argument is made that a good CFD practitioner should have good analytical and physical skills to interpret the results. Almost all of the studies recognize the need to validate the results with either scaled wind tunnel testing or testing in the full scale prototypes.

Meroney (2004) elaborates the important role combining CFD and wind tunnel testing in fluid dynamic analysis of air movement. The author elaborates on the dynamic of dispersion of matter in interior and exterior domains. The author claims that a hybrid methodology combines the advantages of an old tool, fluid (physical or scale) modeling, with the speed and convenience of a new technology, computational fluid dynamics (CFD). Figures 2.1 and 2.2 compare the traditional scientific method with a newer scientific paradigm. The traditional scientific method has two foundations; experimental and theoretical. The newer model includes the role for computing and simulation as an extension of the traditional processes. This newer framework established relationships between the processes of scientific model development, computational model verification, and simulation validation.

Applied on fluid modeling the newer methodology, for example, can initially provide data from which CFD turbulence models are created, CFD calculations can use such turbulence models to quickly survey alternate solution strategies using simplified domain scenarios, then physical modeling can examine in greater depth design consequences, and finally, CFD can extend initial conclusions to a broader set of similar cases. Combining experiments with numerical simulations also provides educational opportunities for the next generation of engineers and scientists.

Meroney (2004) compares wind tunnels to analog computers that have the advantage of “near infinitesimal” resolution and “near-infinite memory.” A fluid modeling study employs “real fluids” not models of fluids; hence, the fluid model is implicitly non-hydrostatic, turbulent, includes variable fluid properties, non-slip boundary conditions, and dissipation and even flow separation and recirculation. All conservation equations are automatically included in their correct form without truncation or differencing errors, and there are no missing terms or approximations. Model studies, while using the same “real material”, are scaled models with necessary simplifications, but are prone to certain inaccuracies due to similitude.

The Scientific Method as Practiced Before Digital Computers

- Practiced by Hippocrates (460-377 BC), In His Rational, Empirical Approach to Medical Science
- Described and Practiced by Descartes (1596-1650)
- Established On Two Foundations:
 - Experimental Science
 - Theoretical Science
- Characterized by Continuous Process of Improvement and Discovery
- Data Validation Process
 - Units of Measurement, Datums
 - Error and Uncertainty Quantification

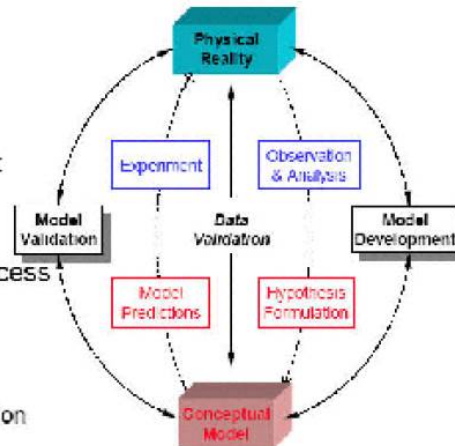


Figure 2.1: The “Old” Scientific Method. (Meroney, 2004)

The “New” Scientific Method (Based on Sargent’s Framework)

- Supported by Three Foundations:
 - Experimental Science
 - Theoretical Science
 - Computational Science
- The Processes of Model Development, Verification, and Validation Deal Respectively, with the Interfaces Between:
 - Reality - Model
 - Model - Simulation
 - Simulation - Reality

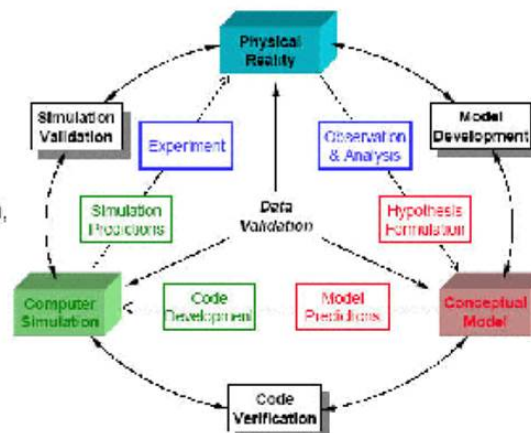


Figure 2.2: The “New” Scientific Method. (Meroney, 2004)

CFD modeling, on the other hand are not intrinsically limited by similitude or scale constraints, although CFD analysis many limitations associated with grid resolution, choice of turbulence model, or assignment of boundary conditions. The author suggests that, in principle, it should be possible to numerically simulate many aspects of airflow transport, dispersion, and/or drift. The tremendous potential of CFD has led wind engineering practitioners to present “colorful and attractive” results of numerical studies in professional and trade journals and promotional materials. Yet the accuracy of the CFD results is directly dependent on the choice of domain resolution, turbulence models, and boundary conditions constrain predictions. The author therefore cautions about the tendency displayed in many CFD applications to believe implicitly in the realism of the beautiful graphical displays Instead the author calls for continued verification and validation at almost every level of CFD prediction.

Clifford et al (1997) suggests that estimating the quantity of ventilation for any particular building at the design stage is still a difficult task. The authors sees the refinement’s wind tunnel testing techniques such as boundary layer simulation and improvements in modelling wind characteristics as powerful tools for the designer which usually give reasonable estimates of ventilation rates. However, factors such as complex topographic features, scaling errors, and influence of architectural features can restrict the accuracy of any estimate. As an alternative approach is to apply the CFD, which has many benefits, such as the avoidance of building a physical model, the possibility to easily simulate different wind

Meroney (2009) reports on validation of CFD simulations with previous wind tunnel experiments. The study investigated how well different numerical options replicate measured natural ventilation situations, but it also examines how well the method of domain decomposition reproduces full numerical simulations and laboratory measurement. In the CFD analysis a wide range of turbulence models was used. The full domain CFD calculation simultaneously modeled the exterior and interior flow field, which means that the computational domain encompassed but exterior and interior air space. Beside the full domain representation, a domain decomposition technique was used that predicts internal flows in buildings, and which considerably reduces the computational effort and expedites design decisions. This technique separately analyzes the building outside region and building inside flow fields. With this technique, CFD analysis is first performed for the flow field outside the building, from which boundary conditions are extracted for the analysis of the indoor situation. Subsequently one uses boundary conditions of wind pressures and flow orientation at proposed opening locations, estimates of internal pressure coefficients based on cross-building surface pressures, and opening discharge coefficients related to a dimensionless internal room pressure to predict opening flow rates. These boundary conditions are imposed on a numerical domain to calculate internal flows also using CFD.

Figure 2.3 compares the results of the experimental data with CFD result from both the full domain and the domain decomposition. As shown in Figure 2.3 Both the PIV and full-field CFD calculations reproduce the vena-contract that occurs downwind of the inlet opening, that results in maximum concentrations occurring about 1/2 opening dimension within the room. The domain decomposition approach does not

produce a vena-contracta, and maximum velocities tend to occur at the inlet opening. Figure 2.4 shows the comparison of average static pressure coefficient obtained by the scaled model tests with coefficients obtained in the full domain and domain composition experiments.

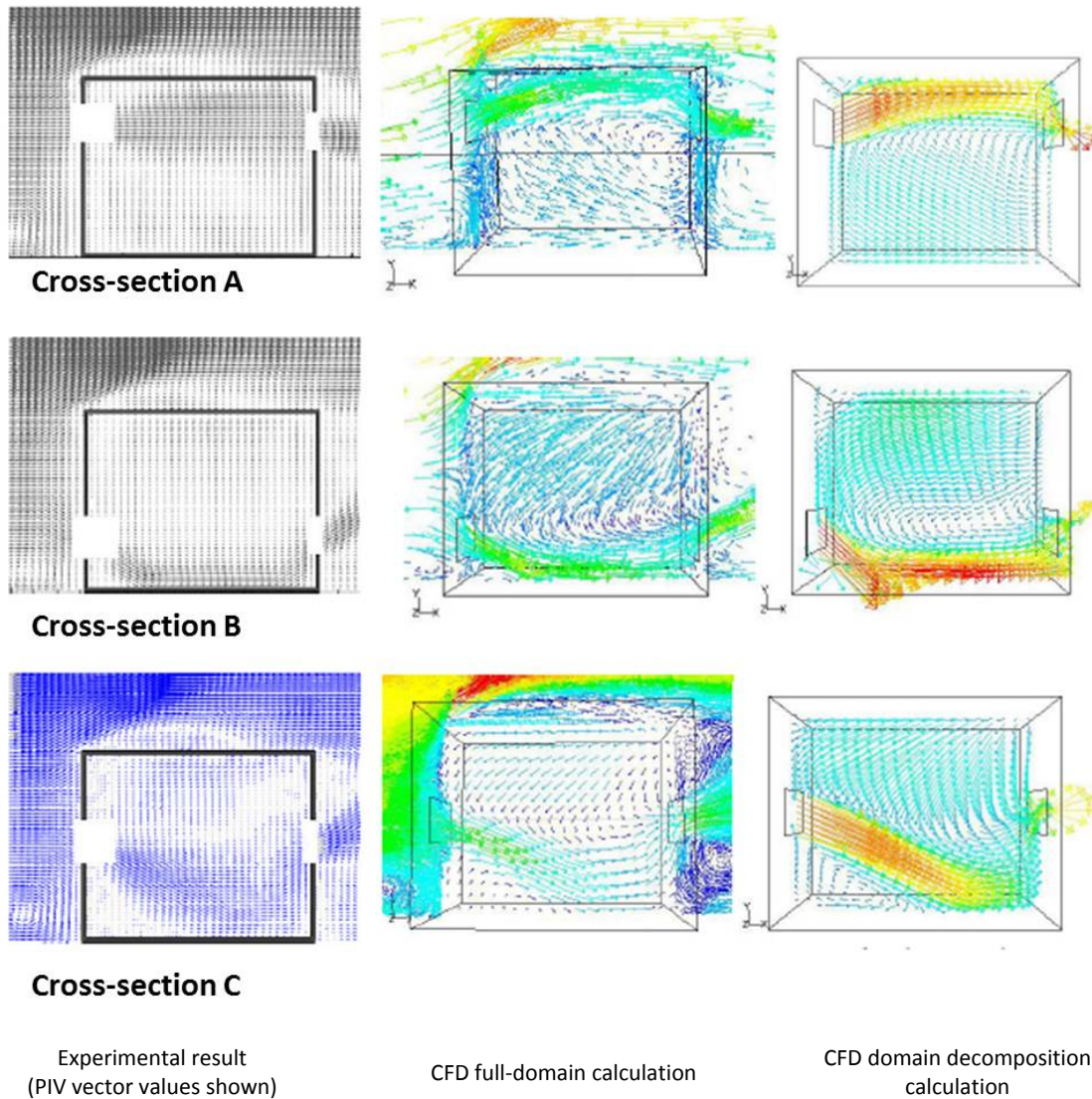


Figure 2.3: Velocity vectors on building vertical midplane for Cases A, C & E. (Meroney, 2009)

The author (Meroney, 2009) concludes that full-domain and domain decomposed CFD calculations could reproduce external flow field characteristics and internal flow channel trajectories as well as cross-

ventilation flow rates and internal pressures that were obtained with wind-tunnel measurements of natural ventilation, within experimental uncertainty. The CFD methods produce results accurate enough to support ventilation designs. The author also concluded that internal flows fields and associated cross ventilation flow rates appear to be fairly insensitive to choice of turbulence model. Domain decomposition worked well, and provides a valuable analysis tool which can significantly reduce computational overhead.

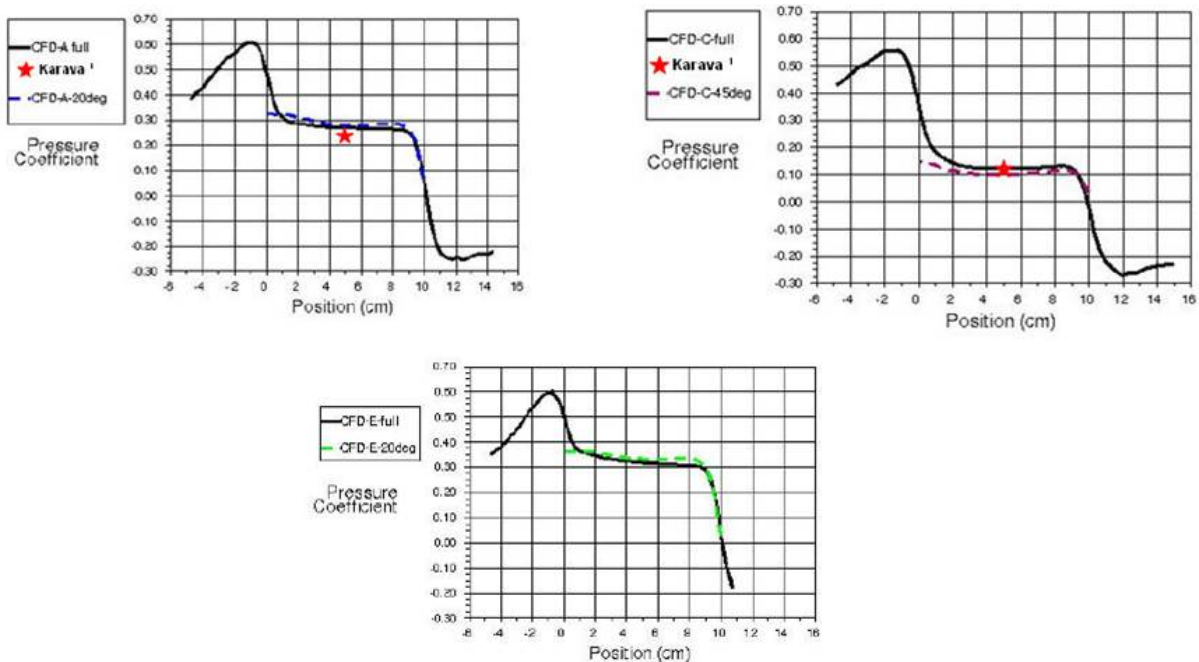


Figure 2.4: Static pressure coefficient, C_p , along line joining inlet and outlet openings (Meroney, 2009)

Kolesnikov (2006) demonstrates the applicability of CFD in a design evaluation of an educational laboratory facility. The design study was done to accurately perform risk assessment studies of human exposure to air pollutants in cases of their accidental release into indoor spaces. A CFD study was conducted to select an optimized layout of the laboratory facility. The author first made a benchmark study of his CFD application program against a well-documented forced convection benchmark study. Figure 2.5 shows the simple physical test prototype and the CFD computational domain.

2. CFD as a Design Tool for Natural Ventilation Design

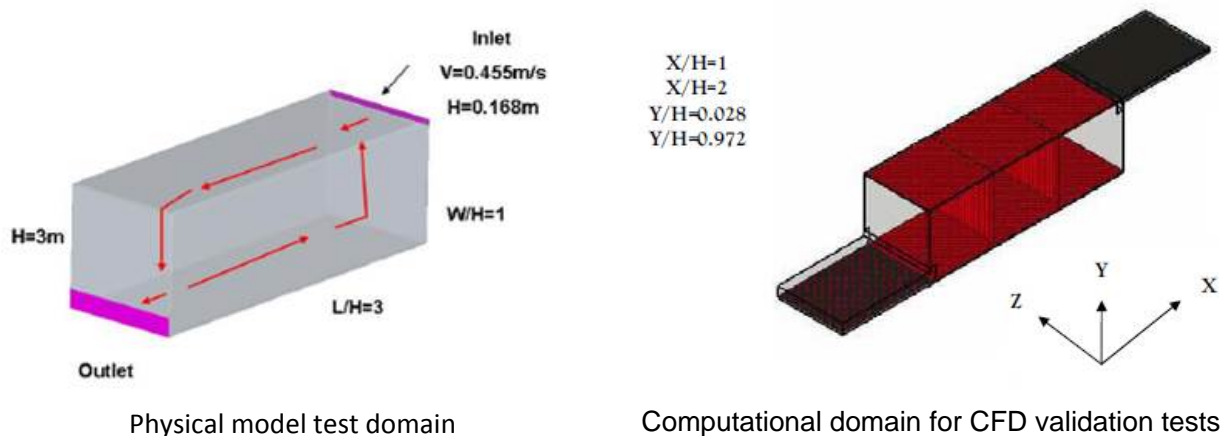


Figure 2.5: CFD validation tests for design analysis of a laboratory layout (Kolesnikov, 2006)

The CFD validation study used several turbulence models including high and low Reynolds number $k-\epsilon$ models and Gibson-Lauder Reynolds stress model (RSM). A comparison of the velocity distribution of the longitudinal cross section is presented in Figure 2.6. As illustrated in Figure 2.6 the flow velocity magnitude diminishes upon incoming airflow propagating into the main room domain. There are large recirculation pattern inside the room, with the bulk-entering airflow moving from right to left along the ceiling, turning towards the floor, partially exiting the room at the outlet and partially proceeding from left to right along the floor completing the recirculation pattern by turning upwards at the right lower corner of the solution domain. An important characteristic of the flow confirmed by experimental results includes two secondary recirculation regions, one in the upper left and one in the lower right corners of test domain.

Figure 2.7 shows, as an example, normalized experimental and numerical results one selected measured cross sections. All CFD solutions show close consistency to experimental measurements for the sample cross-section.

After validating the CFD application and turbulence models the author proceeded with the CFD design study of the layout of the approximately 10,000 square laboratory facility. Figure 8 shows the floor plan section as a three dimensional representation. The lab facility considered in the CFD analysis comprised nine rooms and connecting corridors. The ventilation was modeled with six slot inlets and five outlets. The boundary conditions are uniform velocity inlets and atmospheric pressure at outlets. No-slip boundary condition is used along the walls. The study analyzed the distribution of airflow velocities, temperature and dispersion of selected pollutants in the lab facility. In addition to general floor plan geometry included occupant comfort simulations. For this part of the study a person potentially representing a laboratory worker was somewhat randomly placed inside solution domain as illustrated (see Figure 2.9).

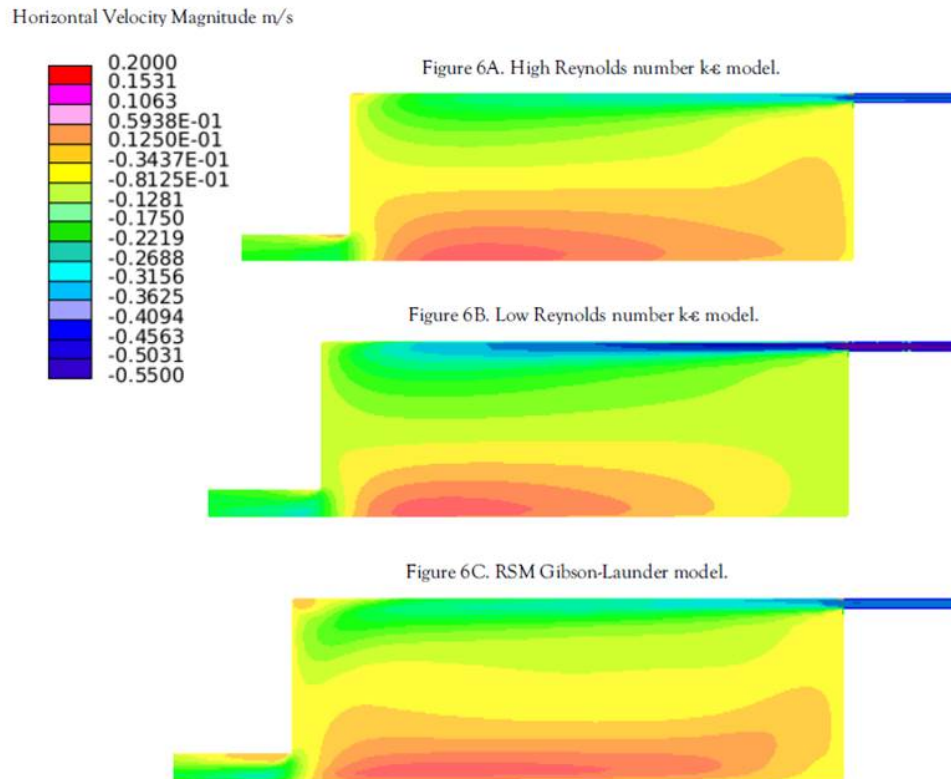


Figure 2.6: Velocity magnitude along the X axis. Cross-sectional view. (Kolesnikov, 2006)

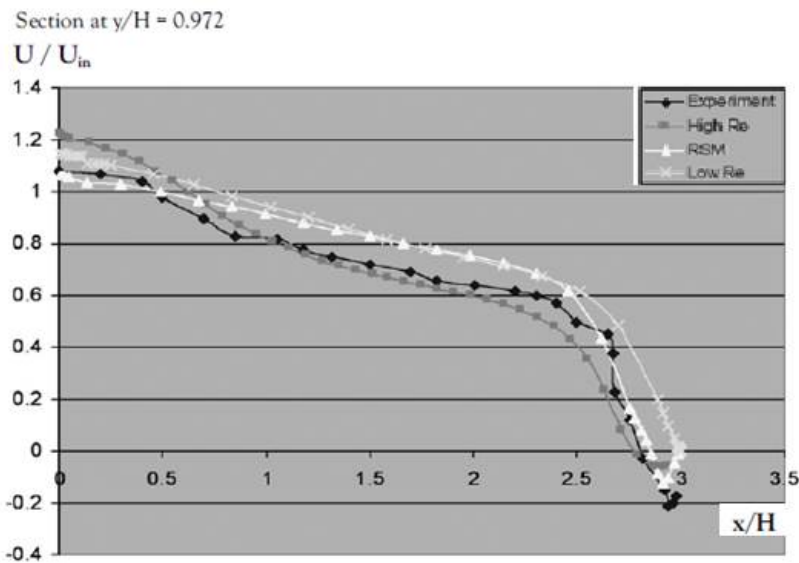


Figure 2.7: Experimental results comparison (Kolesnikov, 2006)

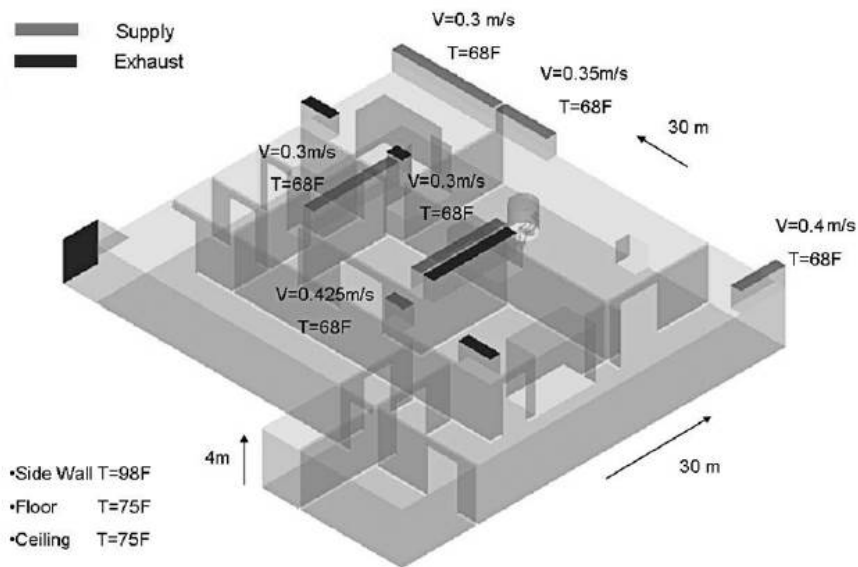


Figure 2.8: Laboratory floor plan. Three dimensional representation and boundary conditions. (Kolesnikov, 2006)

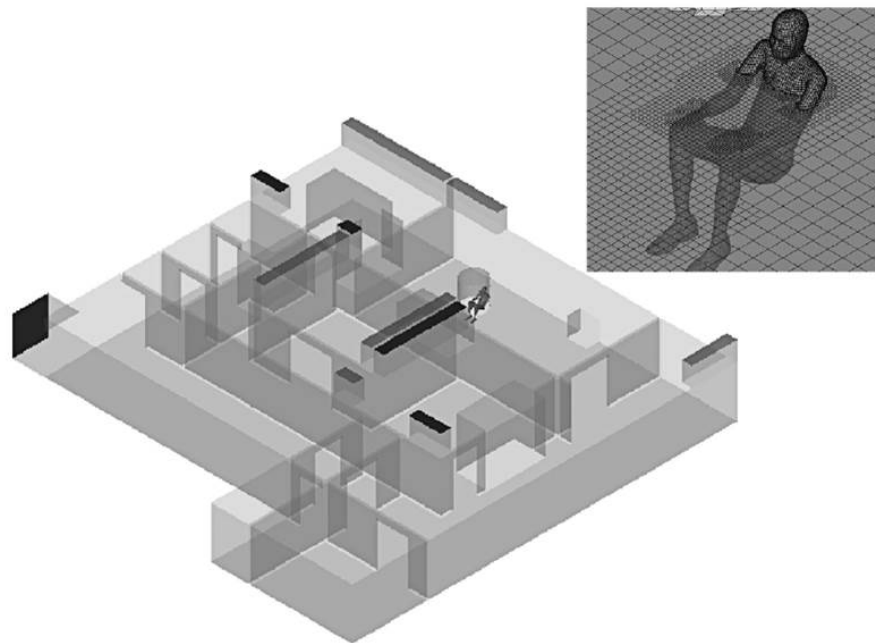


Figure 2.9: Laboratory personnel representation (Kolesnikov, 2006)

Some of the results of the study are presented in Figures 2.10 through 2.11. The results were used in optimizing the floor plan. Figures 2.10 and 2.11 show the distribution of air flow velocities and temperature on the general floor plan in the targeted ventilation approach, respectively. This is steady state data of the analysis.

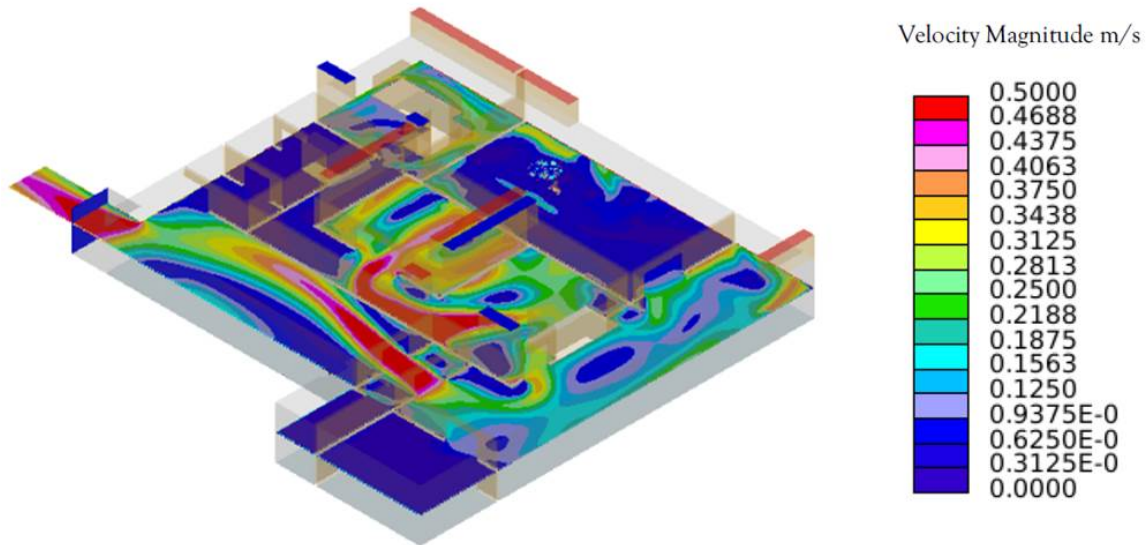


Figure 2.10: Airflow velocity distribution on floor plan (Kolesnikov, 2006)

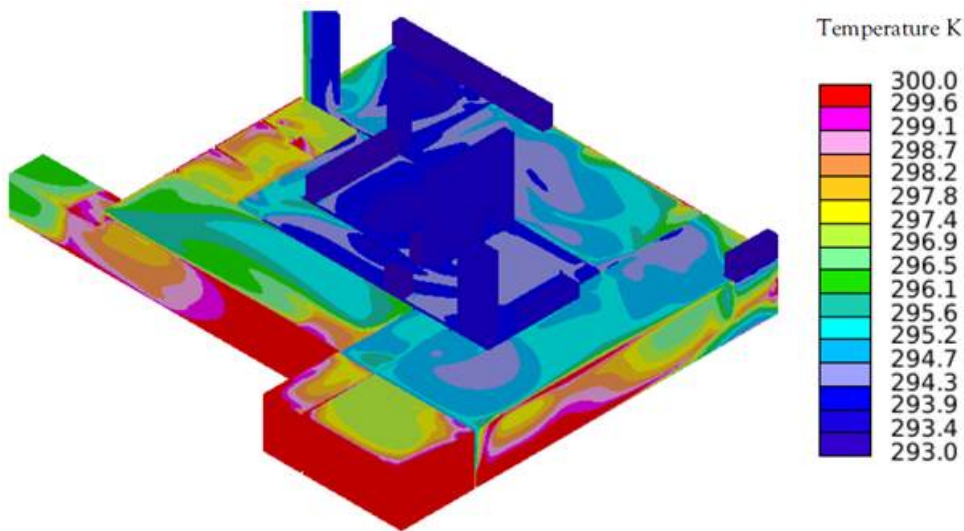


Figure 2.11: Temperature distribution on floor plan (Kolesnikov, 2006)

Figure 2.12 shows the transient (non-steady state) CFD simulation of the dispersion of indoor pollutant through the ventilation system. The times indicated in Figure 2.12 refer to the time after release of the indoor matter. Figure 2.13 indicates the required computational capacities for the CFD analysis. It is apparent that the benchmark tests (“Nielsen Room”) have relatively little complexity and therefore require less time than the CFD analysis of the complicated floor plan. What is also significant is the required long run time for the transient tracer gas dispersion.

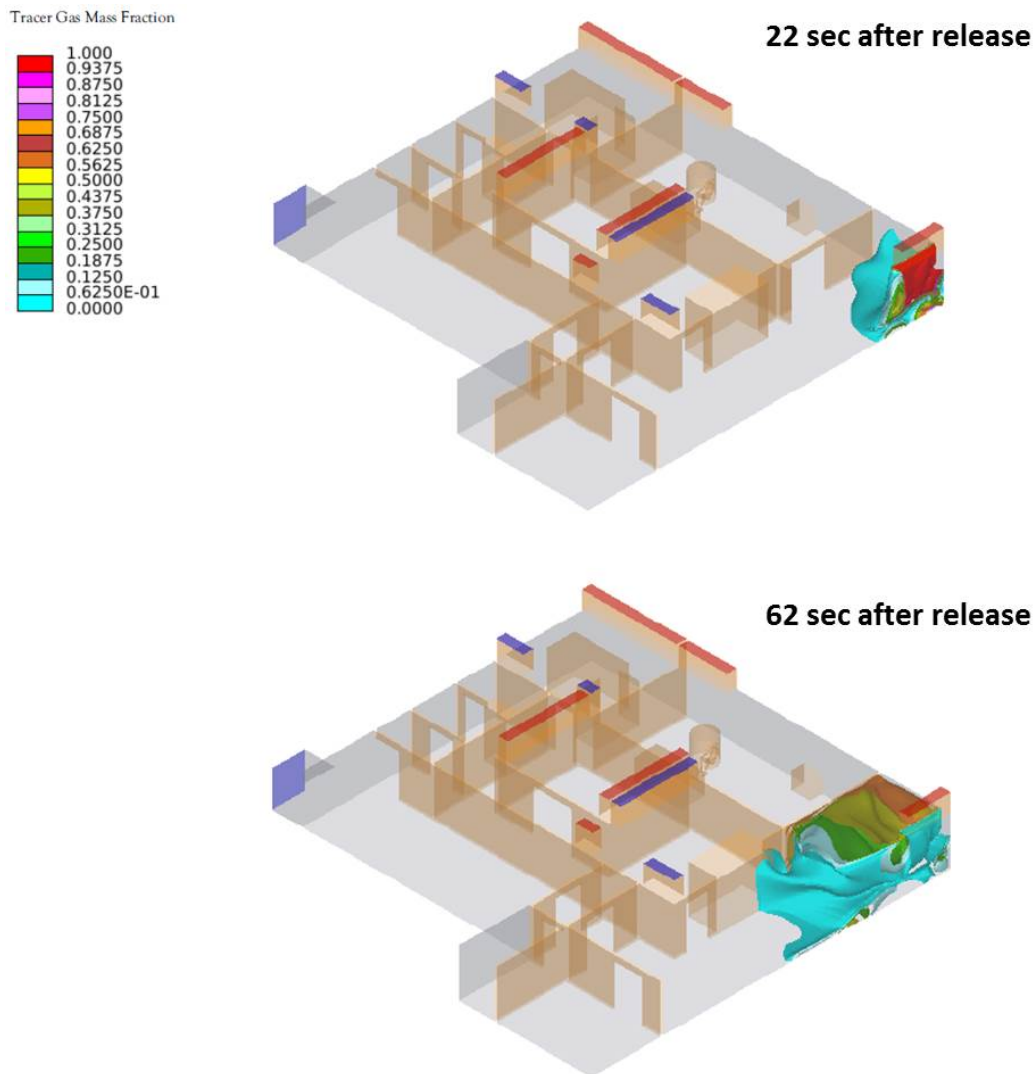


Figure 2.12: Tracer gas concentration profiles after release (Kolesnikov, 2006)

	<i>Mesh size</i>	<i>Computer Platform</i>	<i>Computing Time</i>
<i>Nielsen Room Steady-state</i>	500,000	Dual 3.2 MHz, 8G memory desktop	8 hrs
<i>Lab Floor Plan Steady-state</i>	3,900,000	10 Proc 2.2, MHz cluster	10 hrs
<i>Lab Floor Plan Transient, 90 sec. real time</i>	3,900,000	10 Proc. 2.2 MHz cluster	144 hrs

Figure 2.13: Run time statistics (Kolesnikov, 2006)

The author (Kolesnikov, 2006) suggested that his validation study establishes the ability to closely predict ventilation airflow distribution profiles during CFD simulations. Based on these validation tests, the author feels comfortable to use the validated CFD application in the design optimization for a real-life generic laboratory floor plan. With a moderate capacity on computational resources (e.g. run time) even complicated parametric changes such as the design optimization of an entire laboratory floor plan could be conducted in a one-week period.

The author suggests that a larger-scale problem would simply require a larger number of processors for parallel implementation, thus making it a resource capacity problem readily resolvable with computational means. The author concludes that CFD can provide quality data sets detailing airflow characteristics within built environments which are not available otherwise. Therefore CFD has clearly matured into a design tool of choice at the forefront of building design applications.

Another important description of CFD's emerging role as a principle design tool is presented by Jiang and Chen (2002). The authors describe the study of airflow characteristics of a naturally ventilated building where field measurements are compared to wind tunnel tests and CFD analysis. The importance of this study is the application of a CFD code that includes the modeling of fluctuating wind directions and the inclusion of large scale eddies around the building prototype. The analysis of the airflow pattern inside the building considered the effect of surrounding buildings. Typically surrounding buildings affect the airflow patterns since wind is deflected with wind stagnating on the windward sides and separating into eddies on the leeward side.

The author concluded that cross ventilation is the primary driving force for the naturally ventilated apartments in the buildings.

An effective building design with cross ventilation requires the knowledge of detailed information of air and pressure distributions in and around buildings. Full-scale measurements for a building site can provide reliable data, but experiments are time consuming and hard to control. In most cases, the experimental data obtained from one building site may not be extended to another because of different weather data and building surroundings. Another approach is the use of small-scale models in a wind tunnel to simulate natural ventilation. In general, the mean flow characteristics, such as average pressure, can be adequately modeled for a single building. Modeling of fluctuating components of the flow characteristics, however, are difficult to reproduce. Therefore, the time averaged results obtained from scale models in wind tunnel measurement may contain significant error. An alternative approach the authors suggest to study the airflow in and around buildings is computational fluid dynamics (CFD). CFD is becoming popular due to its informative results and low labor and equipment costs, as a result of the development in turbulence modeling and computer speed and capacity.

While mostly Reynolds averaged Navier-Stokes (RANS) modeling is used in CFD air flow studies, the authors used large eddy simulation (LES) simulations. LES simulation required significantly more computational time, however in recent years, LES has been successfully applied to several airflows related to buildings. RANS modeling requires less computing time than LES because it solves mean flow parameters. Therefore, RANS modeling is the most widely used CFD method in many industrial applications. To simulate natural ventilation in buildings, however, RANS modeling has some deficiencies. LES computes the large eddies in a three-dimensional and time dependent way while modeling the small eddies with a subgrid-scale model. The advantage is that LES modeling can also provide quality data about transient, or non-steady, airflow occurrences around buildings.

The authors explain that most CFD simulations use only one wind approach direction and produce "snap-shots" in time. It is however important to include transient occurrences, for example separation and reattachment of eddies around the building. This analysis can best be carried out with LES.

The authors compared data of the exterior and interior airflow patterns around designed buildings. The data compared were onsite measurements, scaled test on wind tunnel and CFD simulations. For the CFD simulation, LES modelling was used with a single wind direction and varying wind directions. For the analysis a set of buildings was used. A previous study had determined on-site measurement and a scale model measurements conducted in wind tunnel tests. Figure 2.14 shows the building layout, indicating the constellation of building among each other. Figure 2.15 shows where internal air flow measurements were conducted. Figure 2.16 shows the wind data (direction probability) from on-site measurement of a campus. The author suggests that typical variation of wind direction is about 80° during a time period of 15 minutes.

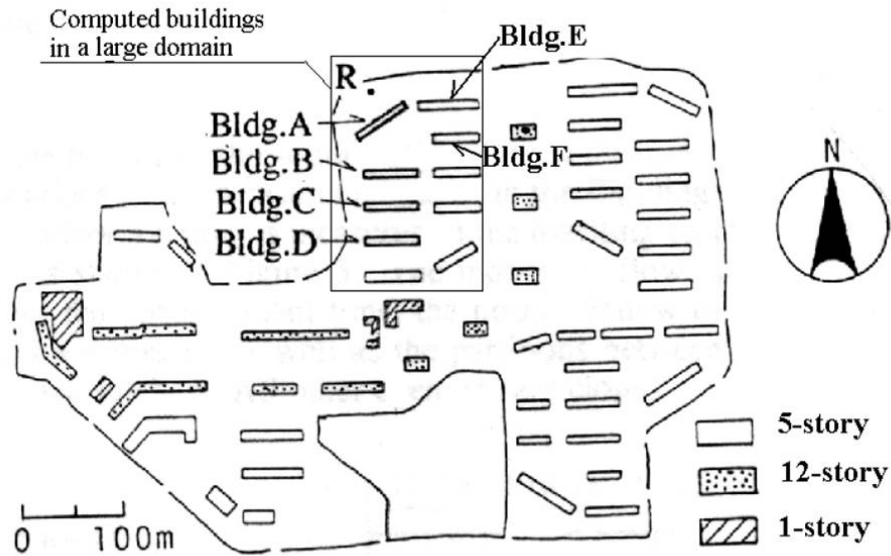


Figure 2.14: Layout of the building group investigated (Jiang and Chen, 2002)

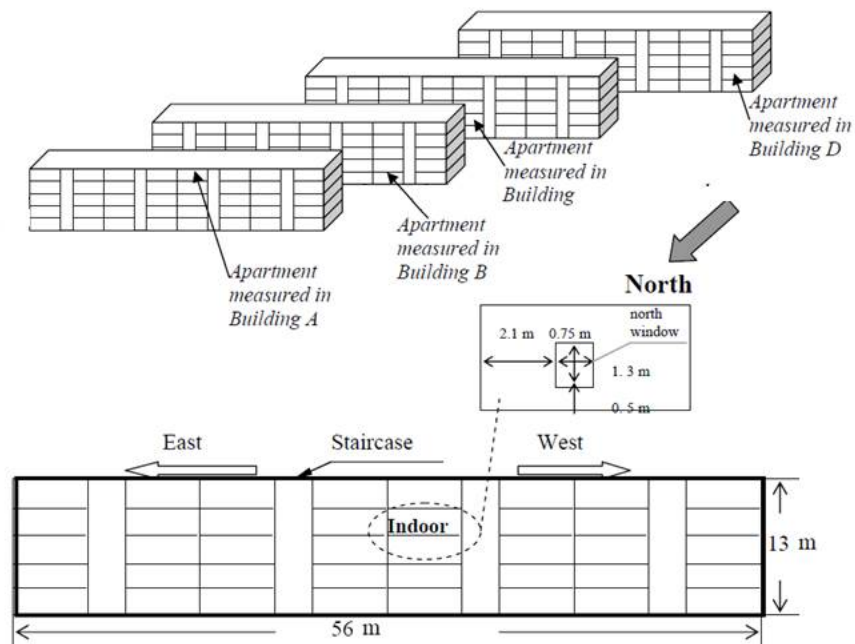


Figure 2.15: Overall dimensions of the building (L56xW13xH7 m) and the locations of apartments where indoor airflow was measured (Jiang and Chen, 2002)

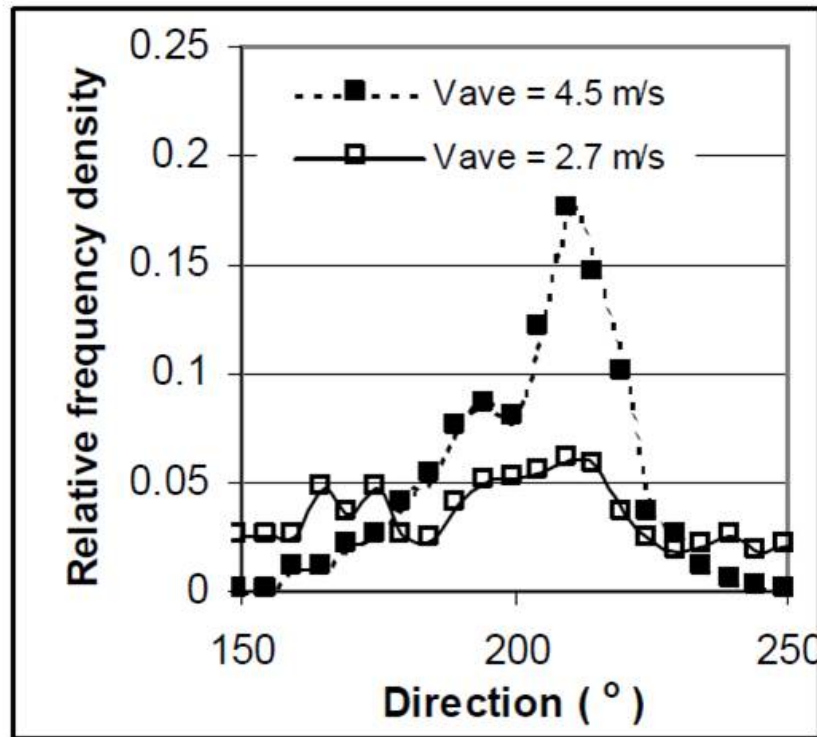


Figure 2.16: Comparison of the histograms of wind data (Jiang and Chen, 2002)

Figure 2.17 show results of the LES simulations which are compared to the experimental from windtunnel test and the onsite measurements. The data shown in Figure 2.17 represent the situation in apartment building A. Sections (a) and (b) of the Figure 2.17 represent the wind tunnel results and the LES with fixed wind direction, respectively. They show similar air flow patterns with higher speed regions in the upper and lower rooms. The on-site measurements show a shallower and wider high-speed region in both rooms. The LES results with the varied wind direction are in reasonable agreement with the on-site data.

The results illustrate that, with a fixed wind direction, the wind can pass through the room openings without too much oscillation and energy loss. Hence, a deep, thin and high-speed core is formed. On the other hand, with varied wind directions, the flow dissipates energy to the corners of the room, which reduces the depth and width of the high-speed core. The wind speed becomes evenly distributed throughout the room than that with a fixed wind direction.

The table in Figure 2.18 shows representative pressure differential coefficients ΔC_p at selected apartments in Buildings A through D. The results support the observation of Figure 16. The results shown in the table suggest that the results are basically distributed in two groups. One group, on-site

measurements and LES (varied wind direction), show a reasonable agreement; whereas the other group, Wind tunnel measurements and LES (fixed wind direction), show also reasonable agreement.

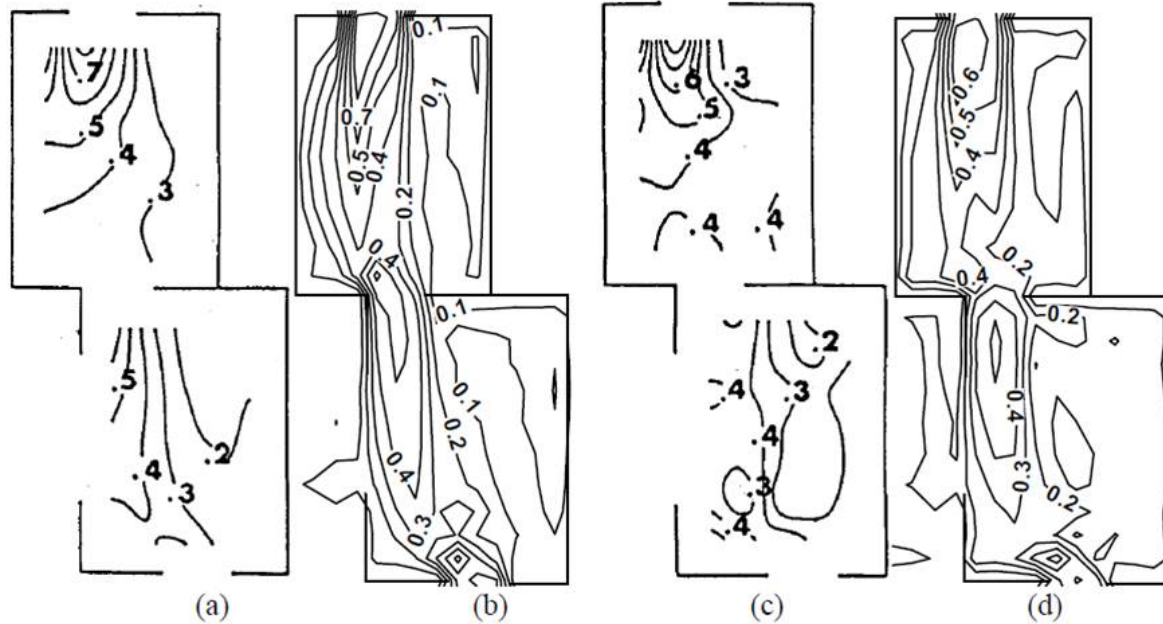


Figure 2.17: Comparisons between the experimental data and LES results. (a) Wind-tunnel; (b) LES (fixed direction); (c) On-site; (d) LES (varied direction). (Jiang and Chen, 2002)

	Building A	Building B	Building C	Building D
On-site measurements	0.85	0.42	0.12	1.03
LES (varied wind direction)	0.87	0.43	0.20	1.00
Wind tunnel measurements	0.85	0.42	0.46	1.26
LES (fixed wind direction)	0.90	0.45	0.50	1.25

Figure 2.18: Results of ΔC_p at selected apartments in Buildings A through D (Jiang and Chen, 2002)

These observations have significant implications, since they point to a fundamental fact that would make CFD simulations less prone to consistent errors than experimental data obtained in wind tunnel. The author concludes that natural wind changes direction over time, which is hard to produce in a conventional wind tunnel. LES can simulate both cases by adjusting inlet boundary conditions: a fixed incoming wind direction for the wind-tunnel test, and a varied incoming wind direction for the on-site

measurements. The measured data and computed results show three significant differences in the airflows for a real building site and for a wind tunnel. The author concludes that:

1. Natural wind at some moments can destroy the formation of large recirculation zones behind a building, and only small eddies can exist. With a fixed wind direction in the wind tunnel, the wind cannot reach some regions of the building façades. Therefore large recirculation zones are easily formed in the downwind direction.
2. The gradient of the pressure coefficient difference across the building, ΔC_p , is more uniform with a varied wind direction than that with a fixed wind direction.
3. The indoor airflow with a fixed wind direction has a thinner, deeper and higher speed core than that with a variable wind direction. This is because the wind in the former case does not oscillate and loses less energy.

A final observation is the required computational resources that are required for transient LES simulation with varying wind directions. Figure 2.19 shows the required computer resources that were required to run the different LES simulations. As can be seen the transient LES required 88 days of CPU time, which might surpass the computer resource capacity of many designers.

No. of bldgs	Include indoor?	Domain size L×W×H (m×m×m)	Smallest grid size	Total grid number	Time step (s)	Total real time (min)	Total CPU (days)
10	Yes	450 × 80 × 400	0.2 m [*]	8 × 10 ⁶	0.05	20	88
10	No	450 × 80 × 400	1.0 m	0.5 × 10 ⁶	0.1	20	2.8
4	Yes	250 × 60 × 280	0.2 m [*]	1.8 × 10 ⁶	0.05	10 ^{**}	6

Figure 2.19: Results of ΔC_p at selected apartments in Buildings A through D (Jiang and Chen, 2002)

3. Internal CFD – Numerical Assessment of Air Movement Inside Buildings

This section discusses specific settings and guidelines that are given in the reviewed literature.

3.1 Best Practices and Quality Control

The quality of CFD simulation is controlled by certain best practice, which are summarized in this section. There are various best practices provided in the literature. The following summarizes the recommendations of Nielsen, P. et al (2007) and Roaches, P. (1997).

Steps of a CFD Simulation

Nielsen, P. et al (2007) suggest that a CFD simulation requires a large number of steps, as CFD simulation is a long and complex work process. Each step is prone to certain errors, and if uncorrected, each error affects subsequent steps so the quality of the entire situation can be compromised. As a result, CFD predictions can significantly differ from the actual situation which the CFD analysis should describe.

The authors categorize error sources into seven groups, where some of these groups contain several procedures. The error groups are listed below and further described in Figure 1:

1. Definition of the problem
2. Grid
3. Models
4. Boundary conditions
5. Numerical procedure
6. Code errors
7. User errors

Figure 3.1.1 shows that the first groups 1 through 4 are about how good the model is selected and set up, this means how well the problem is comprehended in the physical realm and translated into a form that can be used in the CFD process. Groups 5 and 6 indicate how well the equations are solved. Figure 3.1.1 also indicates a distinction between “errors” and “uncertainties”. The distinction and the proper way to address these issues can have a profound effect on the outcome of a simulation.

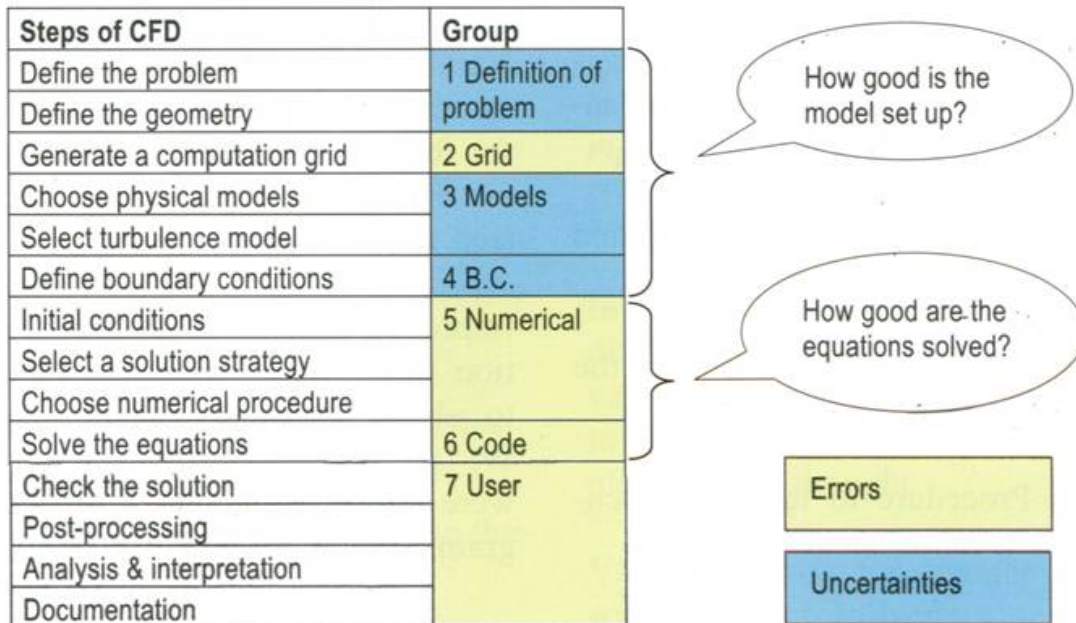


Figure 3.1.1: Steps in CFD simulations (Nielsen, 2007)

Roache, P. (1997) suggests that quantification of **uncertainty**, the estimation or banding of the numerical error of a final calculation in computational fluid dynamics (CFD) and related fields in computational physics, mathematics, and engineering. Quantification of uncertainty may also involve more than just obtaining a good error estimate. Uncertainty can be defined as a shortcoming due to lack of certain knowledge to properly solve a problem. For example, in order to quantify the uncertainty with systematically refined (coarsened) grids, we need the convergence rate p to estimate the error. Once we have produced a CFD solution of the governing partial differential equations, it is clear that we require some additional information in order to quantitatively estimate the uncertainty or numerical accuracy. Uncertainties are not an intuitively quantifiable property and we need a process to quantify it. **Errors**, on the other hand, can be quantified and/or avoided with sufficient care. The distinction between errors and uncertainties is important for the quality of a CFD simulation.

Two other terms have to be distinguished, these are **verification** and **validation**. Roache, P. (1997) makes the following distinction - verification is "solving the equations right," and validation is "solving the right equations." In this sense a CFD code can be verified when it can be shown that the partial differential equations (PDEs) are being solved and demonstrates convincingly that they are solved correctly, this means that the code produces a solution. The author stresses that whether or not those equations and that solution bear any relation to a physical problem of interest to the code user is the

subject of validation. In a meaningful sense, a code cannot be validated; only a calculation (or range of calculations with a code) can be validated.

Definition of the problem:

The important first step is to define clearly the physical objectives of what has to be simulated. The following questions should be clearly stated (Nielsen, 2007):

- What do we want to obtain from the prediction?
- Which are the steps on the way to the final answer?
- How are these single problems defined in the simulation process?

An illustrative example a CFD investigation of an entrance to the building is given. The CFD analysis was prompted by occupant complaints about draft. Various reasons for the draft were identified as possible, such as stack effect through different floors, effects of the façade, and wind. The author suggested that the applicable errors and uncertainties can be divided into simulation method/approach, simplification / modeling level and unsuitability of problem.

Simulation method/approach:

Using an incorrect simulation approach cannot yield the correct effects. For example, the following decisions have to be made:

- Is 2-D treatment adequate or is 3D needed?
- Is the problem steady state or is transient?
- Should the fluid component be treated as a scale or should it be modeled as a multi-component fluid?
- Can a symmetry plane be defined if chances are for asymmetric flows?

For example, Figure 3.1.2 shows the use of a 2D steady state and a 3D transient simulation approach. The space is long and the geometric situation suggests that using a 2D steady state approach could provide an effective solution. The situation results (Figure 3.1.2 (a)) did not show any down draft that could be detected as was observed in the actual building. The only feature observed was a large eddy which could not be the reason for the draft problem. A 3D steady-state approach did not reveal any potential for a draft situation as well. Only a 3D transient simulation approach revealed the draft problem as the result of downward bubbles from vortex shedding at the roof.

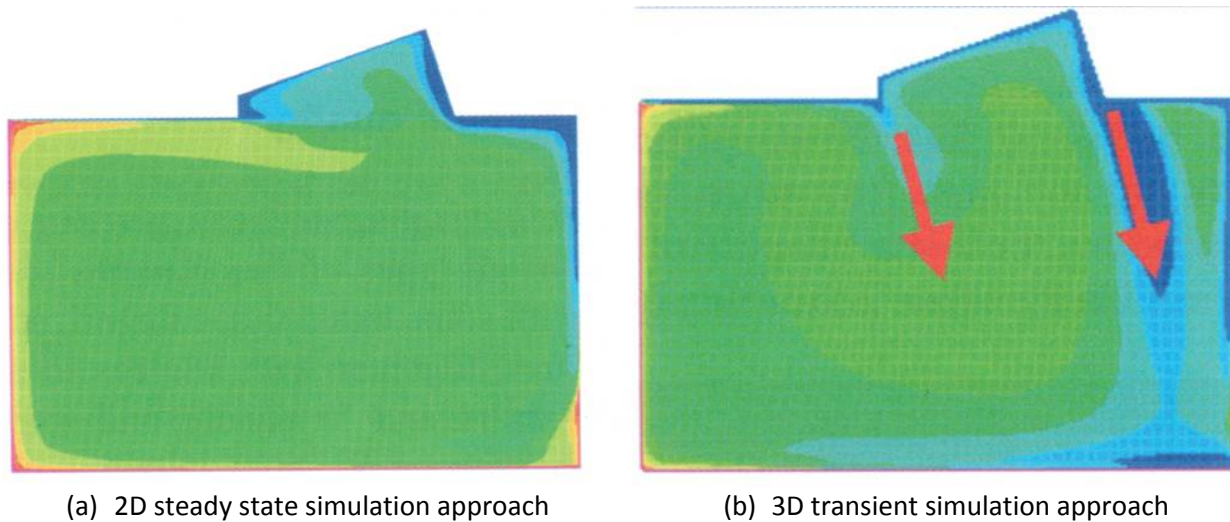


Figure 3.1.2: Comparison of different CFD simulation approach used for a draft problem (Nielsen, 2007)

Another example of a circulation simulation in a room with an inlet jet did not properly predict the interior airflow patterns. In this case a slightly bent inlet jet ruled out the application of a symmetry plane. Even for the full room simulation, without use of a symmetry plane, using a standard turbulence model could not predict the actually observed airflow patterns. Only the use of a higher-order turbulence model with whole room simulation was successful to predict the observe airflow patterns.

Simplification / modeling level:

An elaborate geometrical model or the inclusion of many airflow obstructions and heat transfer boundaries does not necessarily result higher quality CFD results. A CFD model should be simplified to the extent possible. Simplification can drastically reduce the required computer resources.

Figure 3.1.3 serves as an example of a complex interior situation that needs to be simplified in order yield practical results and the avoidance of long and possible erroneous simulation runs. Figures 3 (a) and (b) represent extremes of a degree of simplifications. Figure3.1.3 (a) shows a room with all furniture, heat sources and flow obstructions. Figure 3.1.3 (b) shows the same room without any furniture, only the radiator below the window is kept. The question how much simplification is required depends on the questions that should be answered in the investigation. If the nature of the CFD analysis is the airflow investigation in the vicinity of the window then a very high simplification is required. If an intricate airflow in the room, involving complex inlet and thermal plumes is required much more interior objects should be included. Much care has to be taken that simplification matches the objectives and the computer resources involved.

3. Internal CFD – Numerical Assessment of Air Movement Inside Buildings



(a) Office situation with all details



(b) Simplified office situation

Figure 3.1.3: Comparison of situations to be modeled with different degrees of simplification (Nielsen, 2007)

Nielsen, P. et al (2007) provide the following guidelines:

- Choice of geometric simplification level can be too extreme thereby removing possible airflow characteristics and thermal interactions.
- The appropriate heat sources should be used; for geometrically small but strong heat sources a volume object without airflow obstruction might be selected or an object with heat flux boundaries more appropriate
- Use of square geometry versus round, when possible, to reduce grid complexity.

Figure 3.1.4 (upper image) shows another example where the level of simplification has to be selected in an appropriate way. In this example a high detail in modeling occupants is not needed if general airflow in the rooms required. The shown level of detail of rendering occupant bodies in the upper image might be appropriate if there are very few occupants in the room and detail airflow and thermal performance is required. The detail in Figure 3.1.4 (middle) should probably be appropriate for most CFD simulations. The level of detail in the lower image of Figure 3.1.4 is most likely not sufficient. Nielsen, P. et al (2007) suggest that there are situations where CFD might not be an appropriate design tool to provide quality solution,

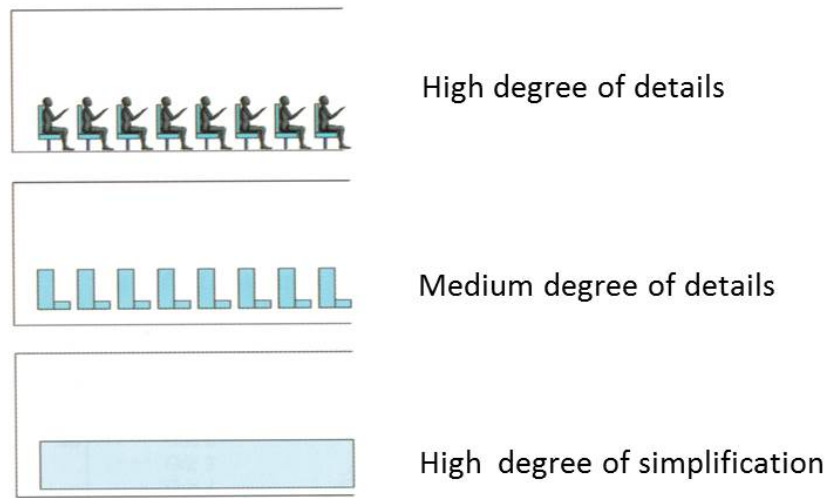


Figure 3.1.4: Representation of heat sources using different levels of simplifications (Nielsen, 2007)

Computational Grid

The next important step in the CFD simulation workflow is the generation of a suitable and effective simulation grid, or mesh. In this step many errors can be made, which could render result of even well-defined CFD problem as unsatisfactory. A variety of grids can be generated with hexahedral cells, tetrahedral cells, with or without boundary prism layers and other cell forms.

Possible errors associated with grid generation are:

- Number of cells (resolution)
- Cell distribution
- Cell quality

Number of cells: Typically the higher the grid resolution the better the results. The drawback is that much more computer power is required, especially for transient problems. Nielsen, P. et al (2007) provide a rough guideline for the typically sufficient number of cells for various rooms. This guideline does not provide information about how boundary layers should be resolved. The guideline is valid for standard turbulence modelling with wall functions. When LES is use, the number of cells should be 100 times higher or more. This illustrates the significant use of computational resources through LES.

$$N = 44.4 * 10^3 * V^{0.38}$$

Where: N= number of cells and V = room volume (m³)

Figure 3.1.5 illustrates the use of the guidelines by example of two different room sizes.

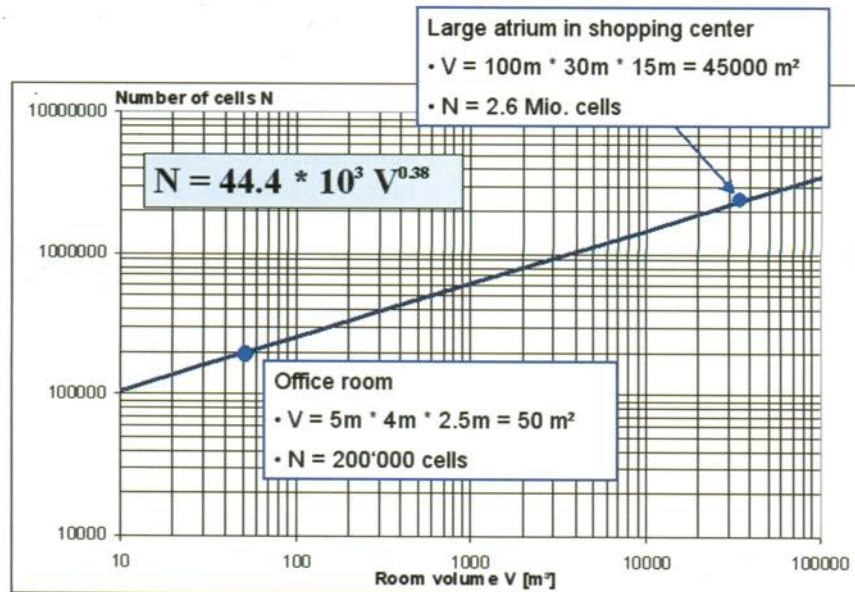


Figure 7.9 Rough guideline formula on number of cells needed in room air flow. An office room, $V = 5\text{m} \times 4\text{m} \times 2.5\text{m} = 50\text{ m}^3$, yields 200 000 cells, and an atrium, $V = 100\text{m} \times 30\text{m} \times 15\text{m} = 45\text{ 000 m}^3$, yields 2.6 Mio. cells.

Figure 3.1.5: Rough guideline to determine cell numbers for internal CFD (Nielsen, 2007)

Cell distribution

Nielsen, P. et al (2007) suggest that a higher resolution of cells be used in areas of relevant flow phenomena, such as boundary conditions, internal heat plumes. The authors suggest that at least 5 – 10 cells in each direction are required to resolve a flow phenomenon.

Cell quality

Cells have to be sufficient “quality”. Low quality cells are those that are distorted, squeezed or degenerated. They introduce numerical error. A measure of quality is represented by cell criteria such as angles, determinates, aspect ratio, expansion ratio and others. Figure 3.1.6 illustrates some of these quality criteria. The author states that the numerical error introduced by the grid cells are larger for tetrahedral cells than for hexahedral. Some CFD codes are more susceptible to low quality cells than others.

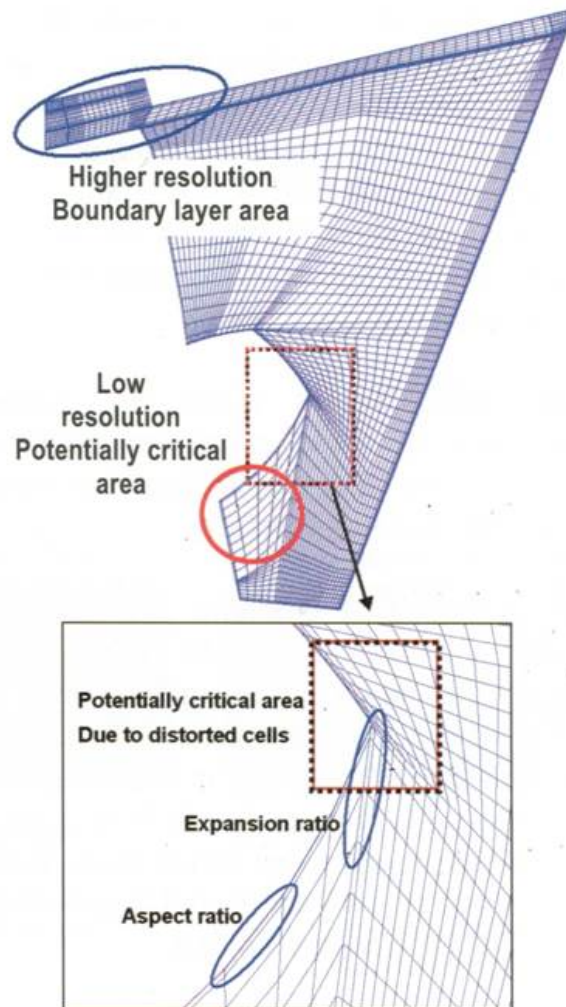


Figure 3.1.6: Different cell quality situations in CFD simulations (Nielsen, 2007)

Nielsen, P. et al (2007) provides rule-of-thumb criteria to avoid ad quality cells. (The author points out that these criteria are code dependent)

- Angles between 20° and 160°
- Expansion ratio < 2
- Aspect ratio < 10 (for hexahedral cells)
- At least 5 to m10 grid points in each direction for areas of important floe phenomena
- As a rule thumb, use 0.1 m for normal rooms (about 5 m) and 0.3 m for larger rooms

The best approach is to perform a grid independent study for each class of problems. Figure 3.1.7 and 3.1.8 illustrates an example of a simple room with air flow. Figure 3.1.7 shows the simple geometry and Figure 3.1.8 indicates the results obtained with different grids. Figure 3.1.8 (a) shows the results obtained with a coarse grid. There is a good convergence but the flow below the window is not plausibly portrayed. In the case of a medium grid, shown in Figure 3.1.8 (b), bad convergence was obtained along with unstable interface between cold layer and warm room. The use of a fine grid, shown in Figure 3.1.8 (c), a good convergence is obtained and plausible results.

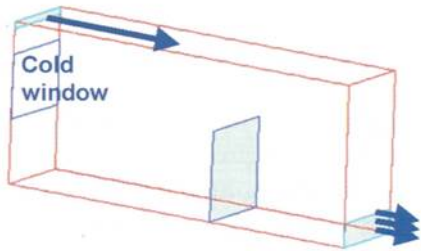


Figure 3.1.7: Simple geometry for room with cross flow (Nielsen, 2007)

Modelling

Nielsen, P. et al (2007) suggest that the following models are important in interior CFD air flow investigation:

- **Turbulence model:** There are various models that can be chosen. Typically high-level turbulence models require more computational resources. The commonly used k- ϵ -model has limitations that can be overcome with the use of SST model. Disagreements with measurements can sometimes, but not always, be attributed to the use of k- ϵ -model.
- **Buoyancy model:** For incompressible flows the Boussinesq approximation can be used to approximate buoyancy. However, for temperature differences higher than 50°C or mixtures of heavy and lighter gases the ideal gas-law and variable density have to be used.

3. Internal CFD – Numerical Assessment of Air Movement Inside Buildings

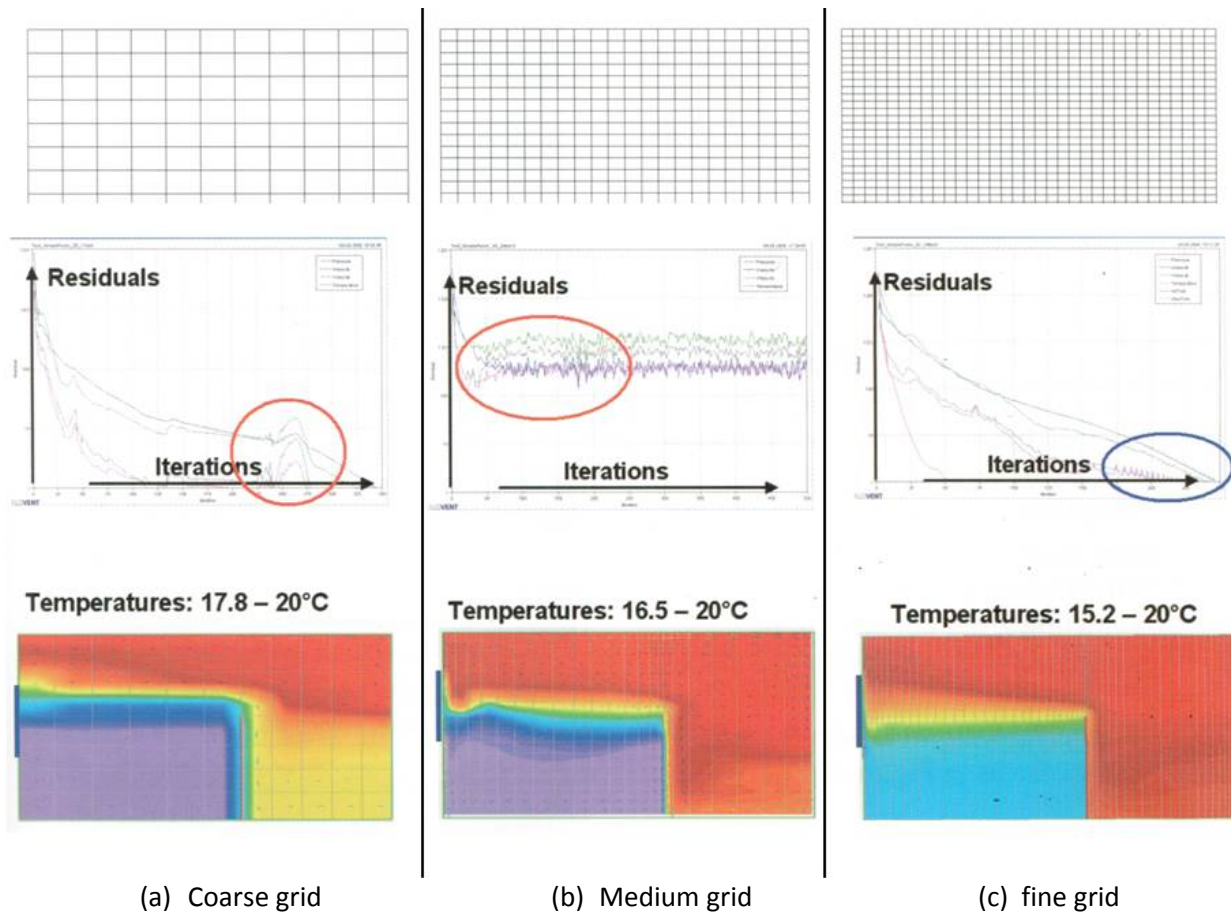


Figure 3.1.8: Three types of grids used in simulating flow in simple room geometry (Nielsen, 2007)

- **Radiation model:** Various radiation models are available. For approximate results CFD simulations should use radiation between surfaces in room air flow in connection with heat flux boundary conditions. Neglecting radiation in ventilation typically results in an incorrect temperature distribution. Figure 3.1.9 shows a basic example (a) without considering radiation and (b) with a simplified radiation model.
- **Other models:** There are other models that might be of importance to simulate interior airflow and thermal phenomena, such as 2-phase flow model, such as phase-change of water vapor to liquid)

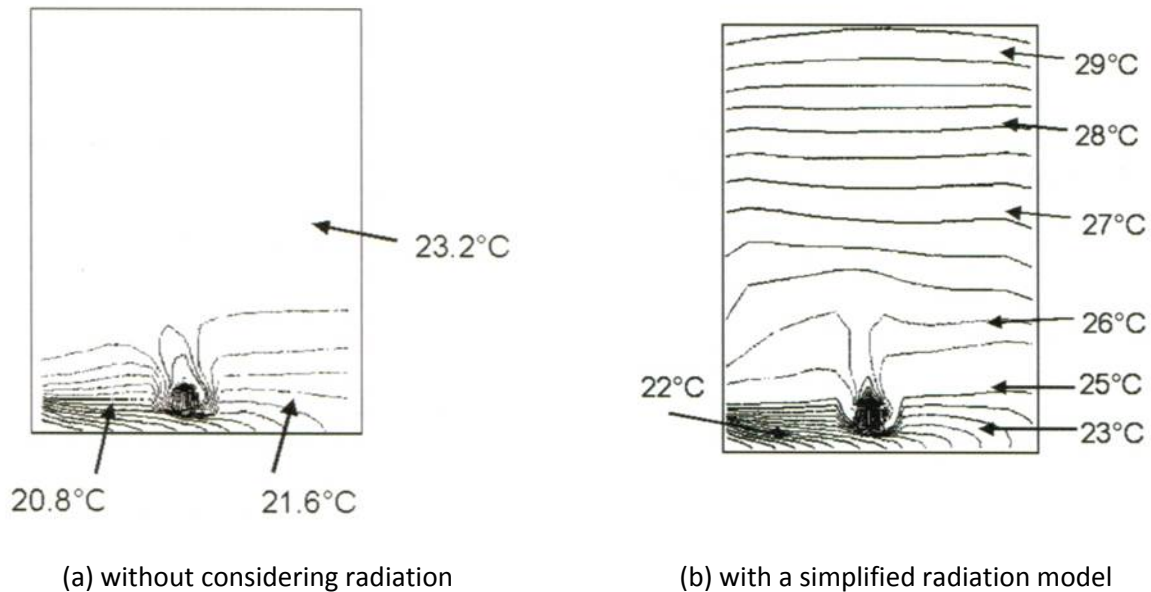


Figure 3.1.9: Use of radiation models in interior CFD simulations (Nielsen, 2007)

Boundary Conditions

The correct selection of boundary conditions is one of the most important sources for errors, since it can result in computational instability. It might be necessary to try several numerical possibilities and make an “informed” judgment which boundary condition is appropriate.

Nielsen, P. et al (2007) suggest the following frequently errors in choosing the boundary condition.

Often the temperature boundary conditions are not well known a priori and that thermal simulations are necessary to obtain plausible boundary conditions

Problems can arise if too small computational domains are chose for inlet and outlet conditions. In these cases the flow problem should be provided that it adjust itself to the real flow

An example of an incorrect and a correct boundary condition for several free flow openings is given in Figure 3.1.10. Using the boundary condition in Figure 3.1.10 (a) will very unlikely predict the free flow through the opening correctly. Figure 3.1.10 (b) shows more suitable boundary conditions where the outer domain is large enough so that the settings at its boundaries do not influence the flow through the connections to the room

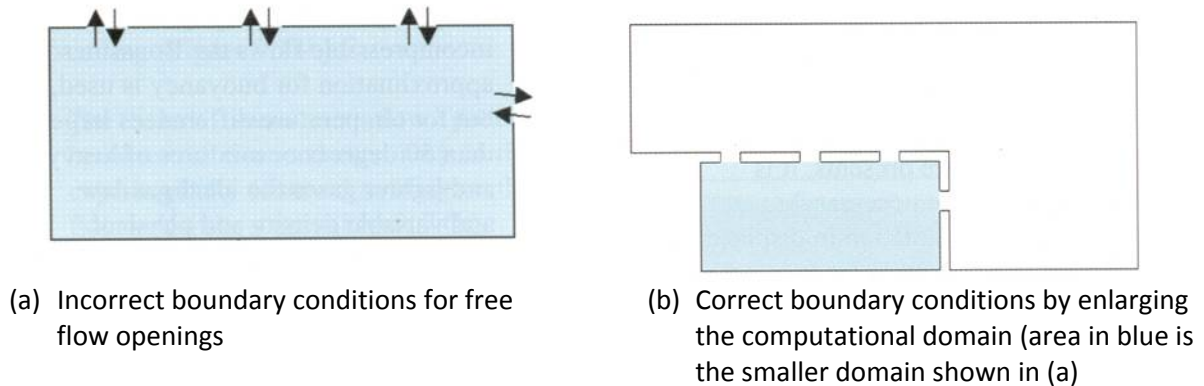


Figure 3.1.10: Examples of boundary conditions in free flow openings (Nielsen, 2007)

Nielsen, P. et al (2007) provide 2 other examples for potentially incorrect boundary condition settings:

- Exhaust openings with prescribed velocity rather than a pressure boundary
- Open window with free flow boundary
- Several exhaust openings at different height levels with pressure boundaries
- Incorrect assumption of symmetry plane
- Wind influence without boundary layer profile at the inlet

Check points to improve quality of the CFD simulation

The quality of the CFD simulation requires that certain aspects, presented earlier are adopted. Not all of these aspects need to be adopted, it depends on the problems that have to be solved with the help of CFD simulations. Generally, with the start to work on certain CFD class of problems, an appropriate set of quality check test should be performed. Some CFD vendors make codes available for which quality checks have already been performed. If the CFD practitioner keeps the major settings the same as the previously tested cases, chances are high that no new quality checks have to be performed.

The following provides a summary of important basic guidance for CFD simulations for internal spaces:

Check for plausibility: Remember that CFD analysis is an analysis of a simplified model of reality.

Understanding the airflow phenomena pays off: Here are things to check:

3. Internal CFD – Numerical Assessment of Air Movement Inside Buildings

- Mass balance of inlet and outlet has to match, this means input and output has to be the same, unless matter is created or stored inside the system boundaries.
- Energy balance of the room has to be conclusive. The energy balance has to result in a zero sum of all internal loads, external loads, and stored loads as well as energy transfer through the boundaries.
- Temperature balance: how the average room temperature compares with the mean temperature for the energy balance.

Check for computational grid:

- Determine what grid was use, a structured or unstructured grid; were prism boundary layers used?
- Grid characterization: number of cells, largest cell, smallest cell in different areas
- Grid resolution

Check for numerical method used:

- A 2nd order scheme is required
- Check for monitoring points

Check for models:

Energy equation needs to be solved including buoyance forces.

- Generally necessary for room air flow simulations with comfort issues
- Boussinesq approximation valid for incompressible flow if temperature $<40^{\circ}\text{C}$, otherwise alternative assumptions for boundary conditions

Radiation model:

- Generally necessary for room air flow simulations with comfort issues
- Turbulence model

Check for boundary conditions:

- Are the locations of inlets and outlets correct and justified
- Are the boundary conditions for supply diffuser realistic
- Can a symmetry plane be used

3. Internal CFD – Numerical Assessment of Air Movement Inside Buildings

- Can volume sources for persons (without obstructions) be used

Check for simulation results:

- Are the airflow patterns plausible
- Are boundary layer flows correlated with high and low temperatures
- Are area of high and low temperatures plausible
- Are there flows around obstacles plausibly simulated

General hints:

- Always start with a simple grid in order to get an understanding and check the proper settings of the model.
- Check the boundary conditions to check for the reasons for results that are unexpected, implausible and expected, even if they have good calculation performance, such as good convergence.
- Keep good documentation of the CFD project, list all parameters used in the simulations.
- Prepare a good overview of all cases investigated
- Use consistent post processing for the results, such as consistent views, the same color distribution and the same value scales.

3.2 Domain Decomposition and Coupled CFD Analysis

There are two approaches to predict internal airflow phenomena through the use of CFD analysis. The first approach is called domain decoupling or “decoupled” approach. In this approach the domain on the exterior of the building is first analyzed and the results in regard to pressure distribution and airflow. These results are then used as boundary condition for the CFD simulation of the interior space. The second approach is the so-called “coupled” approach where the exterior and interior space is combined as the overall computational domain.

The advantage of the decoupled approach is that it requires fewer computational resources than the coupled approach. The disadvantage is that internal airflow cannot be precisely predicted, especially close to free flow openings.

Van Hoff and Bocken (2010a) report that wind flow in urban environments is an important factor for a large number of physical processes that can affect human health and comfort and the durability of man-made constructions. Wind related phenomena that are subject to extensive investigation for the design of structures and planning of neighborhoods are atmospheric transport and dispersion of solid, liquid and gaseous air pollutants, wind loading, pedestrian wind comfort and natural ventilation of buildings. The following describes articles describe wind induced processes that relate to natural ventilation performance of buildings.

With regard to the use of terms, authors use different terms to describe the same CFD domain calculation. The term “full-domain” is synonymous with “coupled flow”. The terms “recoupled domain” and domain decomposition” or “decomposed domain” are synonymous with “un-coupled flow”. Furthermore, it should be noted that the literature also refers to “coupled” CFD models when CFD calculations are coupled with energy simulations. This type of coupling is performed to increase the accuracy of ventilation prediction with reduced computing efforts. When coupling CFD with multizone airflow programs a more accurate ventilation performance can be evaluated. A coupled CFD -multizone system provides more accurate ventilation predictions over a longer duration and achieve a time dependent building ventilation performance, than when using multi-zonal approaches alone. While CFD provide only a snapshot in time of a steady state ventilation scenario, the multi zone results typically extend over a longer time, such as an annual prediction of ventilation. In the following discussion “coupled CFD” only refers to the domains used in CFD calculations.

Nore et al (2010) reports on an investigation of narrow (23 mm) ventilated facade cavities of a low-rise building by coupled and decoupled CFD simulations. In the coupled simulations, the wind-flow pattern around the building and the resulting air flow in the cavities are calculated simultaneously and within the same computational domain. In the decoupled simulations, two separate CFD simulations are conducted: a simulation of the wind flow around the building (with closed cavities) to determine the surface pressures at the cavity inlet and outlet openings, and a simulation of the cavity airflow, driven by

these surface pressures. The author indicated that the results of the coupled simulations compared favorably with those from past experimental studies. Comparing the results from the coupled and decoupled simulations allowed them to assess the local losses (entrance and exit losses) of the cavities.

Ramponi and Blocken (2012c) report on a series of coupled 3D steady RANS simulations for a generic isolated building. The CFD simulations were validated based on detailed wind tunnel experiments with Particle Image Velocimetry (PIV). The authors describe that in in CFD simulations of cross-ventilation involving large openings, a major issue of concern is the accurate modeling of the interaction between the outdoor wind flow around the buildings and the indoor air flow inside the buildings, which interact with each other at the ventilation openings. A distinction can be made between a coupled and a decoupled approach. Figure 3.2.1 indicates the difference between the coupled and uncoupled domains as used in CFD calculations.

In the coupled approach, there is a single computational geometry and computational domain, that includes both the outside and the inside environment of the building (Fig. 3.1.4.A (a)). In this approach, the ventilation openings are considered open, the outdoor wind flow and indoor air flow are solved within the same computational domain and the interaction (coupling) between the outdoor wind flow and indoor air flow is resolved in detail using the appropriate governing equations. Contrary to this, in the decoupled approach, there are two different computational geometries and two different computational domains: one for the outdoor environment and one for the indoor environment of the building (Fig. 3.1.4.A (b)). In this approach, the wind flow simulation is conducted for the building as a sealed body, i.e. the openings are “closed”. This simulation yields the pressure coefficients at the positions of the openings and these coefficients are subsequently used as boundary conditions for the CFD simulation of the indoor air flow.

Ramponi and Blocken (2012) suggest, based on a detailed literature review that, by far, most CFD research on wind induced cross-ventilation has applied the coupled approach. An extensive, but not necessarily exhaustive, overview of coupled outdoor-indoor CFD studies included indicates the type of study (generic or applied), the type of building and surroundings (isolated, building group, urban), the turbulence modeling approach (RANS, LES, DES) and turbulence models used, whether validation was performed, and whether and for which parameters a sensitivity analysis was performed.

The authors suggest that the main reason for the extensive use of the coupled approach is the knowledge that, in case of large ventilation openings, the decoupled approach can introduce important errors. The decoupled domain approach, which includes the so-called sealed-body assumption, implies that the pressure distribution on the building envelope is not affected by the presence of the openings. It assumes that the turbulent kinetic energy is dissipated at the windward opening and that the effect of the dynamic pressure on the air flow passing through the opening is negligible. However, in case of wind

3. Internal CFD – Numerical Assessment of Air Movement Inside Buildings

flow through large ventilation openings, the turbulent kinetic energy is rather preserved and the sealed-body assumption might therefore no longer valid.

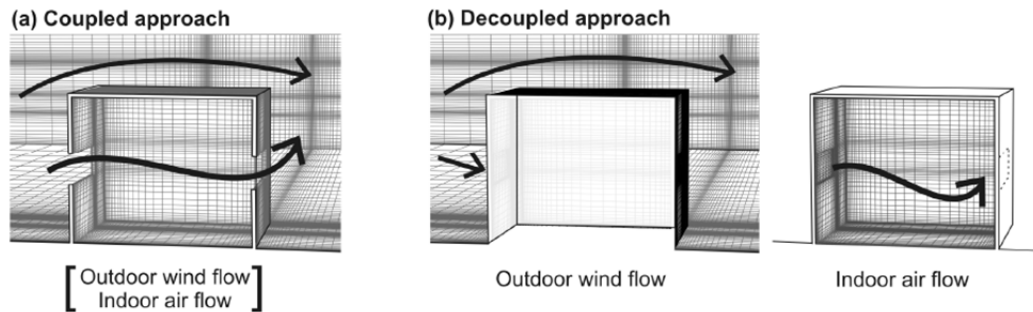


Figure 3.2.1: (a) Coupled and (b) decoupled approach for analysis of wind-induced cross-ventilation of buildings (Ramponi and Blocken (2012))

Figure 3.2.2 illustrates a comparison between measured velocity vector (e.g. “PIV”) and a coupled CFD reference case for the vertical center plane and the horizontal plane at mid-height through the openings (Ramponi and Blocken, 2012). The figure suggests good general correlation of the velocity flow fields between measured (PIV) and coupled CFD reference case. It should be noted that the experimental data obtained by PIV cannot resolve the flow field in close proximity to openings.

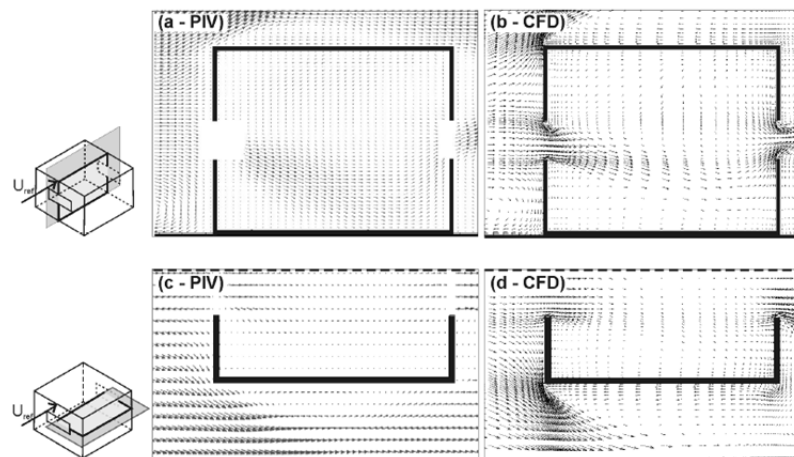


Figure 3.2.2: Comparison of the velocity vector fields obtained with the PIV measurements and the CFD reference simulation case in the vertical centerplane and in the horizontal plane at mid-height through the openings (Ramponi and Blocken (2012))

Figure 3.2.3 shows the comparison of experimental (PIV) and reference CFD case for the streamwise wind speed ratio U/U_{ref} along the centerline. Figure 3.2.3 suggests a very good correlation between the measurements and CFD predictions. Furthermore an increase in wind speed downstream of the openings can be observed with both the measure and CFD predictions.

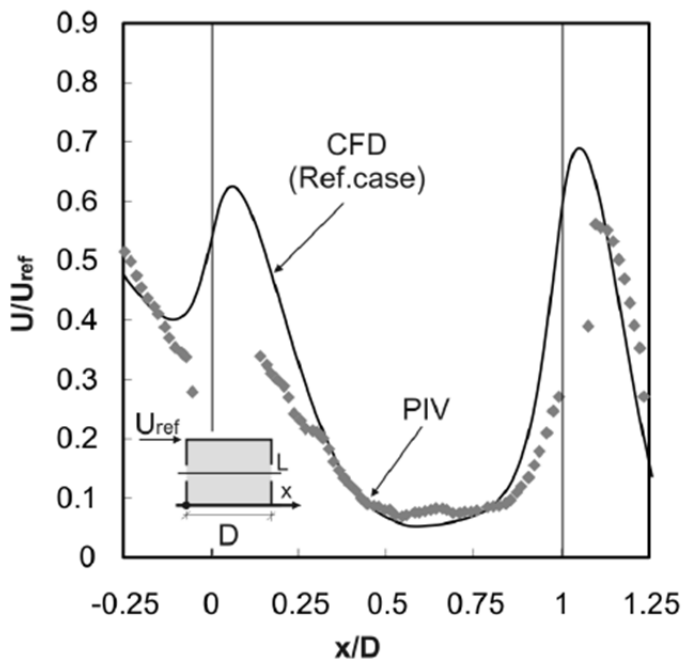


Figure 3.2.3: Comparison of experimental (PIV) and reference CFD case for the streamwise wind speed ratio U/U_{ref} along the centerline.

VanHoff and Blocken (2010a) report on a coupled CFD modeling approach for urban wind flow and indoor natural ventilation applied to a large sports arena. The authors suggest that, to their knowledge, this CFD study was the first coupled CFD simulation of urban wind flow and indoor natural ventilation in complex urban environments, and for complex buildings, geometries have not yet been performed. The authors point out that wind flow is very complex and that appropriate tools are required for characterization of the flow and the related processes. They name three main approaches: (1) on-site full-scale experiments; (2) reduced-scale wind tunnel measurements; and (3) numerical modeling with Computational Fluid Dynamics (CFD). As opposed to experiments, the main advantages of CFD are that it provides information on the relevant flow variables in the whole calculation domain (whole-flow field data), under well-controlled conditions and without similarity constraints. However, the accuracy of CFD is an important matter of concern. Care is required in the geometrical implementation of the model and in grid generation, and solution verification and validation studies are imperative.

The authors point out advantages and disadvantages of coupled and decoupled CFD domains. In the coupled CFD simulation which both the outdoor and indoor air flow are modeled simultaneously and within the same (therefore coupled) computational domain. This method allows the proper calculation of air flow in the proximity of and through ventilation openings. The main disadvantage of this method in urban applications is the large difference in geometrical length scales between the outdoor (urban) environment (1-5 km) and the ventilation openings (e.g., 0.01 – 1 m), resulting in a large and high-resolution grid, and thus in a relatively high computational cost. The authors stipulate that this might probably be the reason why the coupled CFD approach method has only been used for relatively simple outdoor and indoor environments and relatively large ventilation openings.

In the case of the decoupled simulation the authors suggest that very large grids that would be required to include the complex outdoor and indoor environments and/or for small ventilation openings can be avoided. In decoupled simulations two separate simulations are conducted, one for the outdoor flow and one for the indoor flow, each in their own computational domain. In the outdoor flow simulations, the ventilation openings are closed. The information obtained from the simulation of the outdoor flow (generally pressure coefficients at the positions of the openings) can be used as boundary condition for the simulation of the indoor flow. Although this is the standard approach for indoor ventilation studies, its accuracy can easily be compromised because of the simplifications involved. Often, only pressure is passed from the outdoor to indoor environment by means of pressure coefficients at the boundary, and assumptions are made in terms of discharge coefficients and expansion coefficients.

The main objective of performing the coupled CFD ventilation study of the stadium was to determine alternatives in the ventilation openings in the envelope. There have been instances where the thermal (overheating) and ventilation performance, the latter being quantified as air changes per hour (ACH) of the arena was insufficient. Coupled CFD simulations are performed in the stadium study was to verify present natural ventilation configuration of the entire building and evaluate four alternative ventilation configurations to improve thermal and ventilation performance. The alternative configurations consist of one specific geometrical change made to the current stadium geometry with closed roof, except for the last configuration, which has an open roof.

The resulting grid for the stadium is depicted in Figure 3.2.4. A coarse and a fine grid were produced with 3 and 9.2 million cells respectively. The different grid sizes were used in sensitivity tests. The results of the CFD calculations were compared with air flow measurements conducted at various representative points at the stadium envelope. Alternatives of larger ventilation openings in the building envelope were investigated by modifying the grid. The different ventilation configurations were evaluated and compared based on the overall ventilation rate/ACH of the entire indoor air volume. The ACH for the alternatives were calculated based on the mass flow rates through the ventilation openings. Therefore, the most relevant locations are the ventilation openings, and the most relevant parameter is the mass flow rate through these openings. Figure 3.2.5 shows contours of non-dimensional velocity magnitude

3. Internal CFD – Numerical Assessment of Air Movement Inside Buildings

U/U10 in four horizontal planes, for the representative wind direction at different heights. The lower wind speed ratios around the stadium indicate that it is situated in the wake of the surrounding buildings, which causes the lower air exchange rates for this wind direction.

The CFD based design optimization of the stadium ventilation openings in which four alternatives to the current ventilation configuration were evaluated resulted in a significantly improved ventilation performance for two of the alternatives. (See Table 3.2.1)

Table 3.2.1: Calculated air change rate per hour (ACH) for the current situation and for four alternative ventilation configurations, for reference wind speed U10 = 5 m/s, for wind directions = 16°, 151°, 196° and 331° and for fixed indoor surface temperatures. (VanHoff and Blocken, 2010)

Ventilation configuration	ACH (h ⁻¹)				
	φ (°)				
	16°	151°	196°	331°	Average
Current situation	1.51	1.33	1.11	1.49	1.36
Configuration 1	1.56	1.52	1.12	1.33	1.38
Configuration 2	1.91	1.61	1.29	1.54	1.59
Configuration 3	2.19	2.28	1.61	1.72	1.95
Configuration 4	4.57	3.40	2.66	3.41	3.51

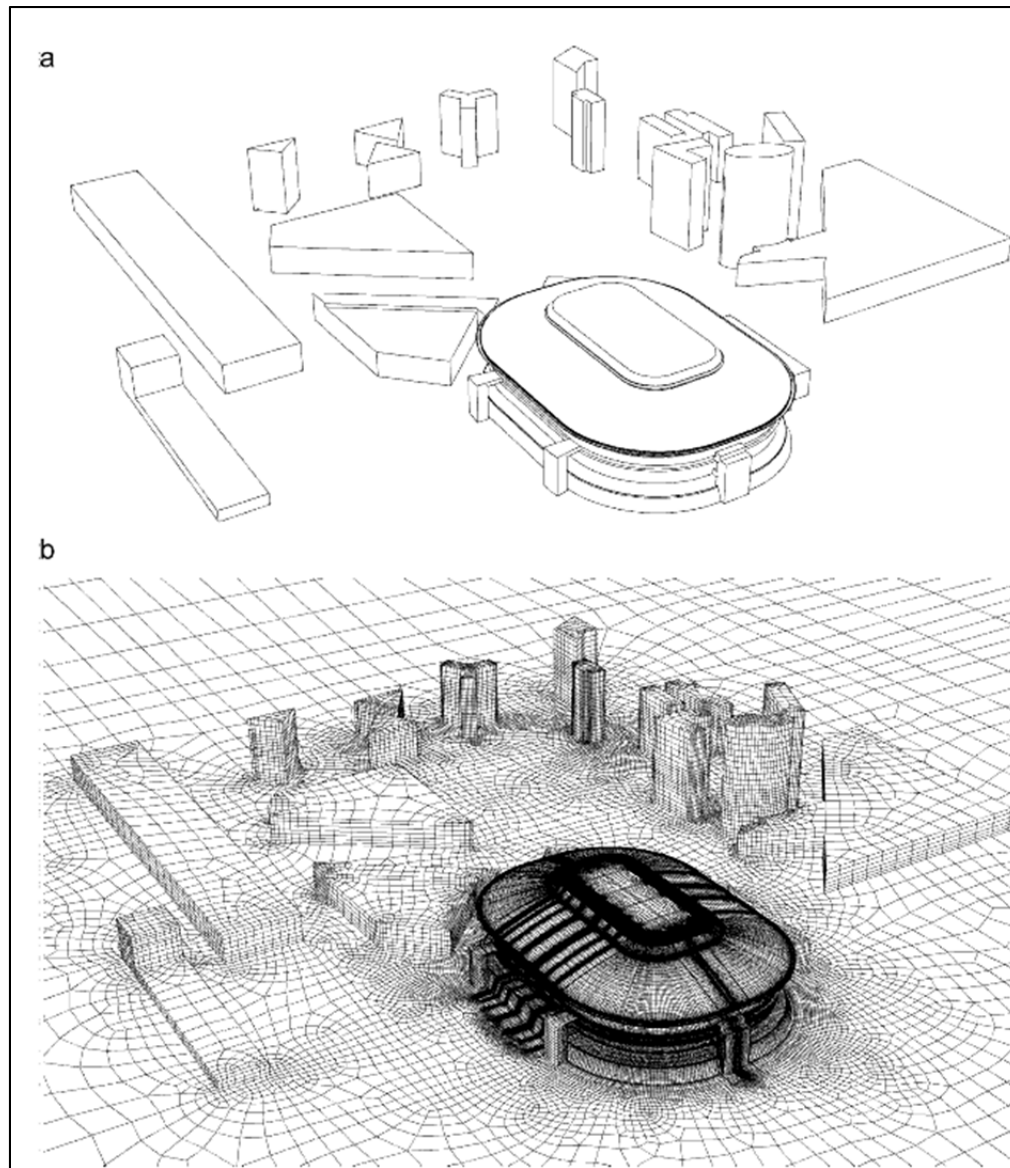


Figure 3.2.4: (a) Computational model geometry, view from northeast; (b) Computational grid on the building surfaces and part of the ground surface. A high resolution is used in the proximity of the stadium, and a lower resolution at a larger distance from the stadium. (VanHoff and Blocken, 2010a)

3. Internal CFD – Numerical Assessment of Air Movement Inside Buildings

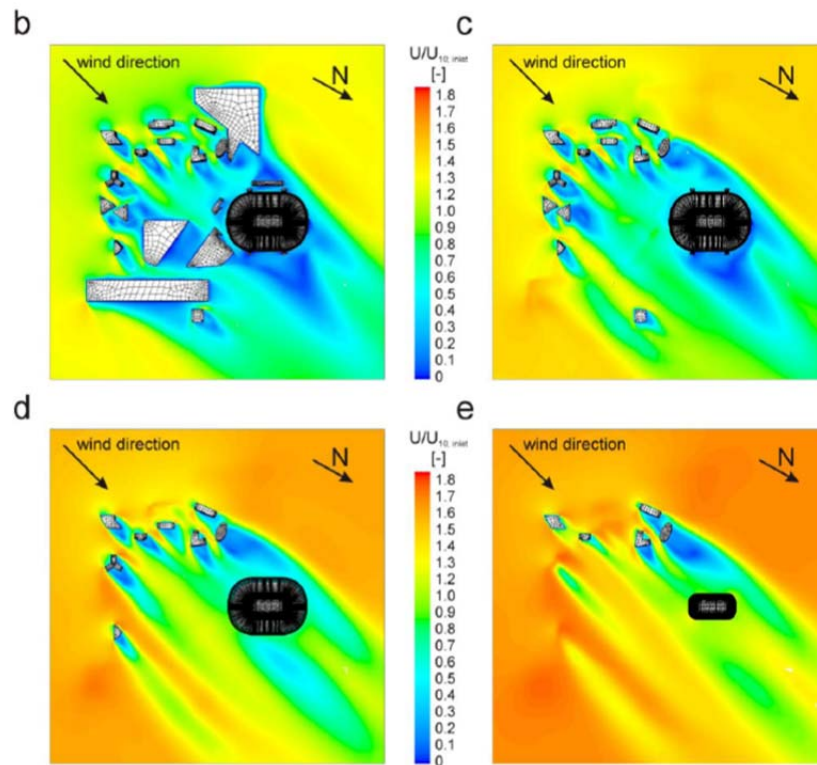


Figure 3.2.5: Contours of non-dimensional velocity magnitude U/U_{10} in four horizontal planes at different heights (VanHoff and Blocken, 2010a; modified)

Meroney (2009) reports on studies that compare results of internal flow evaluated from full domain (coupled) and decomposed (de-coupled) domain investigations. The author points out that CFD analysis is first performed for the flow field outside the building, from which boundary conditions are extracted for the analysis of the indoor situation. Boundary conditions of wind pressures and flow orientation at proposed opening locations are used to estimate internal pressure coefficients based on cross-building surface pressures, and opening discharge coefficients related to a dimensionless internal room pressure to predict opening flow rates. Although the different turbulence models produced significantly different external flows, it appears that since the internal flows are primarily driven by cross building surface pressures which did not vary strongly, the cross ventilation air flow values are very similar.

Meroney (2009) compared internal flow characteristics, expressed as a flow vector field and internal pressure coefficients, between the full and decomposed domain. Both pressure fields were also compared to measured values. The author reports very similar internal flow values for both the full and decomposed domains. Furthermore the values compare well with measured internal pressures. Figure 3.2.6 shows a comparison between values of external and internal air flow for different cases examined measured in the wind tunnel (1), in the full domain (2) and in the decomposed domain. The field

3. Internal CFD – Numerical Assessment of Air Movement Inside Buildings

measurements were unable to provide values near the openings due to generic limitations of data equations. The full-domain predictions are only dependent on domain entrance conditions and building dimensions. The decomposed domain prediction is only dependent on boundary conditions extracted from the full-field sealed building surface results. Both the field data and full-domain CFD calculations reproduce the *vena-contracta* that occurs downwind of the inlet opening, which results in maximum concentrations occurring about one half opening dimension within the room. The domain decomposition approach does not produce a *vena-contracta*, and maximum velocities tend to occur at the inlet opening.

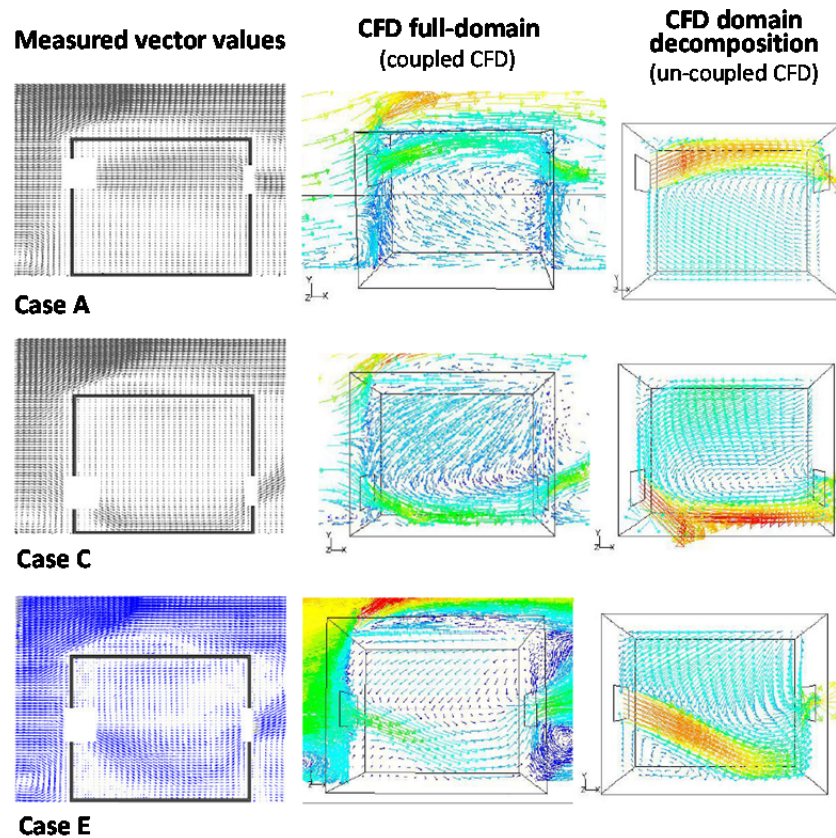


Figure 3.2.6: Velocity vectors on building vertical midplane for three case Cases, obtained from measured air flow and coupled and uncoupled flow domains (Meroney, 2009; modified)

Meroney (2009) further describes the internal flow field by means of the ratio of x-component velocity to reference velocity as a function of the distance along the centerline of the space. Figure 3.2.7 shows an example of the ratio of x-component velocity to reference velocity for Case C (compare Figure 3.2.7).

3. Internal CFD – Numerical Assessment of Air Movement Inside Buildings

The given data suggest measured values and full-domain CFD calculations display a maximum local velocity just downstream of the inlet and outlet openings, but the domain decomposition method does not, although it otherwise reproduces flow variations quite closely. Figure 3.2.8 shows the variation of static pressures along the same line joining the openings for full-domain and domain decomposition CFD calculations. The author suggests that this data again shows that full-domain (coupled) and decomposed domain can reproduced the variations of internal pressures within the building very closely.

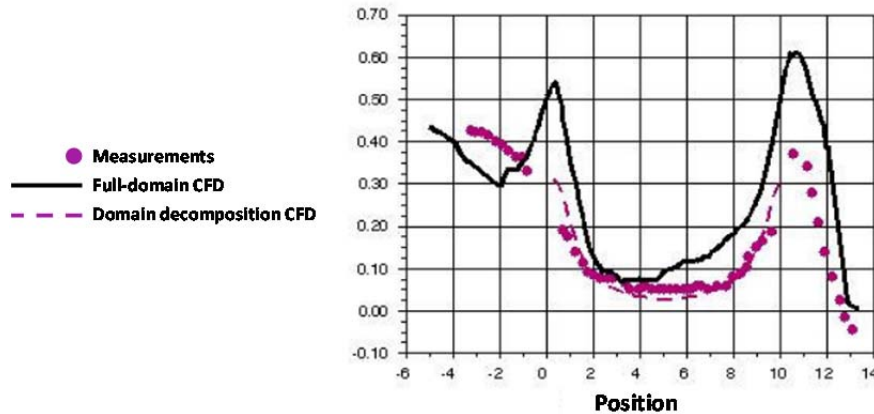


Figure 3.2.7: Velocity ratio VX/V_{ref} along line joining inlet and outlet openings for Case C (Meroney, 2009) modified

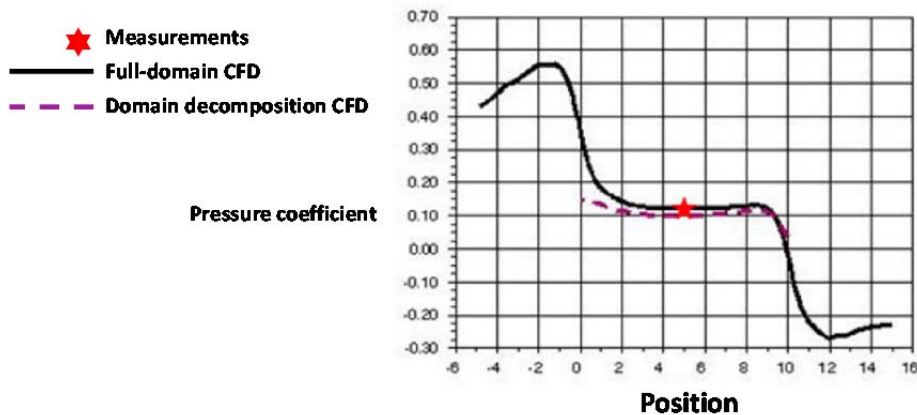


Figure 3.2.8: Static pressure coefficient, C_p , along line joining inlet and outlet openings for Case C (Meroney, 2009)

3.3 Selection of Type of Mesh and Cells

The quality of the mesh plays a significant role in the accuracy and stability of the numerical computation. The attributes associated with mesh quality are node point distribution, smoothness, and skewness. Depending on the cell types in the mesh (tetrahedral, hexahedral, polyhedral, etc.), different quality criteria are delineated in guidelines (ANSYS, 2009):

- Cell squish on all meshes. Cell squish is a measure used to quantify how far a cell deviates from orthogonality with respect to its faces. *Squish index* is computed for cells using the vector from the cell centroid to each of its faces and the corresponding face area vector. A poorly generated cell has a cell squish index close to 1, with better cells having smaller indices, ideally close to zero. For tetrahedral meshes, either skewness or cell squish index can be used to measure the mesh quality. Skewness information is not available for polyhedral meshes therefore must be relied on the cell squish index and an additional index for the face squish (which is computed using the vector connecting the centroids of adjacent cells). A good rule of thumb is that the maximum skewness for tetrahedral cells should be less than 0.95. The maximum cell squish index for all types of cells should be less than 0.99.
- Skewness is defined as the difference between the shape of the cell and the shape of an equilateral cell of equivalent volume. Highly skewed cells can decrease accuracy and destabilize the solution. For example, optimal quadrilateral meshes will have vertex angles close to 90 degrees, while triangular meshes should preferably have angles of close to 60 degrees and have all angles less than 90 degrees. As a general rule the maximum skewness for a triangular/tetrahedral mesh in most flows should be kept below 0.95, with an average value that is less than 0.33. A maximum value above 0.95 may lead to convergence difficulties and may require changing the solver controls, such as reducing under-relaxation factors and/or switching to the pressure-based coupled solver.
- The aspect ratio is a measure of the stretching of a cell. It is computed as the ratio of the maximum value to the minimum value of any of the following distances: the distances between the cell centroid and face centroids, and the distances between the cell centroid and nodes. For a unit cube (Fig. 3.3.1), the maximum distance is 0.866, and the minimum distance is 0.5, so the aspect ratio is 1.732. This type of definition can be applied on any type of mesh, including polyhedral.

3. Internal CFD – Numerical Assessment of Air Movement Inside Buildings

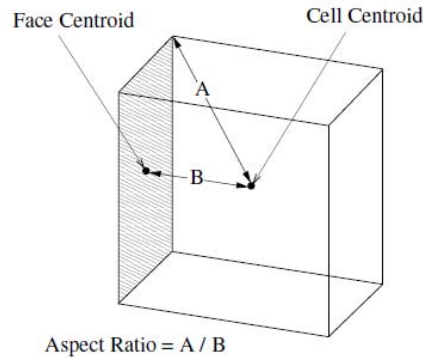


Figure 3.3.1: The aspect ratio for a unit cube (ANSYS, 2009)

Other best practices on computational grids by Franke et al. (2007) summarized several recommendations on the choice of computation grid which affects the computational expense and accuracy. According to these best practices, the grid has to be constructed to: minimize the errors, have adequate resolution and capture the important physics phenomena.

Here are some recommendations:

- Ideally the grid is equidistant.
- The expansion ratio between two consecutive cells should be below 1.3 in these regions.
- The angle between the normal vector of a cell surface and the line connecting the midpoints of the neighboring cells, ideally these should be parallel.
- Hexahedra are preferable to tetrahedral, as the former are known to introduce smaller truncation errors and display better iterative convergence.
- On walls the grid lines should be perpendicular to the wall.
- Prismatic cells should be used at the wall with tetrahedral cells away from the wall.
- In the area of interest, at least 10 cells per cube root of the building volume should be used and 10 cells per building separation to simulate flow fields as an initial minimum grid resolution.
- When a global systematic grid refinement is not possible due to resource limitations, then at least a local grid refinement should be used in the area of the main interest.

Hefny and Ooka (2009) assessed two discretization methods relating to mesh generation: tetrahedral-based meshing and hexahedra-based meshing. Hexahedral-based meshing requires significant time and effort while tetrahedral-based meshing can be constructed much faster in complex geometries. To do so, the authors carried out a CFD analysis of pollutant dispersion around a building using two different cell shapes with four different resolutions ranging from 150,000 to 1,000,000 control volumes. The

3. Internal CFD – Numerical Assessment of Air Movement Inside Buildings

quality of their solution was determined on the observed gas concentration as well as the quantitative grid convergence, which was calculated based on a grid convergence index (GCI).

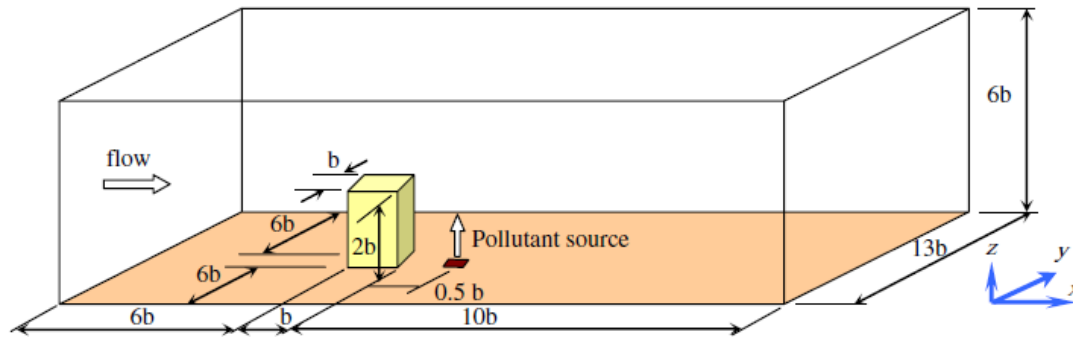
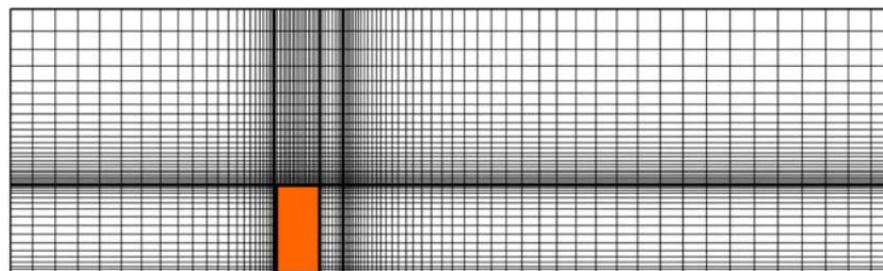
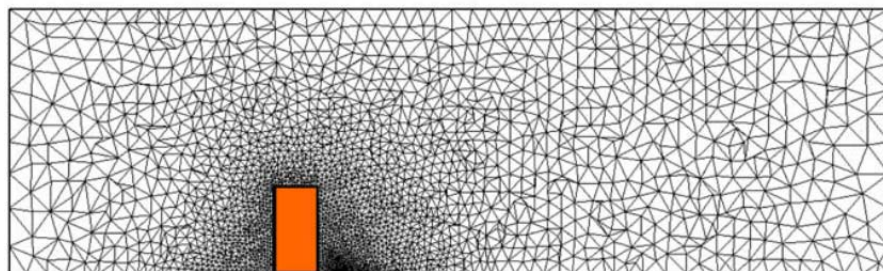


Figure 3.3.2: Computational domain (Hefny and Ooka, 2009)



Hexahedral-based mesh



Tetrahedral-based mesh

Figure 3.2.2.C: Hexahedral-based and Tetrahedral-based mesh (Hefny and Ooka, 2009)

Table 3.3.3: Details of computational cases (Hefny and Ooka, 2009)

Table 1

Details of computational cases.

Grid resolution	Subdivisions ($x \times y \times z$)	Mesh		Min. grid spacing
		Cells (approximate)	Vertexes (approximate)	
Hexahedral-based meshes				
Coarse (H1)	90 × 48 × 35	150,000	163,800	0.07
Medium (H2)	114 × 94 × 44	300,000	322,015	0.05
Fine (H3)	143 × 118 × 55	600,000	634,932	0.035
Very fine (H4)	169 × 140 × 65	1,000,000	1,048,675	0.028
Tetrahedral-based meshes				
Coarse (T1)	–	150,000	27,210	0.07
Medium (T2)	–	300,000	53,780	0.05
Fine (T3)	–	600,000	105,342	0.035
Very fine (T4)	–	1,000,000	175,885	0.028

Hefny and Ooka (2009) found that hexahedral-based meshing produced higher quality solution than tetrahedral meshing. More specifically, the hexahedral-based approach is able to capture the pollutant concentrations around buildings even in the case a coarse mesh is used, while the tetrahedral-based approach failed to adequately capture the pollutant concentrations for most mesh cases considered. The authors points out that where there is no symmetry in the contours around the centerline, there are inaccurate predictions near the pollutant source. The hexahedral-based approach produced the GCI values (truncation error values) below those from tetrahedral-based approach for all resolutions. This study implies taking special consideration when employing an unstructured tetrahedral-based mesh to ensure that the mesh is fine enough and any numerical errors should be documented to assess the quality of the numerical solution.

Biswas and Strawn (1998) presented their work on two unstructured mesh adaptation schemes for CFD problem: the tetrahedral and the hexahedral mesh adaptation procedures using edge-based data structures for efficient subdivision. Tetrahedral mesh adaptation causes poor mesh quality as deploying repeated refinement. Hexahedral meshes have the advantage of allowing for anisotropically subdivided repetition. To eliminate the “hanging vertexes” in the hexahedral meshes, pyramids, prisms and tetrahedral mesh adaptation uses as tetrahedral as buffer elements for refinement. Biswas and Strawn (1998) also asserted that adaptive hexahedral meshes and tetrahedral meshes showed good agreement

but adaptive hexahedral meshes is more computational efficiency than that of tetrahedral meshes in terms of computer resources and calculating time.

Table 3.3.1: Grid convergence index (GCI) for all mesh schemes (Hefny and Ooka, 2009)

Table 2

Grid convergence measures for all mesh schemes.

Cell geometry	Grid size ($\times 10^3$)	r value	ε_{rms} (%)	GCI (%)
			C_g	C_g
Hexahedron	300–150	1.26	1.71	2.91
	600–300	1.26	0.29	0.49
	1000–600	1.26	0.19 ^a	0.33 ^a
Tetrahedron	300–150	1.26	4.54	7.73
	600–300	1.26	2.88	4.90
	1000–600	1.26	0.98	1.68

^a Minimum value for all cases.

3.4 Computational Domain geometry and Grid/mesh Design

Computational domain

Computational domain is the truncation of the real physical domain or system which presents the fluid dynamic characteristics at the area of interest to be considered in a numerical solution. This truncation results in the presence of boundary conditions which represent natural boundaries of the physical domain. The numerical treatment of the boundary conditions is very important to the solution accuracy, the convergence stability. Boundary conditions includes the following types: (1) Solid wall should be considered as slip wall in case of an inviscid flow, the fluid slips over the surface or non-slip wall for viscous flow passes over a solid surface. (2) Inflow/outflow in internal flow; (3) Symmetry plane is used where the fluid is symmetrical to that a plane and there is no flux across such plane or the velocity normal to this symmetrical plane is zero; (4) Coordinate cut; (5) Periodic boundaries for the flow field which is periodic with respect to one or multiple coordinate direction and therefore numerical solution of the flow will only be simulated within one the repeating regions; (6) Boundary between blocks. (J. Blazdek, 2001, p.267)

Space discretization

According to Hirsch (2007), there are two types of discretization consisting of space discretization and equation discretization. Space discretization is related to the repetition of the spatial continuum by a distribution of grid or mesh, by which the spatial continuum “is replaced by a finite number of points where the numerical values of the variables will be determined.” The equation discretization, in the other hand, is related to the discretization based on “the transformation of the differential or integral equations to discrete algebraic operations involving the values of the unknowns related to the mesh points.”

The space discretization includes structured grid and unstructured grid (Figure 3.4.1). The structured grids consist of mesh points spatially distributed on the positions as the intersection of lines corresponding to Cartesian grids in the mathematical space of the curvilinear coordinates. Unstructured grids, however, have arbitrary distribution of mesh points. Structured grid is easy to work with and offers higher chance for convergence but unstructured grid is more flexible to work with complex geometries.

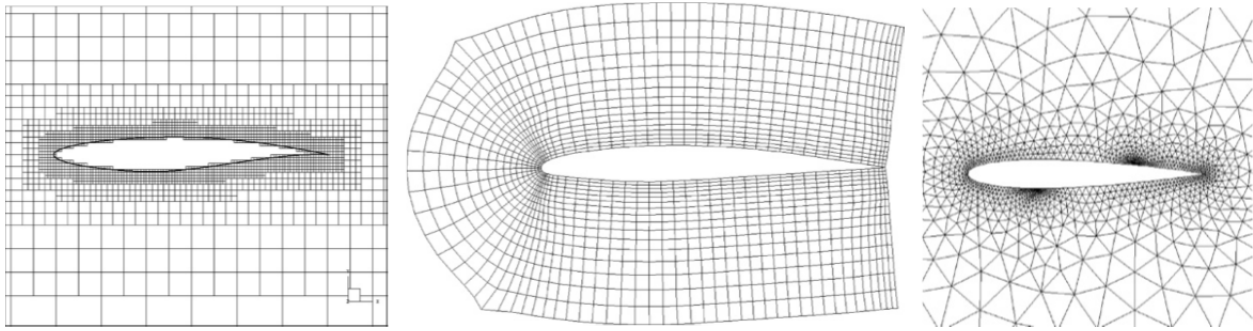


Figure 3.4.1: Examples of different space discretization: (a) Quadtree structured grids around an airfoil; (b) structured curvilinear body-fitted grids; (c) unstructured triangular grids around an airfoil (C. Hirsch, 2007).

Hirsch (2007) introduced some recommendations and best practices on the grid quality, consisting of minimizing the influence and interactions between the flow and the far-field conditions, the grid size continuity and the distortion of a cell relating to the aspect ratio x/y and skewness factor). The placement of inlet and outlet boundaries is as far as possible from the region of interest. Jumps in grid density or in grid size should be avoided. Cells with high distortion always need to be avoided since they will have a negative influence on the accuracy of the solution, deteriorating the solution convergence. Finer resolution (higher number of cells) and the importance of following these recommendations are critical in flow regions with high gradients (i.e. in regions where the flow variables undergo rapid variations).

Grid quality

The quality of the mesh plays a significant role in the accuracy and stability of the numerical computation. The attributes associated with mesh quality are node point distribution, smoothness, and skewness. Depending on the cell types in the mesh (tetrahedral, hexahedral, polyhedral, etc.), different quality criteria are evaluated (ANSYS, 2009):

- Cell squish on all meshes. Cell squish is a measure used to quantify how far a cell deviates from orthogonality with respect to its faces. *Squish index* is computed for cells using the vector from the cell centroid to each of its faces and the corresponding face area vector. The worst cells will have a cell squish index close to 1, with better cells closer to 0. A good rule of thumb is that the maximum cell squish index for all types of cells should be less than 0.99.
- *Skewness* is defined as the difference between the shape of the cell and the shape of an equilateral cell of equivalent volume. Highly skewed cells can decrease accuracy and destabilize the solution. For example, optimal quadrilateral meshes will have vertex angles close to 90

degrees, while triangular meshes should preferably have angles of close to 60 degrees and have all angles less than 90 degrees. A general rule is that the maximum skewness for a triangular/tetrahedral mesh in most flows should be kept below 0.95, with an average value that is less than 0.33. A maximum value above 0.95 may lead to convergence difficulties and may require changing the solver controls, such as reducing under-relaxation factors and/or switching to the pressure-based coupled solver.

- The aspect ratio is a measure of the stretching of a cell. It is computed as the ratio of the maximum value to the minimum value of any of the following distances: the distances between the cell centroid and face centroids, and the distances between the cell centroid and nodes. For a unit cube (Figure 3.4.2), the maximum distance is 0.866, and the minimum distance is 0.5, so the aspect ratio is 1.732. This type of definition can be applied on any type of mesh, including polyhedral.

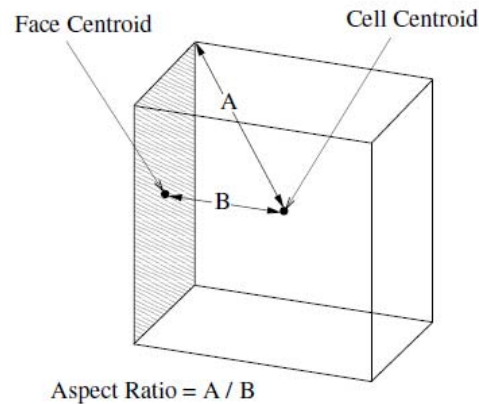


Figure 3.4.2: The aspect ratio for a unit cube

Grid sensitivity analysis

There are three main numerical errors of CFD prediction: the round-off error, the iterative error and the discretization error. The discretization error is resulted from the approximation of discretization method used “to transform the partial different equations of the continuum formulation into a system of algebraic equations.” The discretization error is dominant in comparison to other numerical errors. The discretization error can be reduced by increasing the resolution of the meshing. (L. Eca and M. Hoekstra, 2014)

Roache (1994) proposed the Grid Convergence Index (GCI) based on Richardson extrapolation to provide an objective asymptotic approach to quantification of uncertainty of grid convergence. GCI is calculated as follows:

$$GCI = \frac{3|\epsilon|}{(r^p - 1)}$$

$$\epsilon = (f_2 - f_1)/f_1$$

$$f[exact] = f_1 + (f_1 - f_2)/(r^p - 1)$$

Where r is the cell size ratio between two different discrete solutions f_1 and f_2 with and p is the order of numeric method used in discretization. The cell size ratio r , in case of unstructured grids where the method of grid refinement sometimes could lead to a difficulty of systematically qualify, and therefore, the number of elements used in the coarse (N_2) and fine (N_1) will be used in the following formula:

$$r = (N_2 - N_1)^{1/D}$$

where D is the dimensionality of the problem. By using the common values of grid ratio (r) and the order (p), GCI calculated for coarse grid solutions and fine grid solutions, normalized to $\epsilon = 1\%$ as shown in Table 1:

p	Fine grid GCI			p	Coarse grid GCI		
	$r = 2$	1.5	1.1		$r = 2$	1.5	1.1
1	3.00%	6.00%	30.00%	1	6.00%	9.00%	33.00%
2	1.00%	2.40%	14.29%	2	4.00%	5.40%	17.29%
3	0.43%	1.26%	9.06%	3	3.43%	4.26%	12.06%
4	0.20%	0.74%	6.46%	4	3.20%	3.74%	9.46%

Table 3.4.1: Grid convergence index (GCI) calculated for common values of grid ratio (r) and orders of the basic numerical method (p) for both coarse grid solutions and the fine grid solutions, normalized to $\epsilon=1$ percent (Roache, 1994).

Ramponi and Blocken (2012) studied the cross ventilation cross over openings of a generic buildings with CFD, focusing on sensitivity analysis of computational parameters. In the study, they introduced three different resolution grids with finest/medium grid ratio and medium/coarsest grid ratio equal 2 (Figure 3.4.3). By adopting the uniform reporting of the grid-convergence presented in Figure 3.4.4, their analysis showed the different results (ventilation flow rates through the inlet opening) about 1% between the finest and medium grids (C and B) and up to 7.5% between finest and coarsest grid (grid C and A).

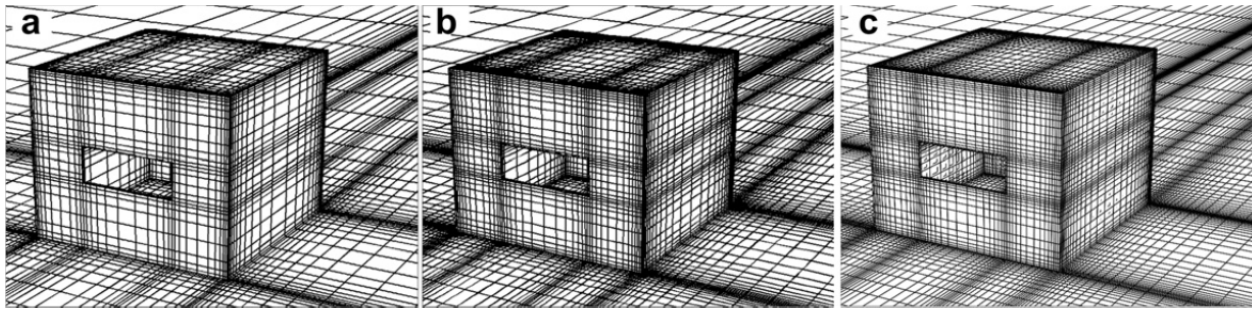


Figure 3.4.3: Perspective view of grids for grid-sensitivity analysis: (a) Coarse grid A with 144,696 cells; (b) Middle grid B with 314,080 cells; (c) Fine grid C with 575,247 cells (reference case) (Ramponi and Blocken, 2012)

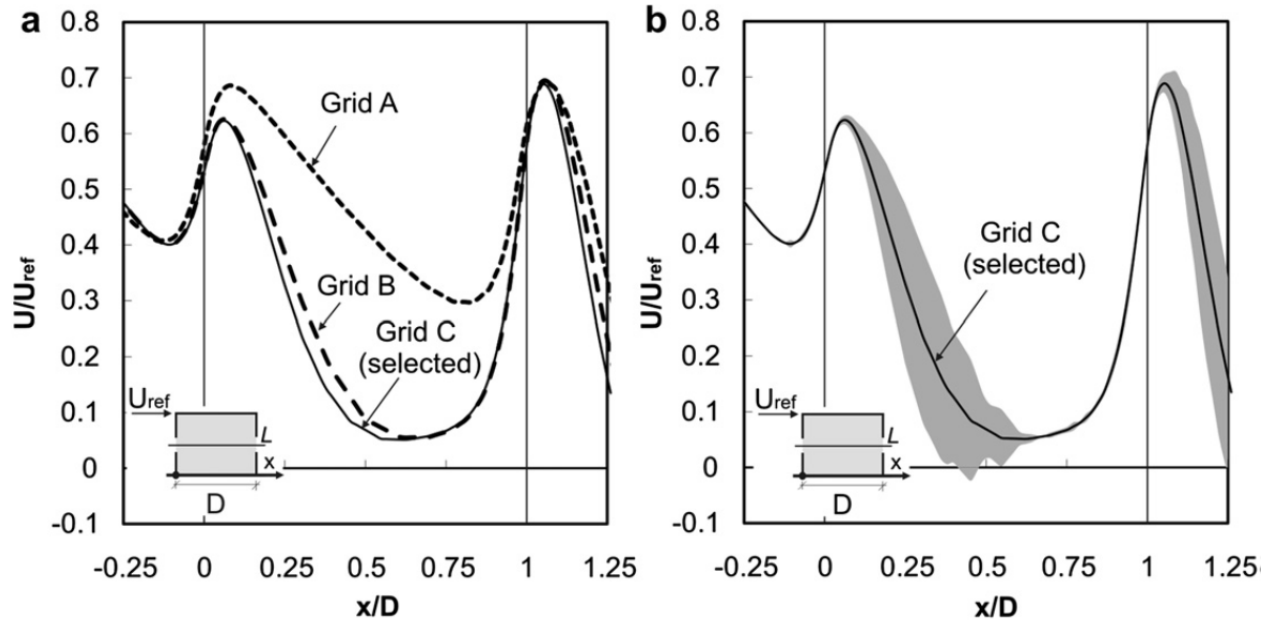


Figure 3.4.4: CFD simulation results for sensitivity analysis: impact of the grid resolution on the streamwise wind speed ratio along the centerline: (a) Comparison of results from the three grids; (b) Results on fine grid with indication of band of $1.25 * GCI$ (Ramponi and Blocken, 2012)

3.5 Surface roughness of grid element

To solve the near-wall fluid, there two approaches consisting of wall function and low-Reynolds number approach. While the low Reynolds number approach requires a very high mesh resolution at the regions

close to wall to capture the characteristics of the wall surfaces and therefore increase the computational load. The wall function approach, on the other hand, using mathematical relations to model the boundary conditions for the near wall fluid, therefore will not require high resolution meshing, with the following assumptions (STAR CCM+ Manual):

- A consistent distribution of velocity, turbulence and other scalar qualities.
- An assumption that the turbulence model is valid only outside the viscous-dominated region of the boundary layer and the viscous-affected region of the boundary layer is not resolve
- The centroid of the near-wall ell lies within the logarithmic region of the boundary layer.

The equivalent sand-grain roughness height r can be obtained either from literature or experiment. From experiment:

- Measure the friction factor for the Reynolds numbers of the experiment.
- Plot the measurement on a Moody diagram as shown in Figure 3.5.1.
- Deduce the equivalent sand-grain roughness height from the Moody curve.

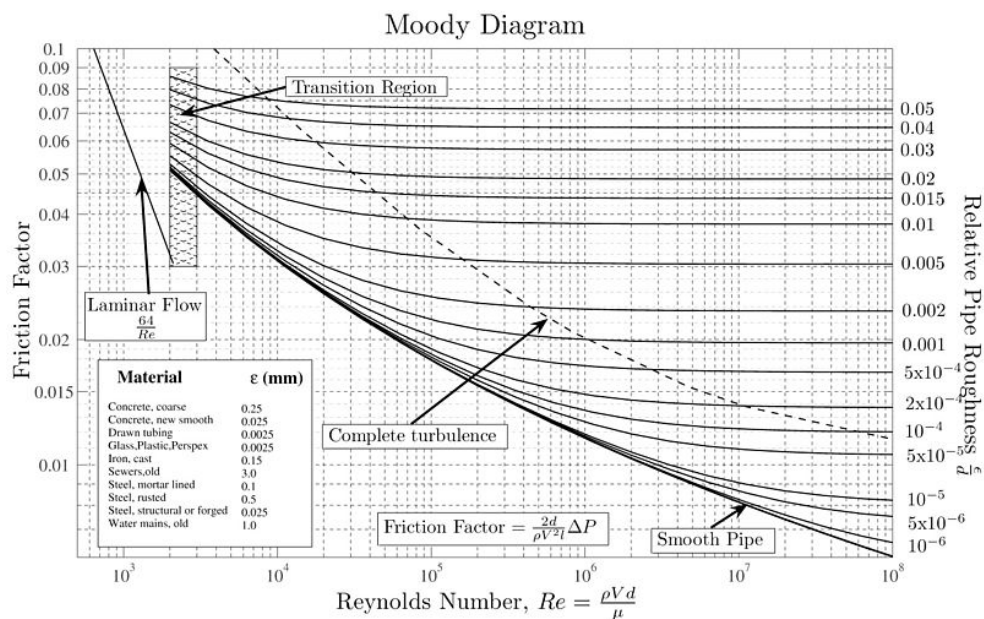


Figure 3.5.1: Moody diagram created by S. Beck and R. Collins, University of Sheffield under GNU Free Documentation License.

Experiment of equivalent sand-grain roughness height was discussed in the study conducted by T. Adams et al. (2012). In this study, the authors proposed a simple algorithm for estimating the equivalent sand-grain roughness of surfaces based on their various measured surface roughness parameters measured from a profilometer. By assuming conversion from a rough surface (Figure 3.5.2a) to a

uniform monolayer of same-diameter sphere surface (Figure 3.5.2b), measured surface roughness parameters from that rough surface were used to represent an approximate value for equivalent sand-grain roughness.

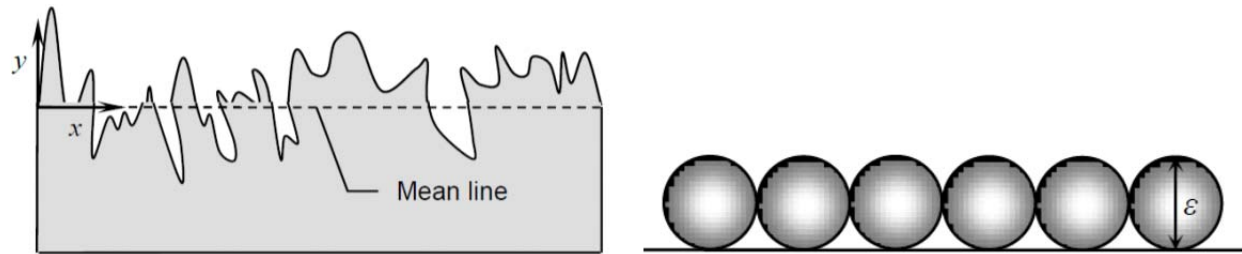


Figure 3.5.2: (a) A rough surface of arbitrary profile (b) A row of uniform spheres on a flat surface (T. Adams et al., 2012).

Three measured surface roughness parameters were defined including arithmetic average of absolute roughness R_a , the root mean squared R_{rms} and the peak-to-valley R_{td} :

$$R_a = \frac{1}{n} \sum_{i=1}^n |y_i|, \quad R_{rms} = \sqrt{\frac{1}{n} \sum_{i=1}^n y_i^2}, \quad R_{td} = \frac{1}{n5} \sum_{i=1}^5 (R_{pi} - R_{vi})$$

Where y_i is the distance from the average height of a profile (the mean line) for measurement, i and n is the number of measurement, R_{pi} and R_{vi} are the largest distances above and below the mean line for one of five measurements. The estimated sand-grain roughness ϵ will be determined based on these three different measured parameters. Adams (2012) concluded that the peak-to-valley surface roughness parameter R_{td} always gives better approximate equivalent sand-grain roughness. The estimated sand-grain roughness is given as following Table 3.5.1:

Table 3.5.1: Estimated sand-grain roughness based on measured surface roughness parameters (T. Adams et al., 2012).

Roughness parameter	Estimated sand-grain roughness, ϵ
R_a	$\epsilon = 5.863R_a$
R_{RMS}	$\epsilon = 3.100R_{RMS}$
R_{zd}	$\epsilon = 0.978R_{zd}$

The equivalent sand-grain roughness height should not be confused from the aerodynamic roughness length z_0 , which is determined by the formula:

$$r = \frac{E y_0}{C} \approx 36 y_0$$

Where E (9.0) and C (0.253) are the wall functions' coefficients (STAR-CCM). Blocken (2007), Hooff and Blocken (2010), however, recommended the equivalent sand-grain roughness height as equal as $30y_0$.

3.6 Boundary Conditions

The review of boundary conditions presented in this report mainly for internal CFD and summarized based on Srebric (2011). In CFD computational domain, boundary conditions representing natural boundaries of the physical domain. They are very important to the mathematical solution of the system of partial differential equations governing the fluid behaviors. In internal CFD, CFD models normally are simplified version of a real detailed geometry. For example, an office is simplified and reduced to a space of a floor, ceiling, walls, cubicle partitions, tables, computers, lamps and etc. (Fig.). These items of the office are considered as boundary conditions since they considerably contribute to the air flow performance of the internal space. There are three main boundary condition types:

- Free boundary: is a boundary surface adjacent to an inviscid stream such as air supply or exhaust. For a supply opening, the boundary conditions are:

$$u_i = u_{supply}, \quad T = T_{supply}, \quad k = k_{supply}, \quad \varepsilon = \varepsilon_{supply}, \quad \text{and} \quad c = c_{supply}$$

Note that these equations **only** apply for supply openings while supply diffusers require more complex specifications of boundary conditions. For supply diffusers, the boundary conditions are complicated due to the complex diffuser geometry and the effects of confined spaces. More information about the boundary conditions of supply diffusers could be found in the original documents. The supply boundary conditions may be specified as a supply velocity, pressure or airflow rate. The airflow inlet condition requires specifying the mass flow rate and the temperature and contaminant concentration at the supply diffuser. The velocities and the pressure are calculated by extrapolation, at the supply diffuser boundaries. For the k- ε turbulence models, turbulent kinetic energy k and turbulent dissipation rate ε can be estimated from the following equations:

$$k = \frac{3}{2} (U_{ref} T I)^2$$

3. Internal CFD – Numerical Assessment of Air Movement Inside Buildings

$$\varepsilon = C_{\mu}^{3/4} \frac{k^{3/2}}{l}$$

$$l = 0.07L$$

where U_{ref} [m/s] is the mean stream velocity, TI is the turbulence intensity, l [m] is the turbulence length scale, C_{μ} is the k - ε turbulence model constant and L is the characteristics length of the supply diffuser (for a duct L is the equivalent radius). The common CFD modeling of supply diffusers consist of: momentum method, box method and prescribed velocity method. The description of these modeling methods should be found in the origin literature (Cen and Moser 1991; Nelsen 1992; Srebric and Chen 2002). Figure shows the example of simplified boundary condition for a supply diffuser with momentum method and box method.

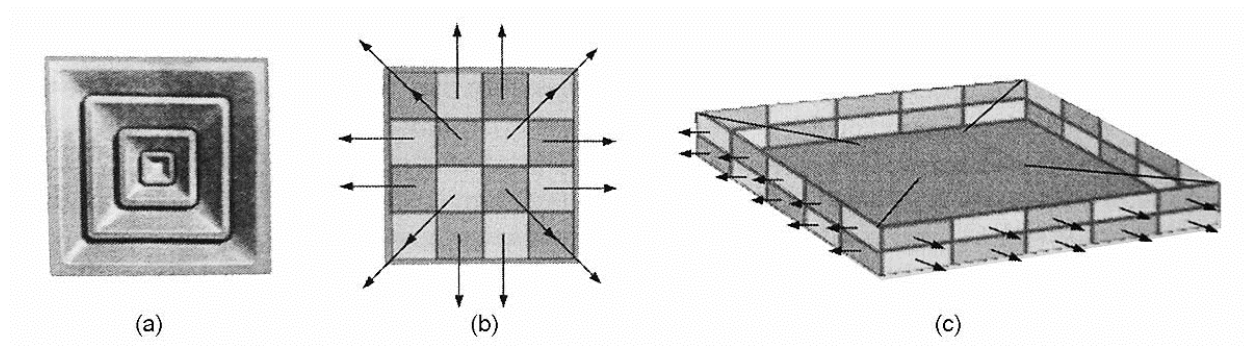


Figure 3.6.1: An example of simplified boundary condition for (a) supply diffuser modeling for square diffuser (b) diffuser modeling by momentum method, and (c) diffuser modeling by box method.

Pressure is normally given for an exhaust opening, and zero gradients normal to the surface are assumed for the other parameters:

$$p = p_{exhaust}, \quad \frac{\partial U_i}{\partial x_i} = 0, \quad \frac{\partial T}{\partial x_i} = 0, \quad \frac{\partial k}{\partial x_i} = 0, \quad \text{and} \quad \frac{\partial \varepsilon}{\partial x_i} = 0$$

where $p_{exhaust}$ [Pa] is the pressure at a return and x_i [m] is the coordinate normal to the surface of the exhaust opening or diffuser.

- Symmetry surface: is used to reduce the size of the computational domains that are symmetric. The boundary conditions of the symmetry surface are:

$$\frac{\partial U_i}{\partial x_i} = 0, \quad \frac{\partial T}{\partial x_i} = 0, \quad \frac{\partial k}{\partial x_i} = 0, \quad \frac{\partial \varepsilon}{\partial x_i} = 0, \quad \text{and} \quad \frac{\partial C}{\partial x_i} = 0$$

where x_i is normal to the symmetry surface

- Conventional boundary: is used to specify the boundary conditions for walls, ceilings, floor surfaces and the surfaces of furniture, appliances and occupants. The boundary conditions are:

$$\tau = \mu_{eff} \frac{\partial U_i}{\partial x_i}, \quad q = h(T_w - T)$$

$$\mu_{eff} = \mu + \mu_t$$

$$h = \frac{u_{eff} c_p}{Pr_{eff} \Delta x_i}$$

where τ is shear stress [Pa] and μ_{eff} is the effective viscosity [Pa-s], h is the convective heat transfer coefficients [W/(m²K)], q is the convective heat transfer rate [W] and T_w is the wall temperature [K], Pr_{eff} is the effective *Prandtl number*. The effective diffusion coefficient for temperature equation u_{eff}/Pr_{eff} is based on *Prandtl numbers* for laminar Pr and turbulent Pr_t :

$$\frac{u_{eff}}{Pr_{eff}} = \frac{\mu}{Pr} + \frac{\mu_t}{Pr_t}$$

It is noticed that the standard $k-\varepsilon$ or RNG $k-\varepsilon$ models developed for high Re numbers. The air flow region near wall region might result in very low Re number and therefore, these models require adjustment for these near wall regions by applying near wall equations. The wall functions are dimensionless velocity, temperature and concentration profiles in the wall boundary region which is consisting of laminar sub-layer ($0 < y^+ \leq 5$), buffer zone ($5 < y^+ \leq 30$) and inertial sub-layer ($30 < y^+ \leq 130$). Where y^+ is the dimensionless distance to the wall by using the following equation:

$$y^+ = \frac{u_* y}{\nu}, \quad u_* = \sqrt{\frac{\tau_w}{\rho}}$$

where u_* [m/s] is the friction velocity at the nearest wall, y [m] the distance to the nearest wall and ν is the local kinematic, τ_w [Pa] is the wall shear stress and ρ [kg/m³] is the fluid density at the wall.

3.7 Turbulence Modeling

The correct choice of turbulence models is one of the key steps in the CFD investigation.

As described by Versteeg and Malalasekera (2007) turbulence causes the appearance of eddies in a wide range of length and time that interact in a dynamically complex way. Three groups methods of numerical methods that can capture the important effect of turbulence. These are;

Turbulence models for Reynolds-average Navier- Stokes (RANS) equation: For this method attention is focused on the average or mean flow and the effects of turbulence on mean flow properties. The nature of the method is that extra terms appear in the time-averaged (eg. Reynolds-averaged) equations due to the interactions with various turbulence models. These extra terms are modeled with turbulence models and Reynolds stress models. The RANS turbulence modeling approach requires only modest computational resources and therefore this approach represents the overwhelming portion of engineering CFD applications.

Turbulence models for Large Eddy Simulations equation (LES): This method represents an intermediate form of turbulence calculations which considers large eddies. The methods uses space filtering procedures for the unsteady Navier-Stokes equations prior to calculations to reject smaller eddies and only use larger eddies. Since unsteady flow equations have to be solved the demand on computational resources is large. LES is starting to be accepted in the industry to address CFD problems involving complex geometries

Direct Numerical Simulations (DES): This method computes the mean flow as well as all turbulent velocity fluctuations. This method requires very significant computational resources and at the present DES is not used for industrial floe computations.

Reynolds-average Navier- Stokes (RANS) equation and classical turbulence models: In most applications it is not required to resolve the details of turbulent fluctuations. Instead for most CFD calculations it is sufficient to provide information about time-averaged properties of the flow, such as mean velocities, mean pressures. While the details of turbulent fluctuations is not calculated the effects of turbulence on the mea flow is needed. For this purpose turbulence models are applied to predict the Reynolds stresses and scalar transport terms and provide closure of the mean flow equations. The most common RANS turbulence models are classified on the basis of the number of additional transport equations that need to be resolved along with the RANS flow equations.

The following list the most common turbulence models. It is noteworthy to point out that there are generalized and specific turbulence models. As the terms suggest the more generalized turbulence models can be used to solve a broader range of flow problems as the more specific models. The following present several turbulence models that are in use in general CFD applications:

Mixing length model: Basically, the mixing length model is typically not used on its own in general purpose CFD, but is found embedded in more sophisticated turbulence models to describe near-wall flow behaviors. The advantages of the mixing length model is the ease of use which requires little computational resources and good predictions of this shear layers. The disadvantages include that the model is incapable to describe flows with separation and recirculation.

The k- ϵ turbulence model: The k- ϵ model a more generic, yet sophisticated and effective, description of turbulence. The model allows for the effects of transport of turbulence properties by means of convection and diffusions and also for the production and destruction of turbulence. The model includes solving for the turbulent kinetic energy k and the rate of dissipation of turbulent kinetic energy ϵ . The k- ϵ model is the most widely used and validated turbulence. The model performs well in confined flows where the Reynolds shear stresses are most important, which includes many engineering flow problems. The model does not perform equally well in unconfined flows. Advantages of the k- ϵ model include that it is the simplest turbulence model for which only initial and/or boundary conditions are required. Other advantages include excellent performance in many industrial CFD applications and a wide application. Disadvantages include poor performance in some unconfined flows, flows with large strains (i.e. curved boundary layers) and other special flow applications.

Reynolds stress equation model (RSM): The RSM is the most complex classical turbulence and is an improvement of the k- ϵ model. RSM is termed the “most general of all classical turbulence models. There are indications the RSM model might be more widely used in the future after some of the difficulties in handling this models have been solved for a wide application. For example, the RSM model outperforms the k- ϵ model in terms of pressure distributions predictions in windward and leeward of flow obstructions. Disadvantages of RSM include very large computing costs and the fact that RSM is not as much validated as the k- ϵ model. In addition, and important to the application of air movement around buildings, RSM shares with the k- ϵ model a rather poor performance to describe unconfined recirculating flow.

In addition to the more classical turbulence models more advanced turbulence models have been developed, which promise good application potential for the simulation of wind movement around buildings. The development of more advanced turbulence models was triggered by the need to produce models with good performance while at the same time reduce the computational cost in comparison to high performance model such as the classical RSM.

RNG k- ϵ model: The model represents an expansion if the classical k- ϵ model. RNG stands for renormalization group. The RNK k- ϵ model represents the effects of small-scale turbulence by means of random forcing functions of the governing Navier-Stoke equations. Basically the RNG

procedure removes small scales of motion from the governing equation. The RNG model performs better for certain flow applications than the classical k- ϵ model.

The Wilcox k- ω model: This model uses a turbulence frequency ω as an additional equation to describe a length scale determining variable. At the inlet k and ω have to be specified. The model has limited use in industrial CFD applications.

Menter SST k- ω model: This turbulence model has advantages over the k- ϵ model in regard to near-wall performance with adverse pressure gradients. The model is actually a hybrid model by first transforming the k- ϵ model into a k- ω model in the near-wall region and using the standard k- ϵ model in the fully turbulent region. The model SST k- ω provides a general model with specific good performance of pressure gradient boundary layers.

Various researchers have tested the validity of different turbulence models for applications describing wind flow phenomena. Some of the reviewed articles are discussed below.

Glover et al (2006) reports that the standard k- ϵ model exhibits problems predicting flow separation and underpredicting turbulent kinetic energy values within street canyons. The practicality of the standard k- ϵ model explains that the model is still widely used in industry and research, thus creating a demand for improved performance from the model. The authors present a comprehensive study in which constants contained within the standard k- ϵ model were investigated on their validity to predict flow situations for which experimental data was available. The authors suggest that often industry leave the constant unchanged from the original values suggested by the developer of the k- ϵ model, Launder and Spalding.

The authors performed CFD calculations with varying constants and they were able to assess their influence on the CFD models capability to simulate flow within and above a street canyon. The authors found that there was a large spread of results, shown in Figure 3.7.1, which suggests these values have a significant impact on the turbulence values. Figure 3.7.1 illustrates the wide spread of results identified by the authors. Furthermore the authors show that the constants can be adjusted to improve model predictions as seen by the use of modified parameters shown in Figure 3.7.2. The authors suggest that they were able to use statistical methods to emulate the CFD model, providing a much improved prediction of the turbulent kinetic energy values within the street canyon by integrating over the range of possible values for the parameters.

Franke et al (2007) recommend that simulations should always be started with the standard k- ϵ model, due to its very good stability. Depending on the application different models are then additionally tested:

- Realizable k- ϵ model for pedestrian wind environment
- Renormalization group k- ϵ model for pressures on buildings, see
- Reynolds stress model(s) (RSM) with and without wall damping for both applications

3. Internal CFD – Numerical Assessment of Air Movement Inside Buildings

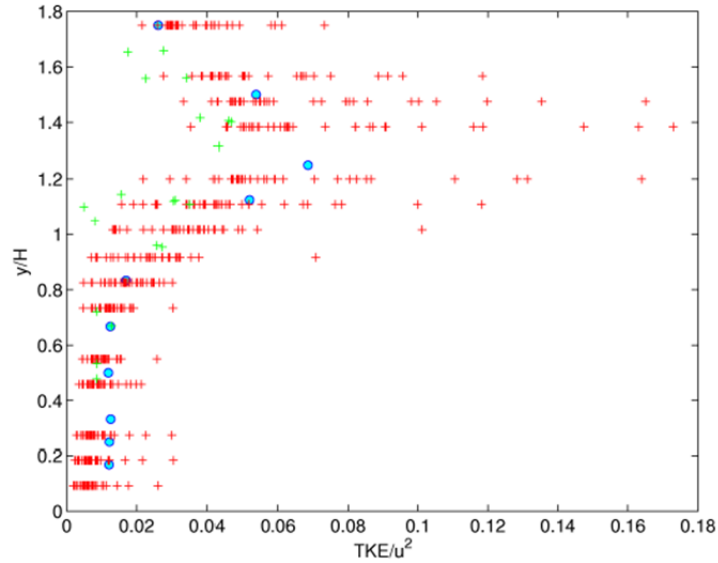


Figure 3.7.1: Normalized TKE (e.g. turbulence kinetic energy) data from wind tunnel (blue circles) and CFD simulation (crosses) against normalized by the height h of the buildings. (Glover et al, 2006)

Ramponi and Blocken (2012) compared the results of CFD for the same building and wind conditions using different turbulence models. In their test they used 3D steady RANS simulations with the following turbulence models:

- Standard $k-\epsilon$ model ($Sk-\epsilon$)
- Realizable $k-\epsilon$ model ($Rk-\epsilon$)
- Renormalization Group $k-\epsilon$ model ($RNG\ k-\epsilon$)
- Standard $k-\omega$ model ($Sk-\omega$)
- Shear-stress transport $k-\omega$ model ($SST\ k-\omega$)
- Reynolds Stress Model (RSM)

3. Internal CFD – Numerical Assessment of Air Movement Inside Buildings

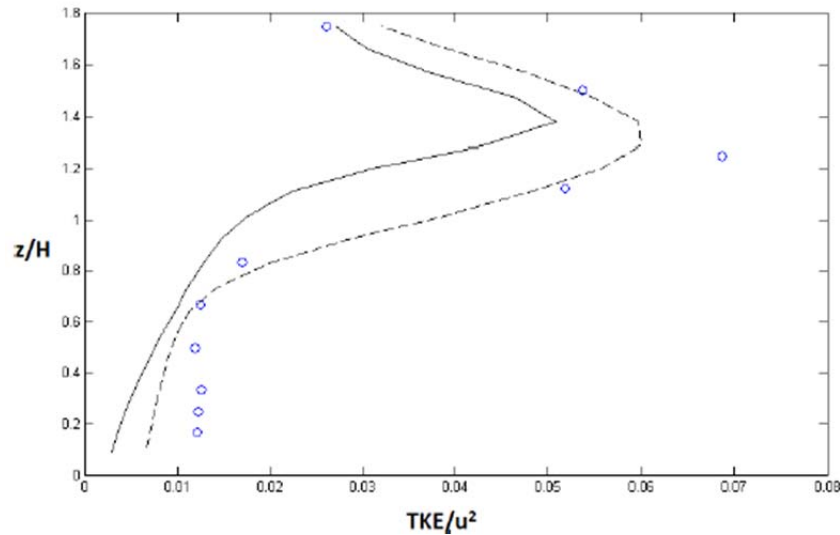


Figure 3.7.2: Normalized TKE profiles from CFD model with un-modified constants (black line), modified constants (dashed line) and wind tunnel data (circles)

The authors report that the effects of the turbulence models on the indoor air flow are illustrated in terms of streamwise wind speed ratio along the centerline of the openings (Figure 3.7.3). Measured ventilation flow rate (referred to as PIV in Figure 3.7.3) compared very well with the SST $k-\omega$ model (also referred to as the Ref. case), followed by the RNG $k-\epsilon$ model, which also provides a fairly good performance. The discrepancies by the other models are very large. In fact, Fig. 3.7.3 shows that the indoor streamwise wind speed obtained with the other $k-\epsilon$ models is up to 6 times higher (at $x/D = 0.75$) than the one obtained using the SST $k-\omega$ model (Ref. case). The result suggest that RSM and the standard $k-\epsilon$ models tend to over predict the experimental values by up to 9 times ($x/D = 0.6$). The authors indicate that in several previous studies, authors pointed out the superior performance of the RNG $k-\epsilon$ model for indoor air flow modeling, especially compared to the standard $k-\epsilon$ model. In the cited study, however, the SST $k-\omega$ model clearly outperforms the RNG $k-\epsilon$ model.

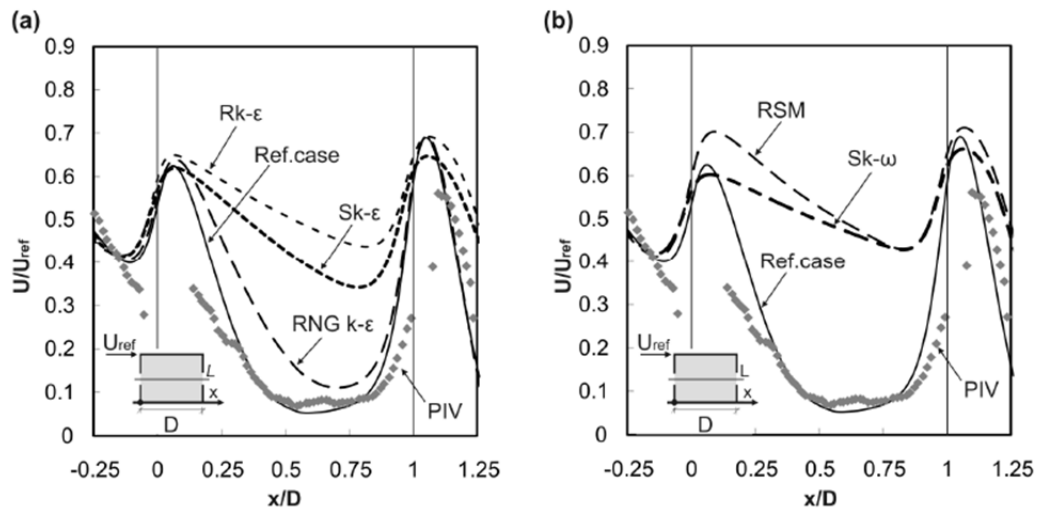


Figure 3.7.3: CFD simulation results for sensitivity analysis: impact of turbulence models on the streamwise wind speed ratio along the centerline. Comparison between the reference case (Ref.case = SST $k-\omega$ model) and (a) the $k-\epsilon$ models and (b) the RSM and standard $k-\epsilon$ model.

3.8 Steady Flow vs. Unsteady Flow

Steady flow is flow that has its properties (e.g. velocity, temperature, pressure, and density) are independent of time. That is,

$$\frac{\partial \phi}{\partial t} = 0$$

Where ϕ represents a fluid property. The properties, however, may vary from point to point, which means that they could be a function of space (i.e., $T = T(x, y, z)$, $p = p(x, y, z)$ and $\rho = \rho(x, y, z)$). It should be noted, steady flow does not mean the velocity and accelerations are constant. Flow in a curved pipe or through a nozzle may be steady, but the velocity and/or acceleration is not constant.

3. Internal CFD – Numerical Assessment of Air Movement Inside Buildings

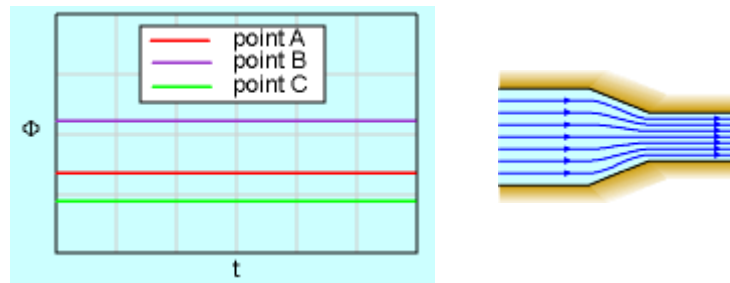


Figure 3.8.14: Steady flow: (a) Steady Flow (b) Flow with changing velocity

Steady flow is the simplification of a flow regime for certain types of analysis. However, most real-world flow problems are unsteady in nature. For unsteady flow, the fluid properties are time dependent (i.e., $T = T(x, y, z, t)$, $p = p(x, y, z, t)$ and $\rho = \rho(x, y, z, t)$). Unsteady flows can be further divided into periodic flow, non-periodic flow and random flow (Fig. a,b,c respectively) (Ngo and Gramoll, 1998)



Figure 3.8.2: Time dependency of unsteady flow: (a) Periodic Flow, (b) Non-Periodic Flow and (c) Random Flow

Suitable analysis for external wind flow in CFD: Since working with turbulent atmospheric boundary layer flow, the principle is the choice of unsteady treatment for the approximate equations (Franken, 2007). There are three common averaging modelling approaches of the Navier-Stokes equations: Steady RANS, Unsteady RANS (URANS), Large Eddy Simulation (LES) and the hybrid RANS-LES (or Detached Eddy Simulation or DES) approaches.

- Steady RANS: this approach uses the time (infinite) average leading to a statistically steady description of the turbulent flow and therefore there are some limitations for applications that model the inherently unsteady meteorology. RANS is adequate representation of the wind tunnel's reality. RANS also can be applicable in studying certain turbulent flows but it requires closure by using one of several available turbulence models.

3. Internal CFD – Numerical Assessment of Air Movement Inside Buildings

- Unsteady URANS: the basic equations of URANS are formally derived by applying ensemble averaging in which the resulting equations comply with the RANS equations now containing the partial time derivatives. URANS also allows for simulating temporal changes in the flow field caused, for example, by different surface temperatures. For an approach requiring a high spatial resolution, the LES or DES is recommended.
- Large Eddy Simulation (LES) and Detached Eddy Simulation (DES): LES provides an alternative approach in which large eddies are explicitly computed (resolved) in a time-dependent simulation using the "filtered" Navier-Stokes equations for reducing the error resulted from turbulence modeling. The DES models often referred to as the hybrid LES/RANS models, combine RANS modeling with LES, in which RANS is used for near-wall region while LES is associated with the core turbulent regions where large unsteady turbulence space plays a dominant role.

Advantages and disadvantages: According to Hertwig et. al (2012), Reynolds-averaged Navier Stokes equations (RANS models) allows fast computation of mean flow and dispersion even in very complex environments, especially applying studying urban ventilation, wind comfort assessment and pollutant dispersion predictions in cities. However, RANS models are only steady state solutions for an inherent unsteadiness of wind phenomena in wind engineering. Particularly within the canopy region (i.e. up to roof level) this can lead to inaccurate predictions of mean flow fields—especially for situations in which unsteady effect like flow separation, impinging, reattachment or vortex shedding play a predominant role in the dynamics of the flow.

For example, Montazeri and Blocken (2013) used 3D steady RANS simulation in their studying of the pressure coefficients of a building with and without balcony and compared with five turbulence models: the standard $k-\epsilon$ ($Sk-\epsilon$), the realizable $k-\epsilon$ ($Rk-\epsilon$), the renormalization group $k-\epsilon$ (RNG $k-\epsilon$), the standard $k-\omega$ ($Sk-\omega$) and the Reynolds Stress Model (RSM). The result unveiled that the RNG $k-\epsilon$ model tends to overestimate the pressure variations near the ground level while the standard $k-\omega$ generally provides a slight overestimation. According to author the $k-\omega$, $Rk-\epsilon$ and RSM models depict some agreement.

Using more detailed models such as models with or without balconies, Montazeri and Blocken (2013) found that the presence of balconies into building causes flow separation, recirculation and detachment on the building façade and therefore has impacted dramatically on the calculation of the pressure coefficients on the windward building façade. Also, the limitation of the steady RANS CFD has been found that it only can be reliable when predicting cases of perpendicular approach flow wind direction. In case of oblique flow wind direction, CFD analysis using RANS depicted large discrepancies against validated from wind-tunnel measurement

3.9 Grid Convergence

Bakker (2006)'s reports on the concept of grid convergence and iterative convergence, errors and residuals. The author provides a general concept and principle of iteration process, residuals, significant of error, and ideal of convergence grid approach.

General approach – convergence: The iterative process is repeated until the change in the variables from one iteration to the next becomes so small that the solution can be considered converged.

- At convergence:
 - All discrete conservation equations (momentum, energy, etc.) are obeyed in all cells to a specified tolerance.
 - The solution no longer changes with additional iterations.
 - Mass, momentum, energy and scalar balances are obtained.
- Residuals measure imbalance (or error) in conservation equations.
- The absolute residual at point P is defined as:

$$R_P = \left| a_P \phi_P - \sum_{nb} a_{nb} \phi_{nb} - b \right|$$

- Residuals are usually scaled relative to the local value of the property f in order to obtain a relative error:

$$R_{P, scaled} = \frac{\left| a_P \phi_P - \sum_{nb} a_{nb} \phi_{nb} - b \right|}{\left| a_P \phi_P \right|}$$

- Residuals can also be normalized, by dividing them by the maximum residual that was found at any time during the iterative process.
- An overall measure of the residual in the domain is:

$$R^\phi = \frac{\sum_{all\ cells} \left| a_P \phi_P - \sum_{nb} a_{nb} \phi_{nb} - b \right|}{\sum_{all\ cells} \left| a_P \phi_P \right|}$$

- It is common to require the scaled residuals to be on the order of 1E-3 to 1E-4 or less for convergence.
- Proper convergence criteria should be defined before using a solution: solutions that do not converge can be misleading.
- Solutions are converged when the flow field and scalar fields are no longer changing.
- Determining when this is the case can be difficult.
- It is most common to monitor the residuals.

Monitor residuals: The author provides the following guidelines for monitoring residuals (see Figure 3.9.1. for illustration of residual monitoring):

- If the residuals have met the specified convergence criterion but are still decreasing the solution may not yet be converged. In this case the convergence criteria should be revisited.
- If the residuals never meet the convergence criterion, but are no longer decreasing and other solution monitors do not change either, the solution is converged.
- Residuals should not infer the solution! Low residuals do not automatically mean a correct solution, and high residuals do not automatically mean a wrong solution
- Final residuals are often higher with higher order discretization schemes than with first order discretization. This fact cannot be interpreted that the first order solution produces more accurate results.

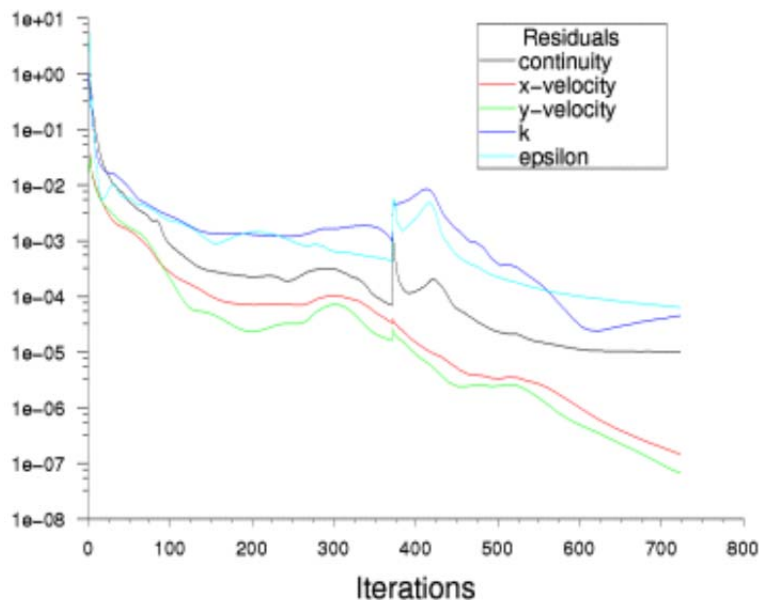


Figure 3.9.1: Residuals monitoring (Bakker, 2006)

Other convergence monitors:

- For models whose purpose is to calculate a force on an object, the predicted force itself should be monitored for convergence. An example might be wind force on an object where one should monitor the predicted drag coefficient. Figure 3.9.2 illustrates the convergence of a predicted drag coefficient.
- Overall mass balance should be satisfied.
- When modeling rotating equipment such as turbofans or mixing impellers, the predicted torque should be monitored.

- For heat transfer problems, the temperature at important locations should be monitored.
- Flow field plots can automatically be generated at predefined iterations (example after 50 iterations) to visually review the flow field and ensure that it is no longer changing.

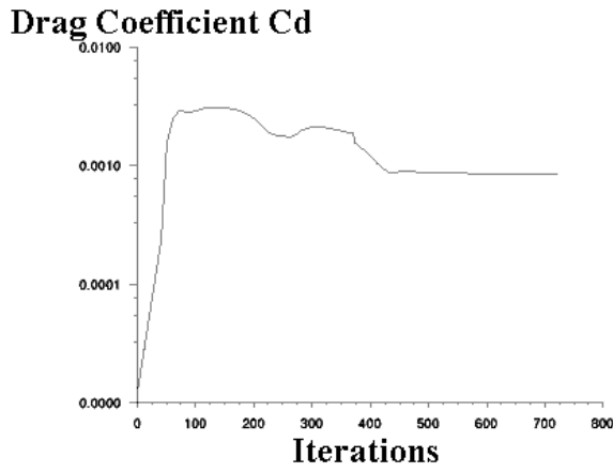


Figure 3.9.2: Drag coefficient (Bakker, 2006)

Accuracy of numerical schemes: The author suggests methods to ascertain accuracy of the numerical solution (see Figure 3.3.4.C as an example):

- The first order upwind scheme only uses the constant and ignores the first derivative and consecutive terms. This scheme is therefore considered first order accurate.
- For high Peclet numbers the power law scheme reduces to the first order upwind scheme, so it is also considered first order accurate.
- The central differencing scheme and second order upwind scheme do include the first order derivative, but ignore the second order derivative. These schemes are therefore considered second order accurate. Quick does take the second order derivative into account, but ignores the third order derivative. This is then considered third order accurate.

Accuracy and false diffusion:

- False diffusion is numerically introduced diffusion and arises in convection dominated flows, for instance in high Peclet number flows.
- False diffusion occurs due to oblique flow direction and non-zero gradient of temperature in the direction normal to the flow.
- Grid refinement coupled with a higher-order interpolation scheme will minimize the false diffusion.

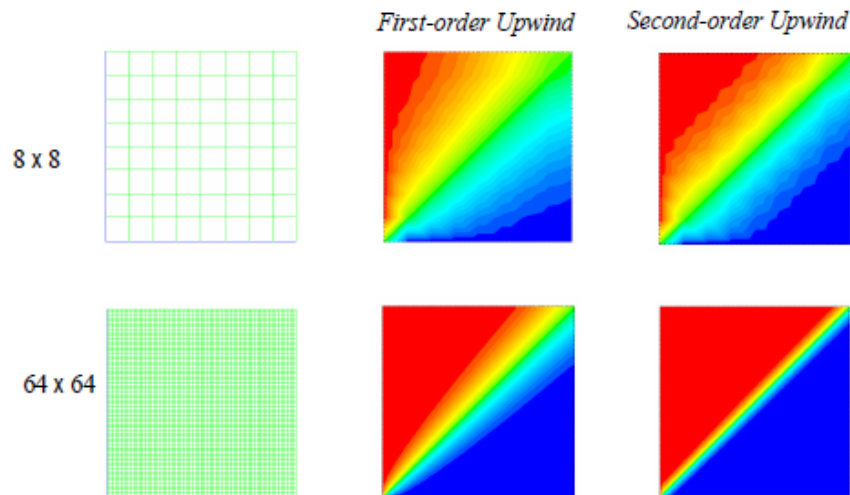


Figure 3.9.3: Grid refinement coupled (Bakker, 2006)

Multi-grid solver:

- The algebraic equation can be solved by sweeping through the domain cell-by-cell in an iterative manner.
- This method reduces local errors quickly but can be slow in reducing long-wavelength errors.
- On large grids, it can take a long time to see the effect of distant grid points and boundaries.
- Multigrid acceleration is a method to speed up convergence for:
 - Large number of cells.
 - Large cell aspect ratios (e.g. $Dx/Dy > 20$).
 - Large differences in thermal conductivity such as in conjugate heat transfer problem.
- The multigrid solver uses a sequence of grids going from fine to coarse.
- The influence of boundaries and far-away points is more easily transmitted to the interior on coarse meshes than on fine meshes.

Fine meshes:

- Fine meshes give more accurate solutions.
- The solution on the coarser meshes is used as a starting point for solutions on the finer meshes.
- The coarse-mesh solution contains the influence of boundaries and far neighbors. These effects are felt more easily on coarse meshes.
- This accelerates convergence on the fine mesh.
- The final solution is obtained for the original (fine) mesh.
- Coarse mesh calculations only accelerate convergence and do not change the final answer.

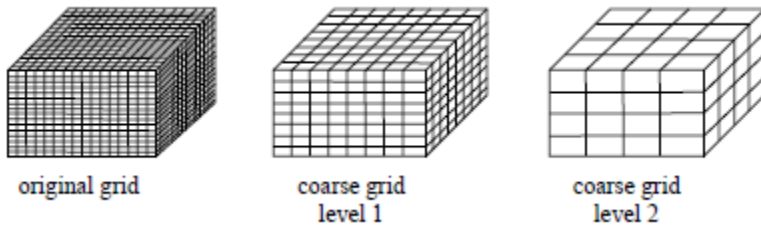


Figure 3.3.4D: Fine meshes (Bakker, 2006)

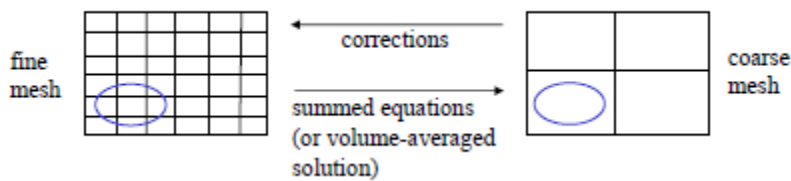


Figure 3.9.4: Coarse mesh calculations (Bakker, 2006)

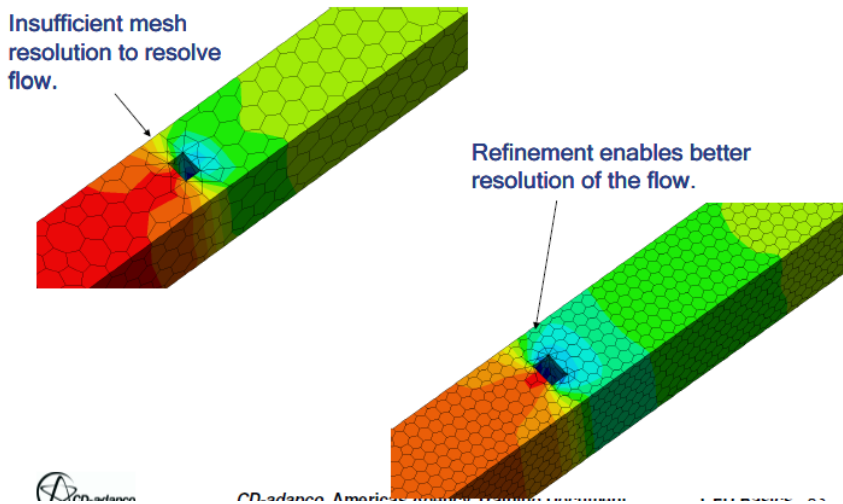


Figure 3.9.5: Grid Generation Guidelines (CD-adapco, user manual)

Iterative error on the numerical uncertainty Eca (2006) describes the influence of the iterative error on the numerical uncertainty of the solution of the Reynolds-Averaged Navier-Stokes (RANS) equations. Two main topics are addressed: the estimation of the iterative error; and the influence of the iterative error on the estimation of the discretization error. Iterative error estimators based on the L_∞ , L_1 and L_2 norms of the differences between iterations and on the normalized residuals are tested on three test cases: the 2-D turbulent flow over a hill, a 3-D flow over a finite plate and the flow around the *KVLCC2M*

3. Internal CFD – Numerical Assessment of Air Movement Inside Buildings

tanker at model scale Reynolds number. Two types of procedures are considered, one using the data of the last iteration performed and the other using an extrapolation based on a least squares fit to a geometric progression. In the latter case, the option of including the standard deviation of the fit in calculation of the error estimator is also tested. The results show that the most reliable estimates of the iterative error are obtained with the extrapolation technique including the effect of the standard deviation of the fit applied to the L_∞ norm of the differences between successive solutions. To obtain realistic estimates of the iterative error the author suggests the use of the L2 and L1 norms and the use of the differences obtained in the last iteration.

3.10 Sensitivity Analysis – Guidelines and Evolving Standards

Results of CFD studies are dependent on a significant number of numerical parameters that comprise the input for the calculations. Sensitivity analyses are recommended to ascertain that suitable attention has been made by selecting the input parameters. There are contradictions among CFD predictions of cross-ventilation through prismatic buildings. Some reproduce experimentally observed inlet jet trajectories and others do not. Meroney (2009) states that it would be desirable to determine prediction sensitivity to approach flow conditions, turbulence levels, and building porosity.

CFD calculations rely on sophisticated models that are used to define the numerical solutions. Jakeman et al (2006) describes some underlying issues related to identifying and mitigating uncertainties. He suggests that identification of model structure and parameters. The underlying aim is to balance sensitivity to system variables against complexity of representation. Uncertainty must be considered in developing any model, but is particularly important, and usually difficult to deal with, in large, integrated models. Uncertainty in models stems from incomplete system understanding, from imprecise, finite and often sparse data and measurements; and from uncertainty in the baseline inputs and conditions for model runs, including predicted inputs.

Jakeman et al (2006) indicates that practical convenience often dictates piecemeal identification of model components, and pre-existing models are often available for parts of the system. The authors suggest that it is wise to test the overall model to see whether simplification is possible for the purposes in mind. Sensitivity assessment plays a large role here. The results from extensive sensitivity testing can be difficult to interpret, because of the number and complexity of cause-effect relations tested. To minimize the difficulty, clear priorities are needed for which features of which variables to examine, and which uncertainties to cover. A good deal of trial and error may be required to fix these priorities.

According to Ramponi and Blocken (2012) the need for accuracy and reliability need detailed sensitivity studies. CFD simulation results can be very sensitive to the large number of computational parameters that have to be set by the user. Therefore, detailed and generic sensitivity analyses are important to provide guidance for the execution and evaluation of future CFD studies. The authors have carried out a comprehensive and exemplary sensitivity analysis, which was based on a reference case. The reference case was found to correlate well with previous results obtained in a wind tunnel. The systematic and detailed sensitivity analysis was conducted by systematically varying a single parameter compared to the reference case and evaluating the impact of this change on the simulation results. The parameters tested were the size of the computational domain, the resolution of the computational grid, the inlet turbulent kinetic energy of the atmospheric boundary layer, the turbulence model, the discretization schemes, and the convergence criteria. Table 3.3.6.A provides an overview of the computational parameters for the sensitivity analysis, with indication of the reference case.

Table 3.10.1. Overview of computational parameters for sensitivity analysis with indication of the reference case (Ramponi and Blocken, 2012)

	Computational domain size (Section 4.1)	Computational grid resolution (Section 4.2)	Turbulent kinetic energy (Section 4.3)	Turbulence models (Section 4.4)	Discretization schemes (Section 4.5)	Level of iterative convergence (Section 4.6)
Ref. case	$H_D = 5xH$	575,247	$a = 1$	SST k- ω	2 nd order	Conv.
	$H_D = 4xH$	314,080	$a = 0.5$	Sk- ϵ	1 st order	10^{-4}
	$H_D = 3xH$	144,696	$a = 1.5$	Rk- ϵ		10^{-3}
	$H_D = 2xH$			RNG k- ϵ		10^{-2}
	$H_D = 1xH$			Sk- ω		
				RSM		

Impact of size of computational domain

For the assessment of the impact of computational grid only the cross-section (width and height) of the computational domain was varied. The upstream and downstream length of the domain remained unchanged at 3H and 15H, respectively, with H the building height. Figure 3.10.1 indicates the variable parameters which included the height H_D of the domain is $H_D = H + d$ and the while W_D of the domain as $W_D = W + 2d$, with W the width of the building. Several researches tend to refer to the blockage ratio (BR) which is the ratio between the frontal area of the model facade and the cross-section of the computational domain. Researchers suggest different yet similar minimum values for the lateral and top clearance that describes the domain cross-section. For example, Tominaga et al (2008) and Frank (2006) suggest a minimum distance (d) equal to 5 times the height (H) to avoid the interference of the domain size on the numerical simulation results. Thus, a distance $d = 5H$ (B.R. = 2%) was applied in the reference case and then reduced to 4H (B.R. = 3%), 3H (B.R. = 4%), 2H (B.R. = 8%) and H (B.R. = 19%). Figure 3.10.1. indicates the influence of the cross-section of the computational domain on the indoor air speed. The result in Figure 3.10.1 suggest that a considerable increase in indoor air speed occurs when the cross-section is strongly reduced ($d=H$).

Impact of computational grid resolution

The sensitivity of grid resolution was tested with three grids of different cell numbers. The grids were obtained by coarsening the reference (fine) grid with twice about a factor 2. The three grids are illustrated in Figure 3.10.2 and the results on the three grids are shown in Figure 3.10.3 the results show that grid sensitivity is most pronounced for the indoor area behind the inlet and behind the outlet. The

sensitivity analysis shows that the reference (fine) grid is a suitable grid. The difference in the ventilation flow rates through the inlet openings is about 1.0% between the fine grid and medium grid, while the difference is 7.5% between fine grid and the coarse (fine) grid and grid A.

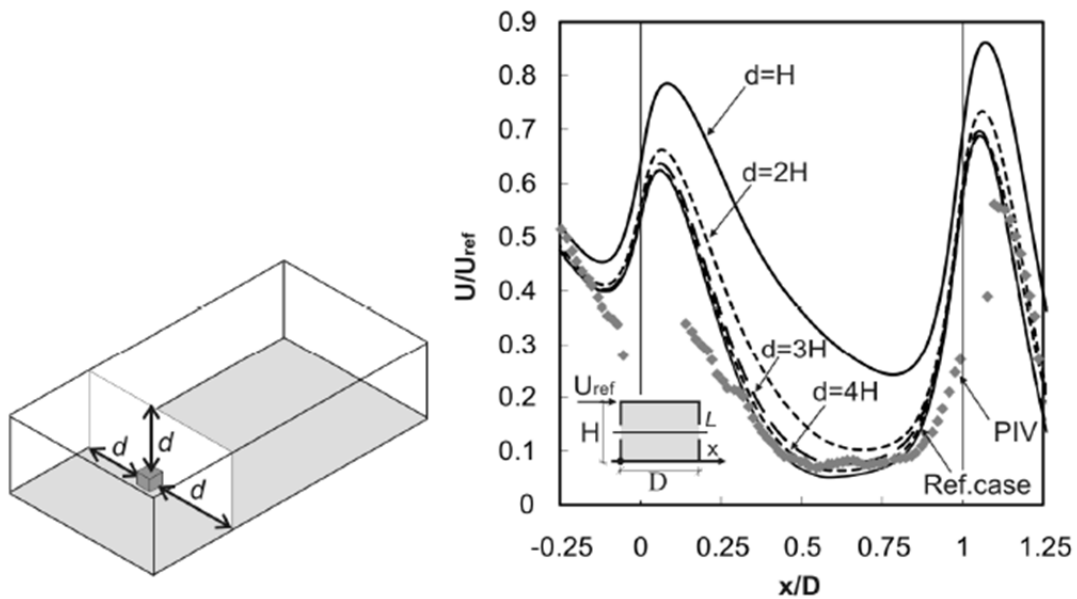


Figure 3.10.1: CFD simulation results for sensitivity analysis: impact of the size (cross-section) of the computational domain on the streamwise wind speed ratio along the centerline (Ramponi and Blocken, 2012).

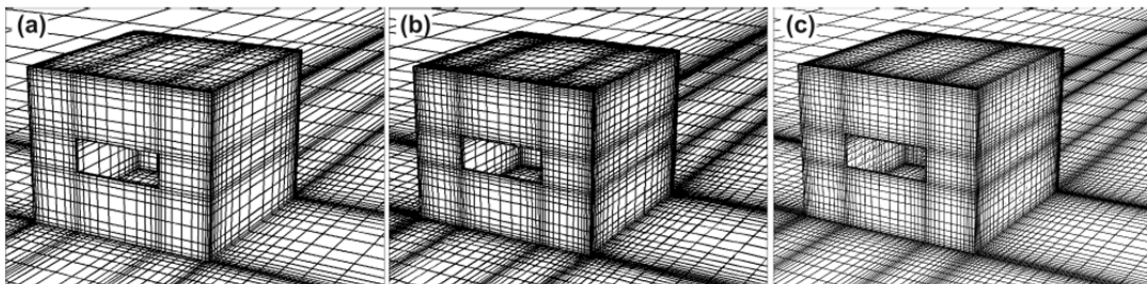


Figure 3.10.2: Perspective view of grids for grid-sensitivity analysis: (a) Coarse grid A with 144,696 cells; (b) Middle grid B with 314,080 cells; (c) Fine grid C with 575,247 cells (reference case). (Ramponi and Blocken, 2012).

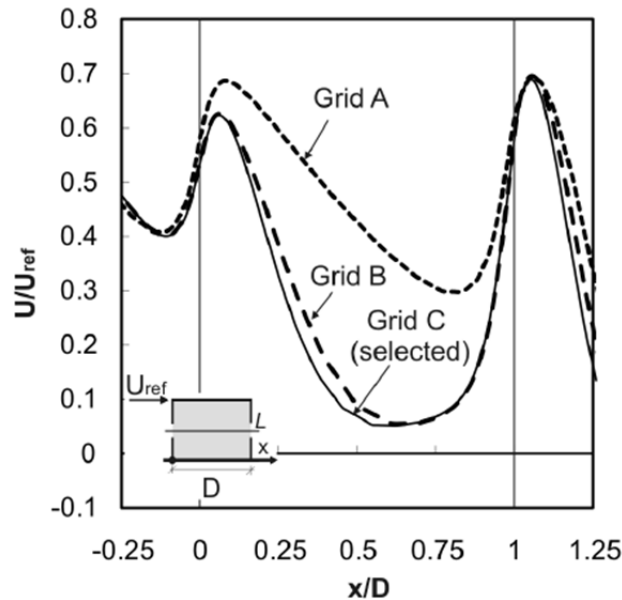


Figure 3.10.3: CFD simulation results for sensitivity analysis: impact of the grid resolution on the streamwise wind speed ratio along the centerline; Comparison of results from the three grids. (Ramponi and Blocken, 2012).

Impact of inlet turbulent kinetic energy

Impact of inlet turbulent kinetic energy profile at the inlet can be estimated from the measured wind velocity and turbulence intensity profiles. In the sensitivity study three values for "a", where a is a linear coefficient that is used to calculate the turbulent kinetic energy. Different profiles of k were defined by varying the parameter a . Results of two values of "a" were compared with the reference case ($a = 1$) for streamwise wind speed ratio along the centerline of the openings (Figure 3.10.4). The functions shown in Figure 3.10.5 shows that varying the inlet turbulent kinetic energy with the parameter "a" has a very large impact on the wind speed ratio along the centerline. Other results indicate that the increased turbulent kinetic energy profiles at the inlet are not significantly affecting the horizontal homogeneity of the approaching flow. Only some small streamwise changes are noted for the turbulent kinetic energy profiles themselves.

Impact of order of discretization scheme

The authors suggest that CFD best practice guidelines consistently stress the importance of at least discretization schemes of second-order accuracy. The authors stress that first-order schemes provide necessary numerical diffusion to achieve convergence with unstructured computational grids that include tetrahedral and/or pyramid cells, rather than hexahedral and prismatic cells. However, the numerical diffusion by first-order schemes also decreases flow gradients, as shown in Figure 10.5, which indeed shows that for this situation accurate results cannot be obtained with first-order discretization schemes

3. Internal CFD – Numerical Assessment of Air Movement Inside Buildings

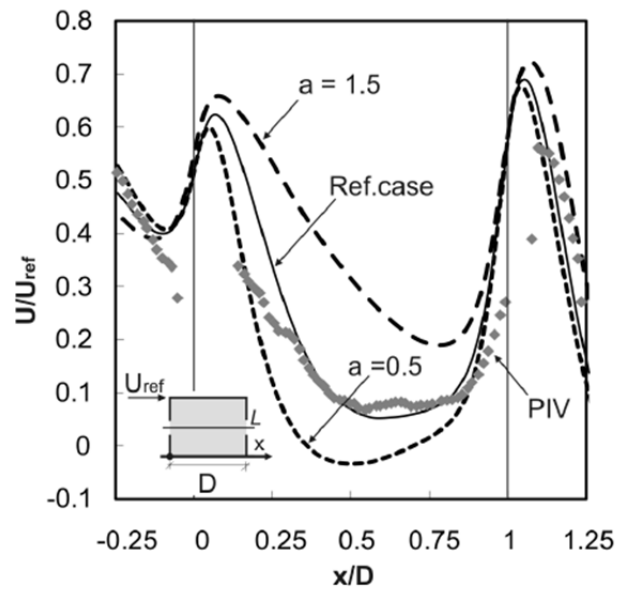


Figure 3. 3.10.4: CFD simulation results for sensitivity analysis: impact of approach-flow turbulent kinetic energy profile parameter a on the streamwise wind speed ratio along the centerline ($a = 1$ for the reference case).. (Ramponi and Blocken, 2012).

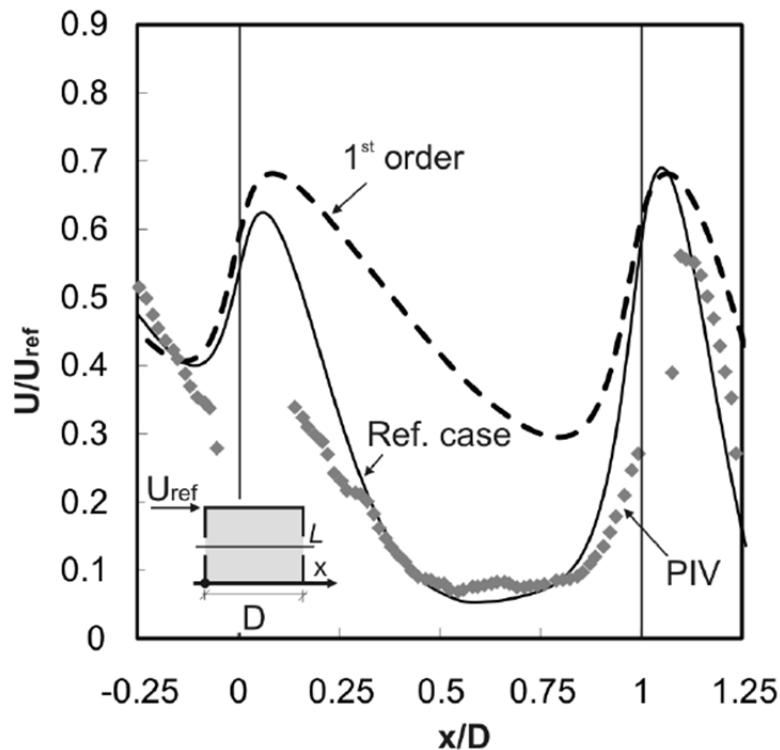


Figure 3. 3.10.5: CFD simulation results for sensitivity analysis: impact of discretization scheme on the streamwise wind speed ratio along the centerline. For the reference case, a second-order discretization scheme is used. (Ramponi and Blocken, 2012).

Impact of turbulence model

The sensitivity analysis used a 3D steady RANS simulation with the following turbulence models:

- standard $k-\varepsilon$ model (Sk-e)
- realizable $k-\varepsilon$ model (Rk-e)
- Renormalization Group $k-\varepsilon$ model (RNG k-e)
- standard $k-\omega$ model (Sk-w)
- shear-stress transport $k-\omega$ model (SST k-w)
- Reynolds Stress Model (RSM)

Figure 3.10.6 shows the effects of the turbulence models on the indoor air flow are illustrated in terms of streamwise wind speed ratio along the centerline of the openings. Figure 3.10.6 shows the contours of streamwise wind speed in the vertical centerplane. Figure 3.10.6 G indicates a comparison with the PIV measurements. The results suggest that the SST $k-\omega$ model (the reference case) is clearly superior, followed by the RNG $k-\varepsilon$ model, which also provides a fairly good performance. The discrepancies by the

other models are very large. In fact, Figure 3.10.6 shows that the indoor streamwise wind speed obtained with the other k-e models are several times higher than the one obtained using the SST k-w model (Ref. case). Figure 3.10.6 also shows that the RSM and the standard k-w models tend to over predict the experimental values by about a magnitude.

The authors point out that several previous studies show a superior performance of the RNG k-e model for indoor air flow modeling, especially compared to the standard k-e model. This is to a large degree confirmed by our study. However, in our study, the SST k-w model even outperforms the RNG k-e model. Figure 3.10.7 shows the differences in flow characteristics obtained with different turbulence models. The figure suggests that the main discrepancies are related to the direction of the jet entering the building model.

Impact of level of iterative convergence

The authors suggest that there is no clear consensus in literature about the level of iterative convergence, apart from the statement that convergence of critical variables should be monitored and confirmed. Care should be taken to avoid convergence criteria that are not tight enough.

The authors point out that the results of their sensitivity analysis substantiate recommendations found in various Best Practice Guidelines. However, they point out that the impact of the inlet turbulent kinetic energy profile was very large. This point is very important since, as the authors stress, this large impact has not been shown before. This is particularly important because there is no consensus in literature on how the inlet turbulent kinetic energy profile should be calculated from the profiles of mean wind speed and streamwise turbulence intensity. In terms of turbulence model, the best performance was shown by the SST k-w model, followed by the RNG k-e model. The other models were found insufficiently capable of reproducing the magnitude and position of the standing vortex upstream of the building facade, and of the resulting direction of the jet through the ventilation opening. The authors recommend the use of at least second-order accurate discretization schemes, as well as sufficiently stringent convergence criteria. It is stressed that the convergence criteria suggested by commercial CFD codes are often too lenient and not stringent enough for accurate simulation results.

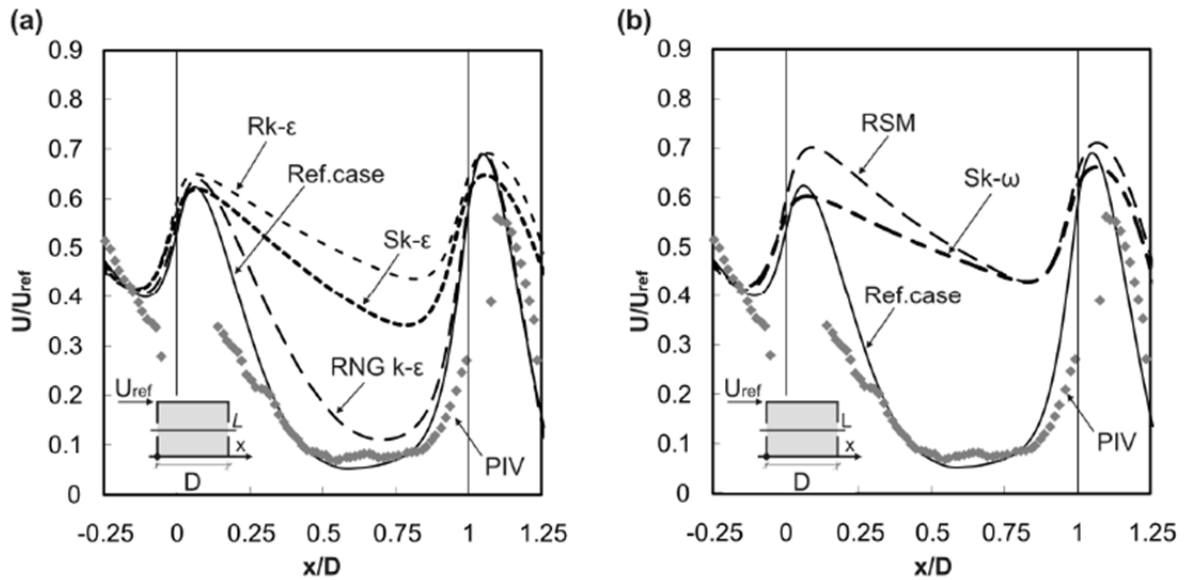


Figure 3.10.6: CFD simulation results for sensitivity analysis: impact of discretization scheme on the streamwise wind speed ratio along the centerline. For the reference case, a second-order discretization scheme is used. (Ramponi and Blocken, 2012).

3. Internal CFD – Numerical Assessment of Air Movement Inside Buildings

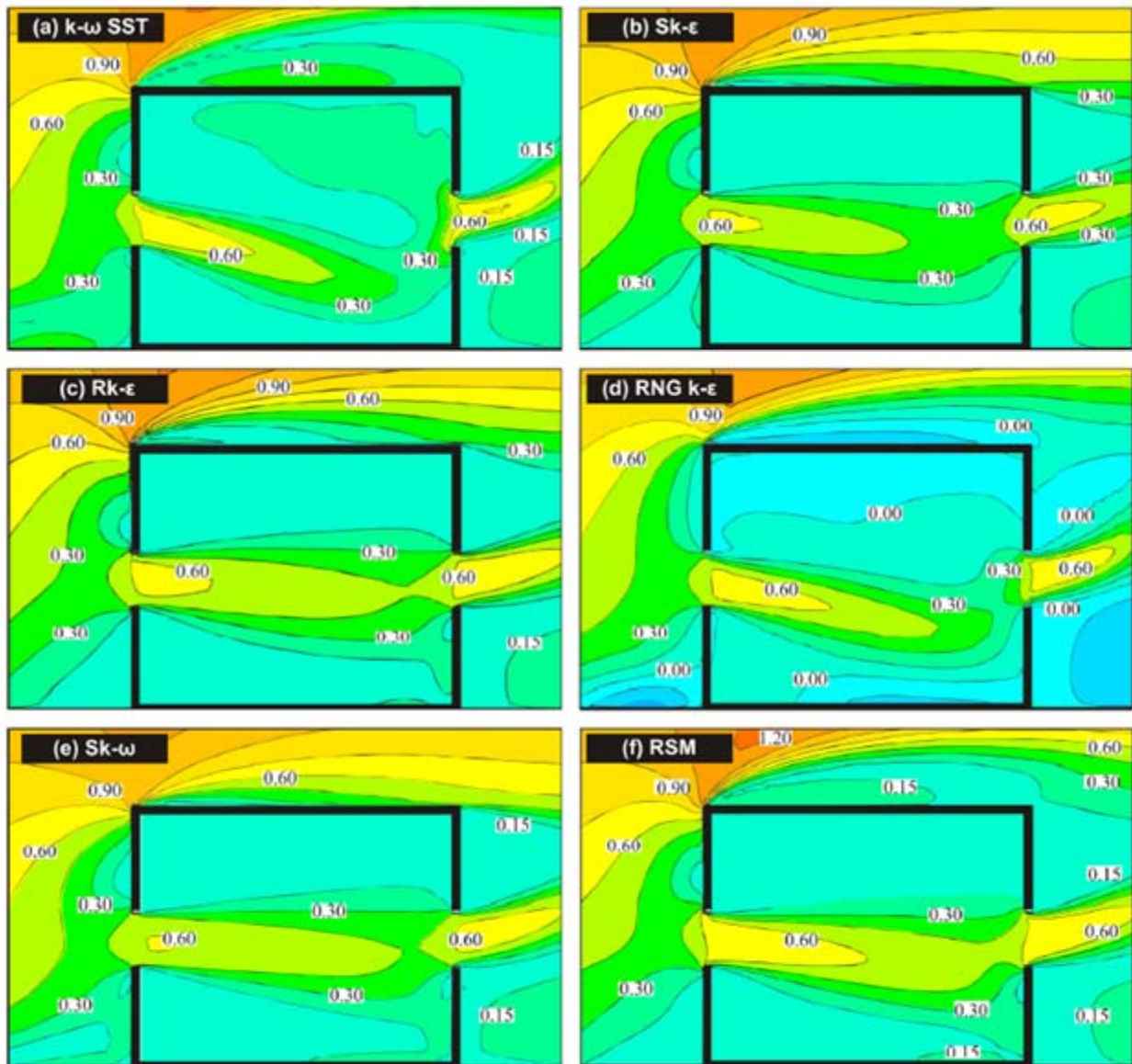


Figure 3.10.7: CFD simulation results for sensitivity analysis: impact of turbulence models on the wind speed ratio contours in the vertical centerplane. The SST k- model is the reference case in this study. (Ramponi and Blocken, 2012).

3.11 Post Processing

Post processing is an important process in CFD modeling workflow to process results from the simulation for quantitative and qualitative assessments. Most CFD packages can provide the following capacities for post processing:

- 2d flow visualization: capability to create a snapshot of the selected solution data as well as provide user-friendly interfaces to locate and manipulate section planes for visualization the solution at specific locations and orientation at specific solution time defined by users. The snapshot of these data can be visualized in many formats such as contoured and shaded fill sections (Figure 3.11.1)
- 3d flow visualization: capability to visualize the selected solution data in 3d such as particle plot, streamlines, iso-surfaces (Figure 3.11.2), etc. or combination of different solution 2d data (Figure 3.11.3)
- Animation.
- Design options/ scenarios: capability to provide design options/ scenarios for comparing multiple steady state solutions in a single simulation file (Figure 3.11.4)
- Report, monitor and graphical plot data/ data export: capability to create reports on certain variables, fields, residuals, monitor those during solution process (Figure 3.11.5) and to access to the results in ASCII format, which is very useful for comparing results with experimental data or other CFD codes (Figure 3.11.6).

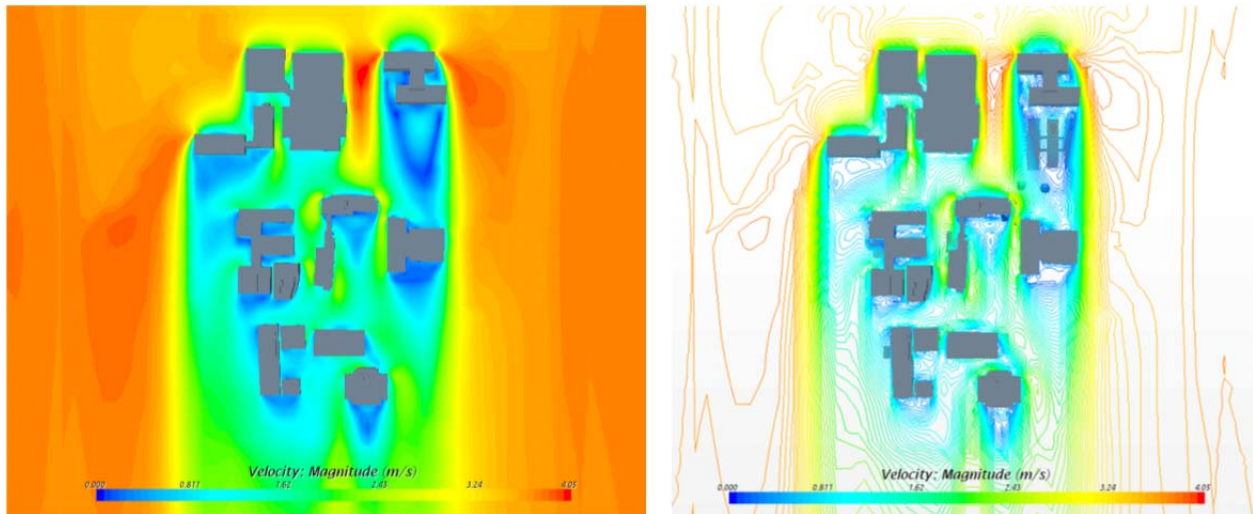


Figure 3.11.1: An examples of 2d visualization in filled region and contour format produced by using STAR-CCM+ showing wind velocities at a section plane.

3. Internal CFD – Numerical Assessment of Air Movement Inside Buildings

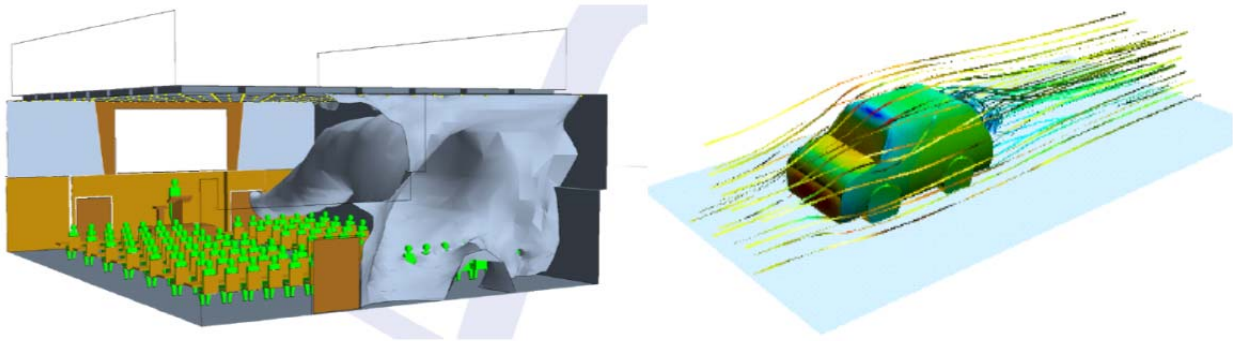


Figure 3.11.2: An examples of 3d visualization in (a) iso-surface showing air change rate and (b) streamline showing airflow (Source: CD-Adapco)

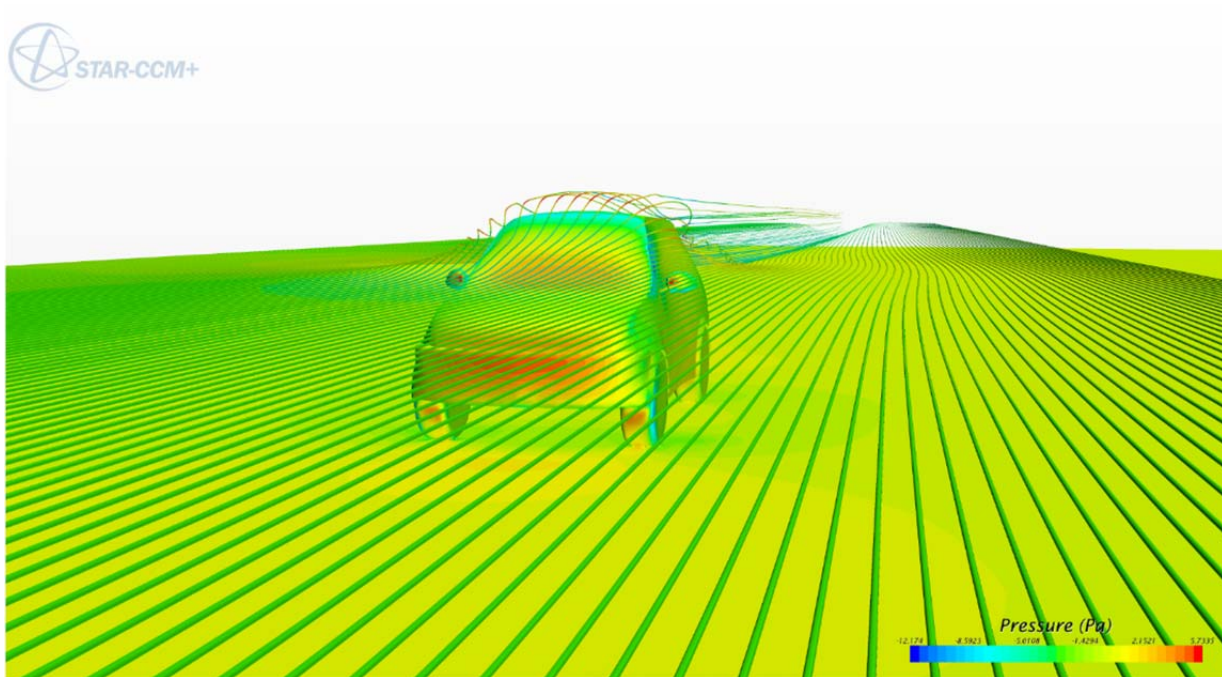


Figure 3.11.3: Combined visualization of two data fields (pressure distribution and velocity streamline) of wind-induced effects around a car.

3. Internal CFD – Numerical Assessment of Air Movement Inside Buildings

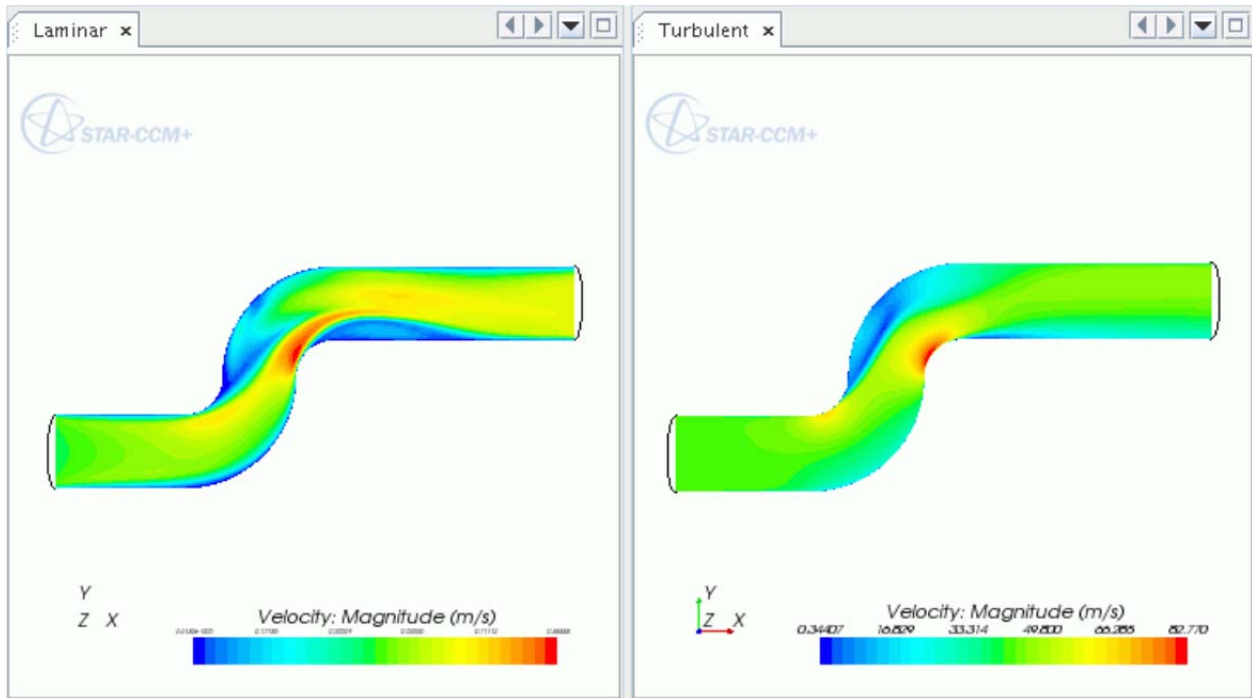


Figure 3.11.4. Multiple snapshot from different design scenarios for comparing the resulting data (STAR-CCM+ Manual 8.02)

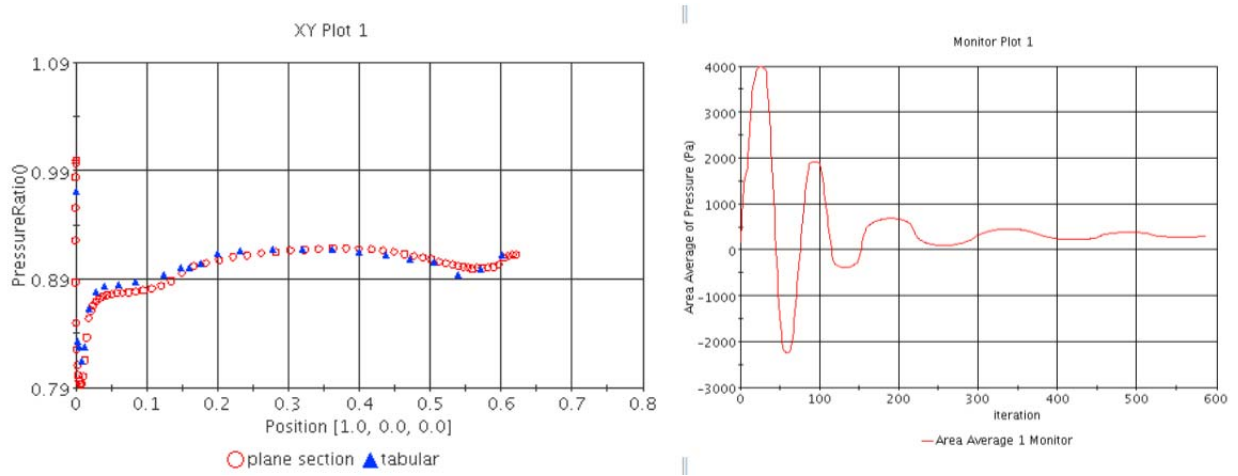


Figure 3.11.5: Example of XY plot and monitor plot with STAR-CCM+ (STAR-CCM+ Manual 8.02)

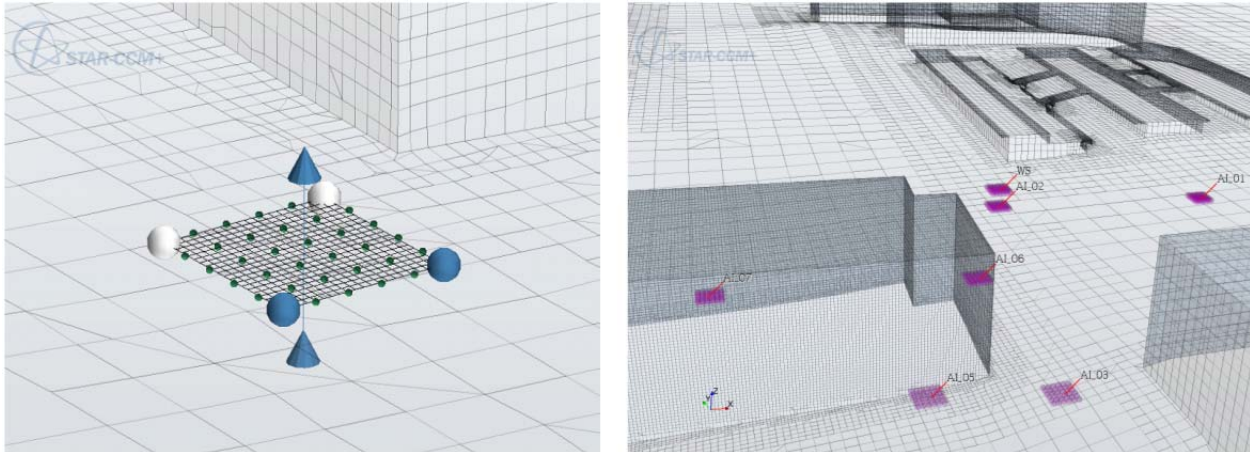


Figure 3.11.6: Presentation grid part in STAR-CCM+ allow to extract resultant data from CFD simulation in ASCII format (e.g. csv) for external post-processing.

3.12 Validation of CFD Data through On-site Measurements

Quality assessment of CFD, which helps to reduce numerical errors and uncertainties, consists of verification and validation. Guidelines for best practices for verification and validation were discussed in ARSHRAE (2005) and AIAA (1988). Verification of a CFD model is process “to start with the assessment of necessary models to realistically represent ventilation transport process and finish with the evaluation of numerical simulation methods”. Verification process includes: airflow and heat transfer models (2) turbulence model and (3) numerical solution methods. For airflow and heat transfer models connecting to convection, diffusion and/or radiation, velocity and temperature fields need to be modeled. Standard $k-\epsilon$ turbulence model is recommended even though some inaccuracy might be found at near wall boundaries (Srebric, 2011).

Numerical errors could be minimized by using double-precision (round-off errors), an increase in the order of magnitude (iterative convergence errors) and high grid resolution (discretization errors) could be minimized by using double-precision (Eça and Hoekstra, 2014). Validation is a process to quantify how accurate a CFD model represents the real ventilation in a building. According to Srebric (2011), validation includes (1) detailed geometry and boundary conditions of simulation domain, (2) detailed measurements of flow properties such as distribution of velocity, pressure and temperature, and (3) complementary overall measurements such as total

mass flow rate and heat fluxes. Uncertainties and errors from acquisition equipment, experiments and data collection process should be considered.

Srebric (2011) presented an example of CFD modeling of a displacement ventilation case of set-up which as available detailed measured data for validation (Figure 3.2.7.1). The results showing the simulated velocities and temperatures at the vertical middle section plane are in very good agreement with the observed flow field and measurement. The model validation confirmed high agreement from detailed comparison between measured and calculated velocity and air temperature (Figure 3.2.7.2)

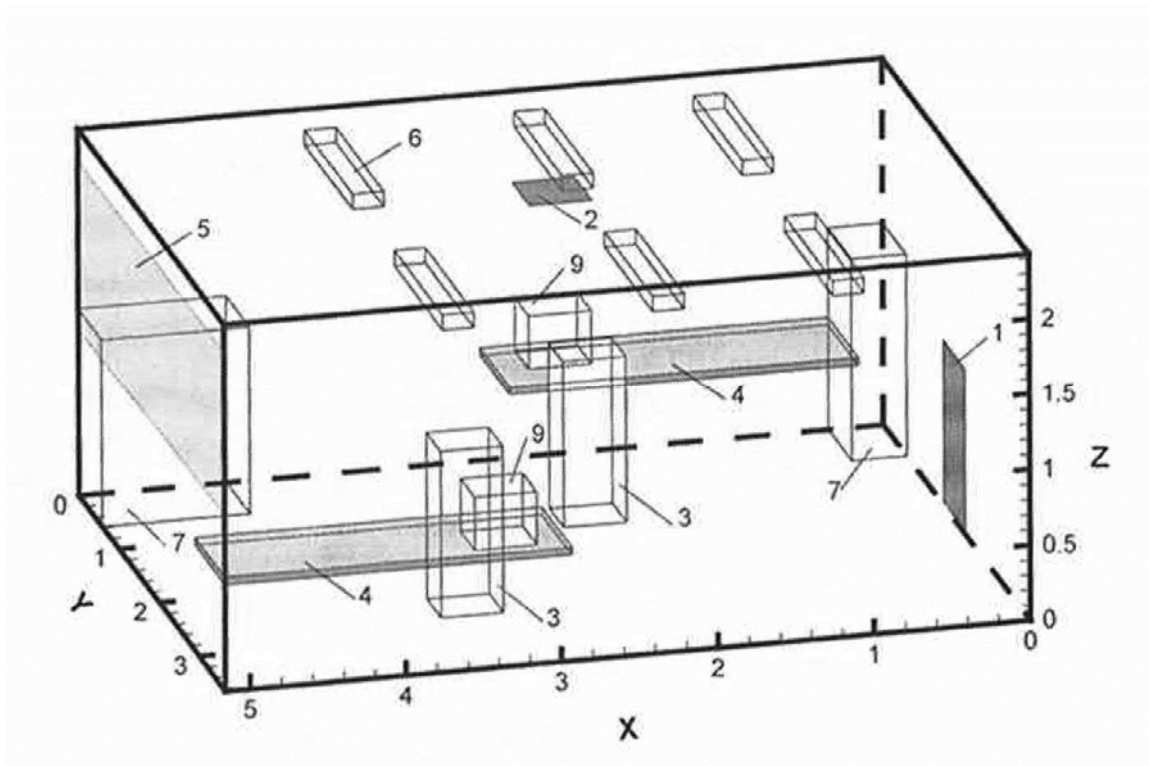


Figure 3.12.1: The configuration of the displacement ventilation simulated and tested in the chamber (inlet -1, outlet -2, person -3, table -4, window -5, fluorescent lamps -6, cabinet -7, computer -9) (Srebric, 2011).

3. Internal CFD – Numerical Assessment of Air Movement Inside Buildings

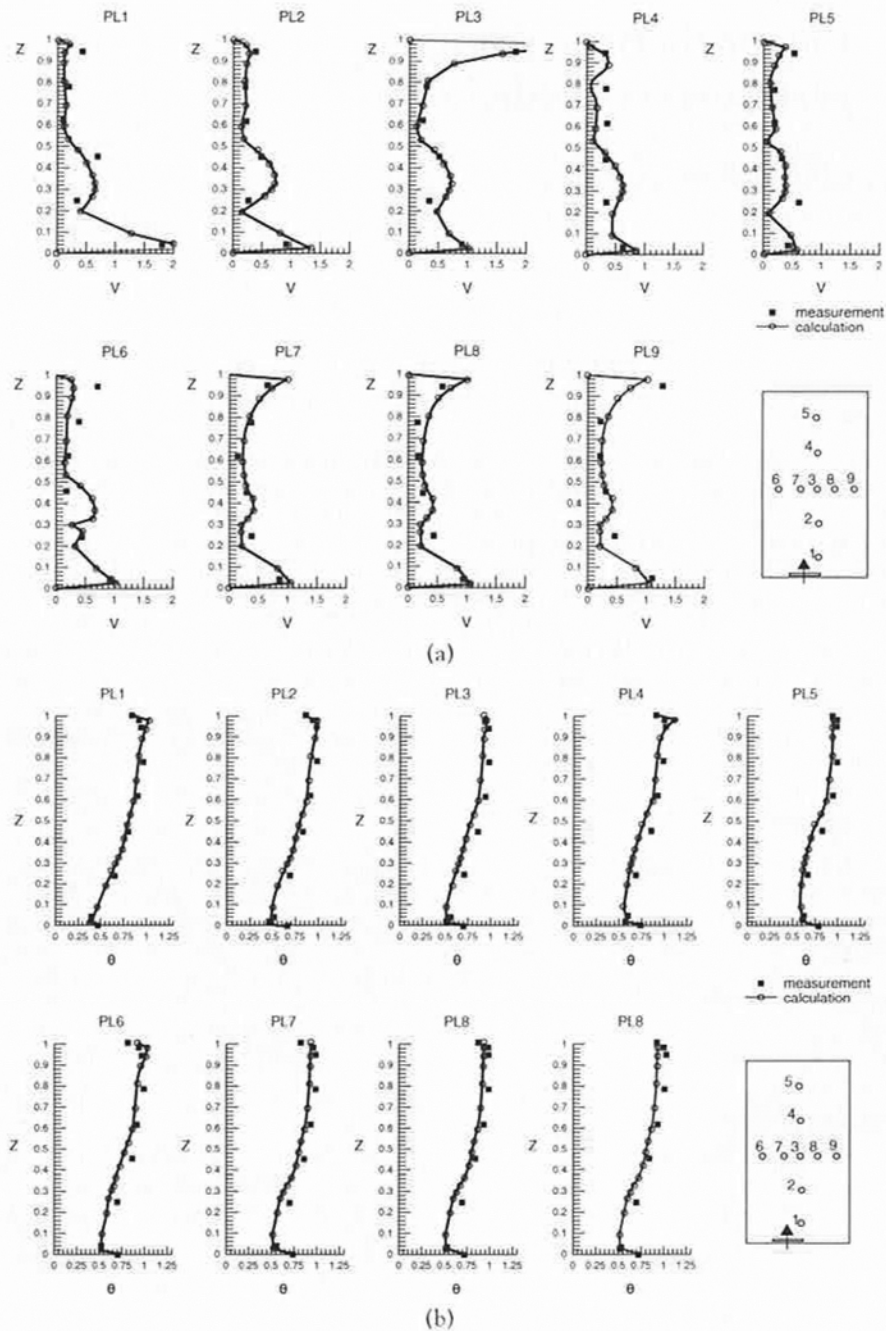


Figure 3.12.2: Comparison of (a) the velocity profiles and (b) the temperature profiles at nine positions in the room between the simulated and measured data for the displacement ventilation (Srebric, 2011).

Hooff T. and Blocken B. (2010) presented their CFD simulation and validated their predictions with the full-scale on-site measurement of the indoor natural ventilation performance of the large semi-enclosed *Amsterdam ArenA* stadium in the Netherlands. The fully coupled outdoor-indoor simulation CFD approach including 3D steady *Reynolds-Averaged Navier-Stokes* (RANS) equation with the *Realizable k-ε* turbulence model, the standard wall function with roughness modification, grid sensitivity analysis via commercial CFD code Fluent 6.3.26 were discussed in the article. Two CFD modeling scenarios were represented. The first one called Case 1 ignored adjacent buildings while the second one called Case 2 included these surrounding buildings in the model. These CFD models and measurement were used to calculate the air change rates as the effectiveness performance indication of the natural ventilation of the stadium for eight every 45 degree wind directions (in respect to the symmetrical axis of the stadium) (Figure 3.12.3). Based on the comparison air change rates from CFD and measurement, the authors concluded that wind directions and surrounding buildings played a big impact on the accuracy of the prediction of indoor natural ventilation of the large stadium.

The full-scale on-site measurement was conducted by using ultrasonic 3D anemometers at four gates of the stadium corners. The reference wind speed was measured on the highest adjacent building at the height of 115m (the building height of 95m plus the height of the weather station's sensor located at 10 m above the roof). To avoid the atmospheric stratification, the authors mentioned that the measurement was conducted during cloudy days with strong winds. In addition, to minimize the standard deviation of the average wind speeds, per wind direction section of 10°, the data of at least 12 10-minute data points of 10-minute averaged were used.

The validation of the CFD was based on the comparison of wind velocities and wind directions between CFD simulation and measurement. The validation showed a good agreement between CFD simulation and measurement on both wind velocities and wind directions, except the location D where the wind direction deviation is as high as 30% (Figure 3.2.7.4). Note that the authors intentionally chose the four locations at large gates where wind with high velocities occur, and where the wind directions would be quite confined. This intent helped the validation to avoid the possible uncertainties such as thermal and turbulence effects.

The authors used the air change rate as indication of the natural ventilation performance in the two different CFD modeling scenarios: CFD model with and without surrounding buildings. The authors found that there were different deviations per wind directions of the estimation of the air change rates between two CFD modeling scenarios. For example, the most significant difference is the wind coming from the upstream area with a large number of buildings ($\varphi=196^\circ$) while this deviation are negligible at the wind coming from the least obstructed upstream area ($\varphi = 16^\circ$) (Figure 3.2.7.5). The author

concluded that this comparison showed that the wind directions and urban surroundings significant influenced the natural ventilation of the stadium.

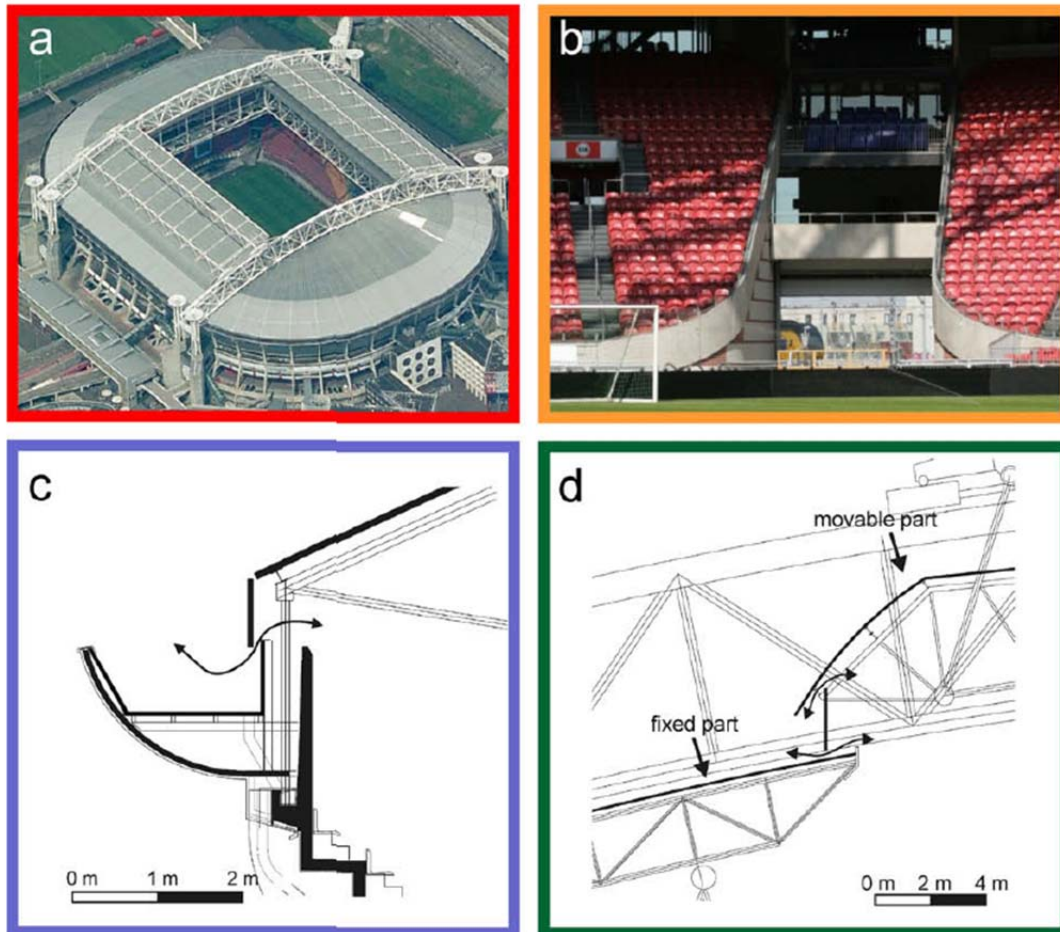


Figure 3.13.3: The ventilation openings of the stadium (Hooff and Blocken, 2010); (a) the opened roof with a surface area; (b) one of the four openings in the corner of the stadium (gates); (c) ventilation opening between the steel roof construction, the gutter and the concrete stand; (d) ventilation opening between the fixed and movable part of the roof.

3. Internal CFD – Numerical Assessment of Air Movement Inside Buildings

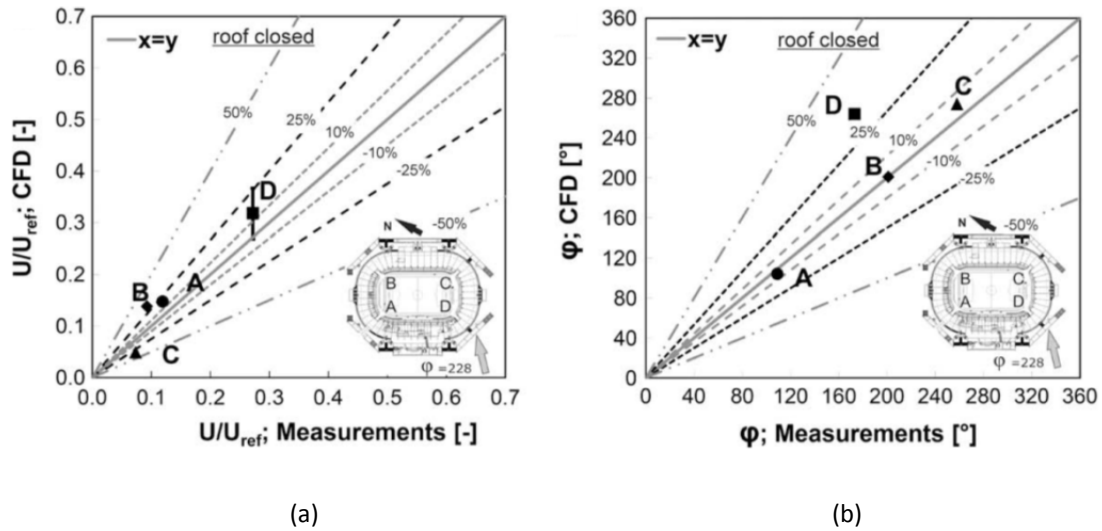


Figure 3.12.4: Comparison between numerical and experimental results in the four gates A, B, C and D, for closed roof and wind direction of 228 (Hooff and Blocken, 2010). (a) non-dimensional velocity magnitude U/U_{ref} ; (b) wind direction ϕ . The error bars are a measure of the local spatial gradients in the CFD simulation. The percentages indicate the deviation between the measurements and the CFD simulations.

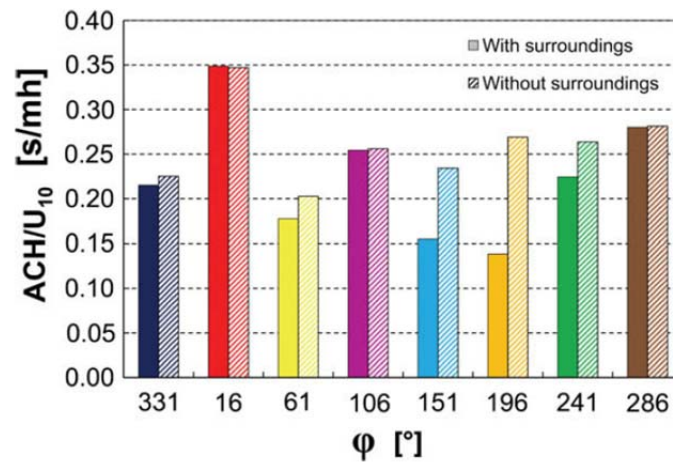


Figure 3.12.5: Comparison of ACH/U_{10} (s/mh) for eight wind directions for Case 1 (without surrounding buildings) and for Case 2 (with surrounding buildings) (Hooff and Blocken, 2010).

REFERENCES

- Adams, T., et al. (2012) *A Simple Algorithm to Relate Measured Surface Roughness to Equivalent Sand-Grain Roughness*, *International Journal of Mechanical Engineering and Mechatronics*, 2012, Vol. 1, Issue. 1, p.66-71.
- Baker, J and Shearin, E. (2010) *Insect screening*, North Carolina Cooperative Extension Service, online article accessed Aug 2, 2014
<http://www.ces.ncsu.edu/depts/ent/notes/O&T/production/note104.html>
- Blazdek, J. (2001) *Boundary Conditions*, In *Computational Fluid Dynamics: Principles and Applications*, Elsevier Science Ltd.
- Blocken B., et al. (2007) *CFD Simulation of the Atmospheric Boundary Layer: Wall Function Problems*, *Atmospheric Environment*, 2007, 41:238-252.
- Bell, M. and Baker, J. (1997) *CHOOSE A GREENHOUSE SCREEN BASED ON ITS PEST EXCLUSION EFFICIENCY*, N.C. Flower Growers' Bulletin - April, 1997 Volume 42, Number 2
- Biswas, R. and Strawn, R. (1998) *Tetrahedral and hexahedral mesh adaptation for CFD problem*, "Elsevier", *Applied Numerical Mathematics*, November 1998
- Building Science Corporation (2010) *Balanced Ventilation Systems (HRVs and ERVs)*, BSC Information Sheet 611, www.buildingscience.com.
- Cóstola, D., et al. (2009) *Overview of pressure coefficient data in building energy simulation and airflow network programs*, *Building and Environment*.
- L. Eca and M. Hoekstra (2014) *A Procedure for the Estimation of the Numerical Uncertainty of CFD Calculations Based on Grid Refinement Studies*, *Journal of Computational Physics*, 2014, 262, p. 104-130.
- Emmerich, Steven J. (1997) *Use of Computational Fluid Dynamics to Analyze Indoor Air Quality Issues*, NIST U.S. Department of Commerce, Building and Fire Research Laboratory, National Institute of Standards and Technology, Gaithersburg

- Harrington, K. and Ray, J (2014) *How Louvers Work*, Architectural Louvers, accessed Aug 2014, http://www.archlouvers.com/How_Louvers_Work.htm
- Hefny, M. and Ooka, R. (2009) *CFD analysis of pollutant dispersion around buildings: Effect of cell geometry*, Building and Environment, Volume 44, Issue 8,
- C. Hirsch (2007) *Numerical Computation of Internal & External Flows, Volume 1: Fundamentals of Computational Fluid Dynamics*, 2nd. ed. Elsevier Science Ltd.
- Hooff, T. and Blocken B. (2002) *On the Effect of Wind Direction and Urban Surroundings on Natural Ventilation of a Large Semi-enclosed Stadium*, Computers & Fluids 2010, 39
- Hult, E. , et al (2009) *Using CFD Simulations to Improve the Modelling of Window Discharge Coefficients*, Lawrence Berkeley National Laboratory, Berkeley, CA
- Jiang, Y. and Chen, Q. (2002) *Effect of fluctuating wind direction on cross natural ventilation in building from large eddy simulation*, Building and Environment, 37(4), 379-386.
- Kesik, Ted (2014) *Moisture Management Concepts*, National Institute of Building Sciences, accessed July 2014 <http://www.wbdg.org/resources/moisturemanagementconcepts.php>
- Lstiburek, J. (1999) *Air Pressure and Building Envelopes*, Research Report - 9905, Building Science Press
- Lstiburek, J. (2000) *Toward an understanding and Prediction of Airflow in Buildings*, Ph.D. Dissertation, University of Toronto
- Lstiburek, J. (2006) *Building Science Digests*, 109, Building Science Press
- Meroney, R.N. (2004) *WIND TUNNEL AND NUMERICAL SIMULATION OF POLLUTION DISPERSION: A Hybrid Approach*, Wind Engineering and Fluids Laboratory Colorado State University
- Meroney, R. (2009) *CFD Prediction of Airflow in Buildings for Natural Ventilation*, 11th Americas Conference on Wind Engineering
- Nielsen, P. et al (2007) *Computational Fluid Dynamics in Ventilation Design*, Federation of European Heating and Air-Conditioning Associations, Guidebook No. 10

- Pedersen, C.O., et al (1997) *Development of a Heat Balance Procedure for Calculating Cooling Loads*, ASHRAE Transactions, Vol. 103, Pt. 2, pp.459-468.
- Quirouette, R. (2004) *Air pressure and The Building Envelope*, accessed Aug 20104. <https://www.cmhc-schl.gc.ca/en/inpr/bude/himu/coedar/upload/Air-Pressure-and-the-Building-Envelope.pdf>
- Ramponi R, Blocken B. (2012a) *CFD simulation of cross-ventilation flow for different isolated building configurations: validation with wind tunnel measurements and analysis of physical and numerical diffusion effects*. Journal of Wind Engineering and Industrial Aerodynamics 104-106: 408-418.
- Ramponi R, Blocken B. (2012b). *CFD simulation of cross-ventilation for a generic isolated building: impact of computational parameters*. Building and Environment 53: pages 34-48
- Roache, P. (1997) *QUANTIFICATION OF UNCERTAINTY IN COMPUTATIONAL FLUID DYNAMICS*, Annual. Rev. Fluid. Mech. 1997. 29:123–60
- Roache, P. (1994) *Perspective: A Method for Uniform Reporting of Grid Refinement Studies*, Journal of Fluids Engineering, Vol. 116, p.405-513
- Russell, M. et al (2005) *Review of Residential Ventilation Technologies*, ERNEST ORLANDO LAWRENCE BERKELEY NATIONAL LABORATORY, LBNL 57730
- Santamouris, Mat, et. al (1998) *Natural ventilation in Buildings*, European Commission Directorate General for Energy Alterer Program, Publisher James & James, London
- Srebric,J. (2011) *Ventilation Performance Prediction*, In J. Hensen and R. Lamberts (Eds.), Building Performance Simulation for Design Operation, p.143-179
- STAR-CCM+ User Guide 8.02, CD Adapco, 2013
- Straube, J. (2007) *Air Flow Control in Buildings*, Building Science Digest 014, Building Science Press
- SuperFlow Technologies Group (SFTG) (2007) *Airflow Basics*, accessed Aug 2, 2014
http://www.superflow.com/support/supportDocuments/airflow_basics.pdf

VanHooff, T. and Blocken, B. (2010) *Coupled urban wind flow and indoor natural ventilation modeling on a high-resolution grid: A case study for the Amsterdam Arena stadium*. *Environmental Modeling & Software* 25(1): 51-65.

Versteeg, H.K and Malalasekera, W. (2007) *Introduction to Computational Fluid Dynamics; The Finite Difference method*, Second Edition, Pearson Education Limited,

Walker, Andy (2010) *Natural Ventilation*, National Renewable Energy Laboratory, web page accessed July 2014, <http://www.wbdg.org/resources/naturalventilation.php>